Aalto-yliopisto
Aalto-universitetet
Aalto University

Master’s Programme in Environomical Pathways for Sustainable Energy Systems

Recycling of Future Batteries

Laleh Ghaheri Badr

Master’s thesis
2025

Aalto-yliopisto
Aalto-universitetet
Aalto University

Author Laleh Ghaheri Badr
Title of thesis Recycling of Future Batteries
Programme Environomical Pathways for Sustainable Energy Systems
Major Sustainable Biomass Processing
Thesis supervisor Prof. Mari Lundström
Thesis advisor(s) Anssi Karppinen, MSc and Heikki Lappalainen , MSc
Date 27.09.2025 **Number of pages** 111 **Language** English

Abstract

Rapid development in future battery technologies, including solid-state batteries (SSBs) and sodium-ion batteries (SIBs), is diversifying battery chemistries, bringing both opportunities and challenges to end-of-life (EoL) battery recycling with the existing recycling infrastructures. This study explores the feasibility of integration of emerging battery chemistries into existing lithium-ion battery (LIB) recycling flow sheets, with a focus on hydrometallurgical and pyrometallurgical approaches. Also, a novel type EoL Sodium-SO_2 battery CAM characterization and leaching behaviour has been studied.

In theory, pyrometallurgy offers high tolerance to compositional variability, yet further hydrometallurgical treatment is needed. In contrast, hydrometallurgy enables selective, high-yield material recovery but faces uncertainties related to contamination risks of battery-grade materials and needs extra purification steps. Water-based selective leaching emerges as a potential preliminary treatment for certain solid-state electrolytes (SSEs) and to remove sodium ions from the cathode active material (CAM), potentially mitigating contamination during CAM separation. In the experiments, while effective leaching of NaCl is detected in the sodium deactivation step, a new phase formation in the presence of halide and sulfur is observed. Leaching efficiency out of this new phase shows fast leaching behavior in the first few minutes using different lixiviants for Al and S (~90% Al in 1 M H_2SO_4, 60-70% Al and 50-65% S in 1 M HCl).

In conclusion, the results highlight the potential for separating new chemistries, while underscoring the need for accurate battery identification, aided by tools like the battery passport, to ensure safe and efficient recycling.

Keywords Solid-state batteries, Sodium-ion batteries, Industrial battery recycling, Hydrometallurgy, Pyrometallurgy

Table of contents

Preface and acknowledgements

This master's thesis was conducted as part of the BATCircle 3.0 project (Business Finland grant number 1754/31/2024). The work was supported by the Research Council of Finland through funding for the Aalto JUST Materials Research Infrastructure at Aalto University. The thesis was hosted by the Hydrometallurgy and Corrosion Research Group within the School of Chemical Engineering at Aalto University, Espoo, Finland. I would also like to thank BroadBit Batteries for their support in providing battery samples.

First and foremost, I sincerely thank my supervisor, Professor Mari Lundström, for welcoming me into her leading research group and giving me the opportunity to contribute to the field of battery recycling. Her invaluable guidance throughout this journey has been instrumental, and I have learned so much from her expertise and mentorship.

I am deeply grateful to my advisers, Heikki Lappalainen and Anssi Karppinen, for their consistent support, insightful guidance, and positive attitude. I had the privilege of learning from them in all aspects of the research process, including experimental analysis, result interpretation, and scientific writing.

I also wish to thank Dr. Jere Partinen and Jere Vänskä for their generous help and support with laboratory analyses. Special thanks go to Docent Jari Aromaa, Dr. Sipi Seisko, and Dr. Mika Sahlman for their valuable advice and guidance throughout this journey. I would also like to thank Mikko Oksanen (BroadBit Batteries) for his kind collaboration.

Finally, I am deeply thankful to the entire Hydrometallurgy and Corrosion Research Group for their kindness, openness, and warm attitude. Their welcoming environment made this experience truly enriching.

Last but not least, I would like to thank my family for their unwavering encouragement, for being by my side, and for supporting me every step of the way.

Otaniemi, 27 Sep 2025
Laleh Ghaheri Badr

Abbreviations

CAM	Cathode Active Material
CEI	Cathode Electrolyte Interface
CSSE	Composite Solid-State Electrolyte
CRM	Critical Raw Material
EoL	End of Life
EI	Economic Importance
EnAM	Engineered Artificial Mineral
EU	European Union
EV	Electric Vehicle
GHG	Greenhouse Gas
ICP-OES	Inductively Coupled Plasma Optical Emission Spectrometry
LCO	Lithium Cobalt Oxide
LFP	Lithium Iron Phosphate
LIB	Lithium Ion Battery
NCA	Lithium Nickel Cobalt Aluminium Oxide
NMC	Lithium Nickel Manganese Cobalt Oxide
PGM	Platinum Group Material
PPE	Personal Protective Equipment
PSD	Particle Size Distribution
QR	Quick Respond
REE	Rare Earth Element
RFID	Radio Frequency Identification
RIR	Recycling Input Rate
SDR	Sodium Deactivated Residue
SIB	Sodium-ion Battery
SEI	Solid Electrolyte Interface
SSB	Solid-State Battery
SSE	Solid-State Electrolyte
TRL	Technology Readiness Level

XRD	X-ray Diffraction
XRF	X-ray Fluorescence Spectroscopy

1 Introduction

One of the foremost objectives of the EU in driving the green revolutionary transition is the decarbonization of transport, made possible by the mass use of electric vehicles (EVs) that have recorded phenomenal expansion during the last decades[1],[2]. Electrification via batteries will be the core to eliminating greenhouse gas (GHG) emissions from road transportation[2], which was responsible for 11.8% of total worldwide emissions in 2021[3]. Furthermore, batteries have an important role in the storage of surplus electricity generated by renewable technologies, enhancing storage efficiency, facilitating electricity arbitrage through the storage of energy during low demand, and releasing it at peak times[4], frequency regulation, and grid balance applications to maintain grid stability[5].

Electrochemical energy storage systems, or secondary rechargeable batteries, have developed remarkably in the past decades, and new technologies have entered the market. Some of the most common technologies having a considerable market share are lead-acid, nickel-cadmium, and lithium-ion (LIB) technologies. Lead-acid batteries accounted for roughly 90% of the global battery market until 2010; however, LIB technology outperformed them in 2021, with increased demand for electromobility being largely responsible[6]. In spite of upcoming emerging battery chemistries, LIB technology is expected to keep up market dominance until 2030, due to successful market penetration and a well-established industrial value chain[7].

Although the technical performance of LIBs in the green transition has been proven, there are still some life cycle issues, especially related to material constraints in their production. These constrained resources primarily affect cathode materials and the lithium-based electrolyte[8]. Since policymakers and vehicle manufacturers are more and more motivating consumers toward EVs, the growth of LIBs in the next 5-10 years is projected to be exponential. This, in turn, drives the demand for raw materials and resources, particularly critical raw materials, to their limits[9].

The constraints on the availability of resources are one of the motivations for the development of next-generation batteries. Potentially increasing economic instability for lithium extraction has raised long-term energy security alarms that have led to a need for other battery chemistries. The limited availability of resources, coupled with growing costs of lithium, have motivated scientists to replace battery cathode materials with abundant metals, including sodium, aluminium, calcium, potassium, magnesium, and zinc. The inclusion of these aspects within battery technologies would allow for a greater prevalence of supply security and an advancement of a more robust and sustainable energy storage ecosystem[10].

Another approach to developing conventional LIBs is derived from technological advancements in next-generation batteries. Incremental demand for LIBs is leading to higher capacities of battery manufacturing infrastructure. Cost reduction and higher energy densities are growing requirements for improvements in traditional battery technologies. For this approach, further post-lithium-ion batteries are under investigation[11]. Among these technologies, solid-state batteries (SSBs) stand out as a promising innovation due to their higher energy densities and improved safety. Their use of solid-state electrolytes (SSEs) eliminates electrode crosstalk, reducing chemical instability, while bipolar stacking and lithium metal or silicon anodes can boost performance[12].

As mentioned above, there are different types of future batteries being studied. Meanwhile, sodium-based and solid-state batteries have attracted lots of attention among other emerging battery types with a higher Technology Readiness Level (TRL) Factor.

Having this in mind, the main goals of the current master's thesis are as below:

1- Theoretical evaluation of the recyclability of solid-state and sodium-ion batteries with integration to the existing hydrometallurgical and pyrometallurgical recycling plants, and assess alternative recycling processes.

2- Theoretical investigation on selective water separation potential of solid-state and sodium-ion batteries.

3- Experimental analysis of novel end-of-life disassembled sodium-SO_2, cathode active material characterization, and leaching behaviour with the main focus on Na, S, and Al elements, under different lixiviants.

2 Future Battery Materials and Criticality

Studying the criticality and environmental impacts of raw materials being used in batteries is of the highest importance for the battery stakeholders. Lead acid batteries and LIBs are mostly used and mature secondary battery types, which have a variety of compositions with materials of a wide range of criticality. Nowadays, more than 98% of the mass of lead acid batteries is being recycled, which is mainly because of the simplicity of battery chemistry, composed of Pb and PbO_2 for anode and cathode, respectively. Achieving the same yield with lithium-ion batteries is still challenging. This arises from the complexity of the materials being used and the cell design[6].

Based on information in Table 1, for a car with 100 kWh capacity of lithium nickel cobalt aluminium oxide (NCA) battery, there would be a need for a considerable amount of metals: 10 kg of lithium, 13 kg of cobalt, and 67 kg of nickel. Only for the EV batteries and energy storage, an 18-fold increase in lithium and a 5-fold increase in cobalt demand are projected by 2030. Inevitably, this can cause a supply risk not only in the EU but also worldwide, and due to that, both of the materials have been added to the EU's Critical Raw Materials (CRMs) list. Although nickel is not as critical as lithium, its reserves are of concern. As nickel is increasingly replacing cobalt in LIB cathode materials, the nickel demand may have a 60-times boost in the EU from 2017 to 2060[13].

Table 1. Different Lithium-ion batteries, Raw material requirement in kg/kWh[14]

Battery Type	Lithium	Cobalt	Nickel	Manganese
LCO	0.11	0.96	0	0
NCA	0.1	0.13	0.67	0
NMC 111	0.15	0.4	0.4	0.37
NMC 662	0.13	0.61	0.19	0.2
NMC 811	0.11	0.75	0.09	0.09
LFP	0.1			

The next material is manganese, which poses considerable supply risk related to the substitutability and the limited lifespan of known reserves at current extraction rates. Current available manganese reserves will be depleted in 34 years, and there are limited alternatives capable of providing the same range of battery capacity and life span. The rest of the materials in LIBs are copper, aluminium, steel, and graphite or silicon in future generations[6].

Rapid changes in the chemical composition and structure of the batteries in the market are the main issues for recycling plants. Thus, more generic recycling plants capable of digesting different types suffer from lower recycling yield and lower purity levels. For the existing battery types, the absence of compositional labelling for identification and ease of shredding is a constraint on employing more advanced recycling methods. Most battery packs do not provide information about the anode, cathode, or electrolyte chemistry, so all cells from various packs must be processed in the same way. Due to that, pyrometallurgy and shredding are the most available recycling techniques[14]. This raises the importance of the battery passport that would enable sorting of different batteries in various forms by providing labels to QR codes or even RFID tags. Scanning of the above-mentioned labels would enable the separation based on different chemistries and battery types[15].

While market penetration predictions of the batteries at 2030 mainly show the dominance of different types of NMC (NMC811, NMC622, NMC900), being followed by LFP, coupled with graphite or some minor SiO_2 anodes, other novel types of batteries are expected to occupy a market share[16].

In this chapter, reviews from different materials involving future batteries are presented with a focus on their availability and criticality. This is to introduce the major materials utilized in future batteries, their supply risk level, and the main precursors. With this in mind, the foundation for determining how material selection influences the circular economy and long-term sustainability of battery technologies is being established.

Although the emergence of future batteries relying only on abundant materials would decrease the raw material risk in terms of material scarcity, there are still environmental aspects to be considered. These motivations for recycling can stem from environmental concerns, either mining or the deposited end-of-life battery contamination of water, soil, and air.

Among different emerging battery types, some have higher Technological Readiness Levels (TRL) and seem promising for commercialization in the near future. Considering this, the focus of the current thesis is on solid-state lithium-ion batteries and liquid electrolyte sodium-ion batteries with high TRL factors.

2.1 Solid-state Batteries

Solid-state batteries (SSBs) are one of the future batteries in the pre-commercialization stage, likely to partially replace market-dominant conventional LIBs in the future. This projection is primarily due to their claimed advantageous features, particularly with higher energy densities, besides greater fire safety. Being a significant development, SSBs may provide improved energy and power densities facilitated by bipolar stacking, along with the utilization of lithium metal or silicon anodes. Further, incorporating solid-state electrolytes (SSEs) may improve safety through the elimination of electrode cross-talk, thereby reducing the chemical interactions that lead to the long-term instability of liquid-electrolyte LIBs. A characteristic of inorganic solid electrolytes is enhanced high charging capability with no electrolyte polarization, hence providing high power density. The mentioned characteristics render solid-state batteries a potential additional future battery, an alternative to traditional LIBs, efficiently solving performance and safety issues of energy storage applications. Although there may be clear advantages of these types of batteries, their commercial feasibility still highly depends on issues related to specific capacity, safety, and finally, the availability of material resources, as well as the costs. Cost not only includes the material but also the scalability, synthesis, and processing[12].

At the level of the cell, considering all internal components of the batteries (including materials, binders, current collectors, housing, poles, and gaskets), a cost comparison shows a comparable commercial potential for SSBs to conventional LIBs. This is because a conventional LIB using NCA ($LiNi_{0.8}Co_{0.15}Al_{0.05}O_2$) with a graphite anode delivers specific energy and energy density of 265 Wh/kg and 635 Wh/L, respectively, and a lithium metal anode SSB can reach 393 Wh/kg and 1143 Wh/L (based on theoretical values). This potential has become so promising that it has initiated progress by leading companies like Samsung, Solid Power, QuantumScape, and Toyota. However, the broad commercialization of SSBs will depend not just on electrochemical advancements relative to LIBs but also on engineering challenges and cost-related factors, as different process units are required for manufacturing[12], [17]. Figure 1 illustrates the main material structures being used in SSBs. As it is shown, the cathode material remains the same as in typical LIBs, while for the solidification of the current LIB batteries, lithium metal anode or silicon can be combined with a wide range of available SSEs[12].

Various types of SSEs have been developed, which can be classified into two main groups: inorganic (e.g. oxides, sulfides, and halides) and organic polymer[18], [19]. While garnet-type (e.g. $Li_{7-y-3x}Al_xLa_3Zr_{2-y}Ta_yO_{12}$) oxide-based SSEs have been the main material discussed in the literature due to their high ionic conductivity, perovskite-type (e.g. $Li_{3x}La_{2/3-x}TiO_3$), NASICON-type (e.g. $Li_{1+x}(Al,Ge)_xTi_{2-x}(PO_4)_3$), and glass-ceramic materials (e.g. LiPON), have also been researched for their electrochemical stability and potential compatibility with lithium metal[20], [21], [22], [23], [24]. The main methods of synthesizing the above-mentioned materials are either through solid-state reactions at high temperatures or solvent-based methods such as sol-gel and spray-pyrolysis, followed by sintering to improve ionic conductivity[25], [26], [27], [28], [29]. Despite the advantages of sintering, the SSB fabrication using these approaches poses challenges such as volumetric changes in the electrode materials, impacting cycling stability. To overcome these drawbacks, studies have been conducted on the creation of hybrid electrolytes, integrating ceramic and polymeric components to achieve mechanical flexibility and superior electrochemical performance[30], [31], [32].

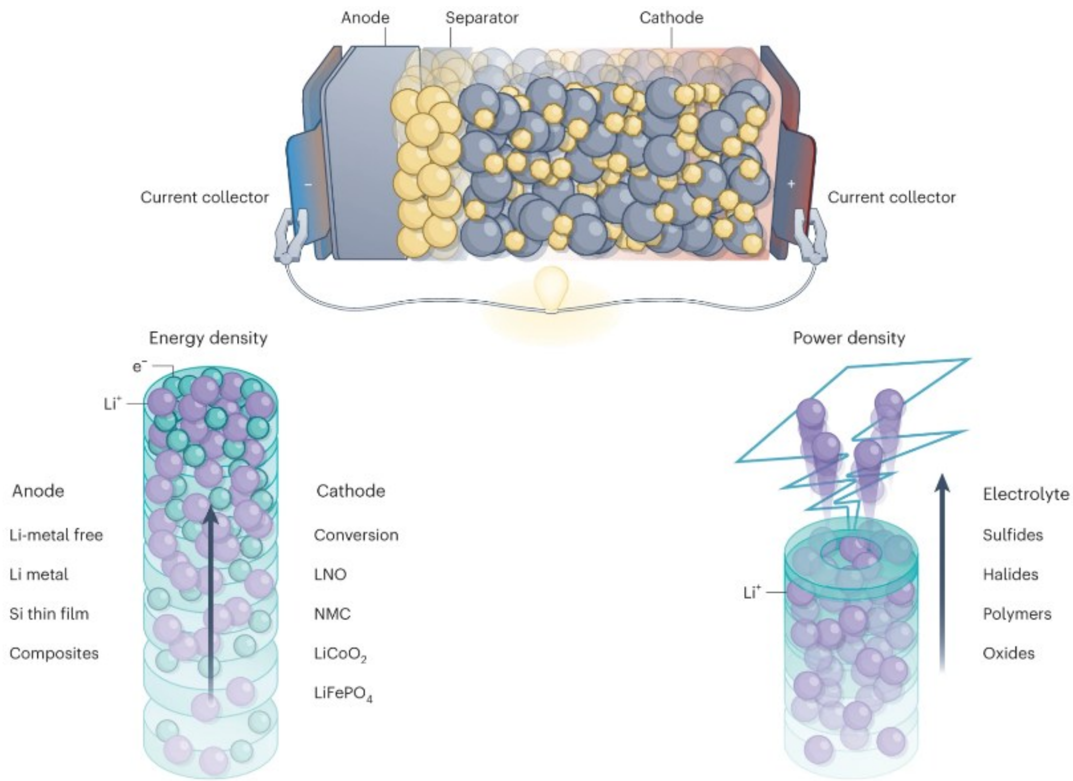

Figure 1. Typical structure of lithium SSB[12]

Figure 2, illustrates a comparative assessment for three different compositions of the electrolyte. As it is obvious, besides the ionic conductivity, chemical stability to both cathode and anode is of importance in SSBs. In this master's thesis, halide-based SSE has also been evaluated as a newly evolved type.

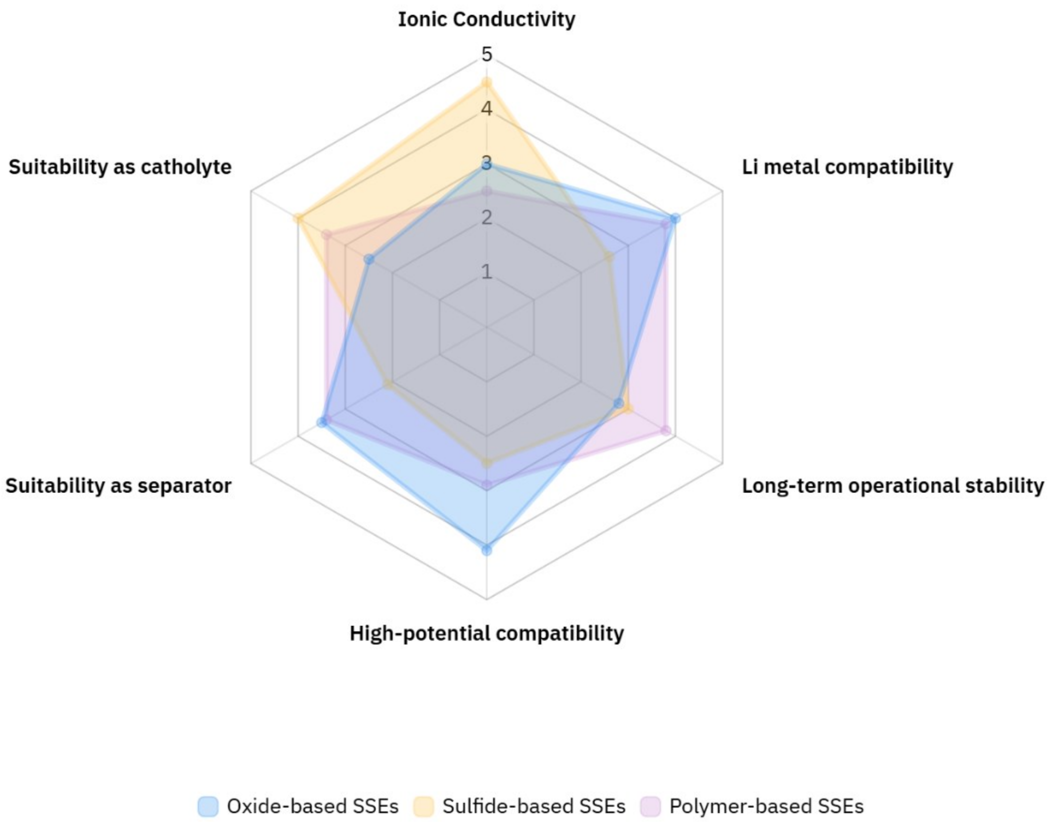

Figure 2. Properties comparison of Oxide/Sulfide, and Polymer-based electrolyte(modified from D. T. Schmaltz, "Solid-State Battery Roadmap 2035+"[33]).

The term solid-state battery refers to the specific all-solid-state battery category. Due to the similar cathode active materials being used as LIBs, the focus of this master's thesis would be the introduction of anode and different electrolytes as the main deviations from traditional LIBs.

2.1.1 Anode

There are different types of SSB designs coupled with different SSEs combined with a wide range of materials, and the mass of these materials can sometimes be different from that of LIB, as their predecessors[34]. Typically, the interface of electrolyte and electrode is of much importance in SSBs. Thus, studies are focused on choosing the most compatible materials. In this regard, various types of anodes have been used, such as lithium, silicon, tin, etc. The most common anode type in the majority of the studies is lithium metal[35]. Particularly due to the implementation of the lithium-based anode and SSEs also containing lithium, the recovery of lithium is more critical[34]. Lithium as a pure metal is very reactive and can oxidise easily, so there are some requirements to reduce the risk of reaction both during the manufacturing and usage[36], as well as recycling.

2.1.2 Oxide-based SSEs

Oxide-based solid electrolytes are a large variety of lithium- and oxygen-containing compounds combined with elements like phosphorus, titanium, aluminum, lanthanum, or zirconium. This category of electrolytes has been investigated with early solid-state rechargeable battery efforts, initially with thin-film batteries in the 1970s. Around 1980, with the invention of lithium-ion batteries, solid oxide batteries with bulk electrolyte layers were researched. Oxide-based solid electrolytes have high mechanical and chemical stability, a wide electrochemical window, and compatibility with lithium metal anodes and high-voltage cathodes. Figure 2, illustrates the properties window of the oxide-based electrolytes. Due to the chemical stability, there are no high processing requirements. Mechanical properties of these electrolytes can also introduce some disadvantages in terms of brittleness and stiffness to the structure. This is an obstacle in terms of industrial manufacturing of these types of batteries, which can be reduced by hybrid SSEs combined with polymers. Also, in order to increase the ionic conductivity, oxide-based solid electrolytes are sintered to the cathode[33], which needs to be considered in the recycling efforts.

Schneider et.al, evaluated the material criticality and the recyclability potential of the garnet-type $Li_7La_3Zr_2O_{12}$(LLZO) SSE as one of the most promising solid electrolytes. Regarding their study, LLZO SSE accounts for above 50 wt% of the cell without considering the housing, followed by the cathode, accounting for roughly 30 wt%. Adding to the complexity, elements such as La and Zr are introduced to the battery cell, as well as Ta, which is the main doping element, while the current LIB battery cells do not contain them[37].

Critical Raw Materials (CRMs) are defined by the European Union as those elements strictly necessary for the EU economy and with a high risk of supply problems. Criticality is evaluated using two primary parameters: Economic Importance (EI), which indicates the contribution of a material to final-use applications, and Supply Risk (SR), which estimates the risk of disruption of supply. The materials with SR ≥ 1 and EI ≥ 2.8 are being classified as CRMs. Moreover, aspects such as the End-of-Life Recycling Input Rate (EoL-RIR, ratio of recycled material replacing primary raw material input within the EU) are also included [38].

In Table 2, the highlighted rows show the critical materials involved in LLZO SSEs. Considering LLZO SSEs, 3 out of 4 elements involved in their structure are being classified as CRMs; thus, there should be a great focus on the recycling of these elements.

Oxide-based solid electrolytes are composed of metals whose oxidation states in their final compounds resemble those found in natural minerals. Regarding the strong metal-oxygen bonding, the electrochemical stability of these materials is high, resistant to reduction and oxidation, even in contact with highly reactive metallic lithium[39], [40]. However, the scarce natural amounts of key oxides like ZrO_2, Ta_2O_5, La_2O_3, TiO_2, and Li_2O have a strong impact on recycling efforts. Significant energy input is required for the reclamation of these materials since the reduction of their oxides to the metallic state is much more energy-intensive than the reduction of first-row transition metals during traditional pyrometallurgical recycling methods[40].

Table 2. EU CRM assessment for Oxide and Sulfide-based SSEs (Data from "Study on the critical Raw Materials for the EU 2023"[37], [38]).

Raw material	Electrolyte	Stage[1]	Supply risk(SR)	Economic importance(EI)	EoL-RIR(%)	Compared to 2020
Germanium	LGPS	Processing	1.8	3.6	2	SR ↓ & EI ↑
Lithium	LLZO,β-Li_3PS_4, Li_6PS_5X, LGPS	Processing	1.9	3.9	0	SR & EI ↑
Light rare Earth elements	LLZO	Processing	3.7	5.9	3	SR ↓ & EI ↑
Phosphorus	β-Li_3PS_4, Li_6PS_5X, LGPS	Processing	3.3	4.7	0	SR ↓ & EI ↑
Sulfur	β-Li_3PS_4, Li_6PS_5X, LGPS	Processing	0.3	5.0	0	EI ↑
Tantalum	LLZO	Extraction	1.3	4.8	3	SR ↓ & EI ↑
Tin	LGPS	Processing	0.9	4.5	31	EI ↑
Zirconium	LLZO	Extraction	0.8	3.5	12	EI ↑

1) The stage refers to the material stage within the life cycle at which the criticality assessment has been performed. The extraction stage concerns mining, while the processing stage concerns refinement.

2.1.3 Sulfide-based SSEs

Research on sulfide-based SSEs has attracted much attention for next-generation energy storage systems, such as SSBs[40]. Their excellent performance stems from the high polarizability of sulfur atoms and the softness of the material, which together reduce interactions with Li-ions and enhance ionic mobility[41]. The softness and plasticity also improve processability and electrode interface quality. They may be produced through cold pressing or calendaring at high pressure, avoiding costly high-temperature sintering.

These processing pathways also yield dense, low-grain boundary resistant layers, improving electrode contact and inhibiting dendrite growth. Unlike fragile oxides, sulfides are more tolerant of volume change upon cycling, further facilitating their deployment in next-generation solid-state battery designs[33].

Thiophosphate-based electrolytes (e.g. β-Li_3PS_4), argyrodite-type compounds (Li_6PS_5X, where X = Cl, Br, I), and $Li_{10}GeP_2S_{12}$ (LGPS), which are the three classes of materials currently under consideration as sulfide-based SSBs[42], [43], [44]. These materials share the common characteristic that their synthesis depends on sulfide precursors (Li_2S, P_2S_5, GeS_2, SnS_2) and lithium halides (LiX, X = Cl, Br, I). These types of sulfides are not common in nature, and their chemical transformation processes pose supply constraints. In contrast to oxide-based electrolytes, which are usually extracted from nature, the precursors of sulfide-based SSE can only be prepared by chemical synthesis from their elemental species like Li, P, Sn, Ge, and S. This can be accomplished by the reaction of the elemental sulfur and elemental Li, P, Ge, Sn, or their oxides (e.g. GeO_2) with H_2S[40].

As it is demonstrated in Table 2, all of the listed elements, except for sulfur and tin, are being categorized in the EU CRMs list. Same as oxide-based electrolytes, the incremental reliance on lithium sources (expanding the lithium dependence from cathode to electrode and anode) exacerbates the material scarcity caused by LIBs.

Development of sulfide-based SSEs was triggered with Li_2S-SiS_2 systems in the 1980s[45]. Weak bonds between lithium and sulfur elements have been reported as the main reason for the free movement of lithium ions and contributing to high conductivity. Although the softness and mechanical flexibility of sulfide-based SSEs over their oxide counterparts provide a higher compatibility of cathode/electrolyte, their chemical instability in contact with humidity raises safety concerns in the manufacturing and recycling processes[41].

Sulfur is a non-critical material that can be obtained from natural sources or as a by-product of other industries. The criticality of sulfide-based SSEs is primarily driven by concerns regarding the availability and supply chain vulnerabilities of other involved materials: Li, P, Ge, and Sn. Lithium, phosphorus, germanium, and tin are more limited as they are primarily extracted from unique mineral ores or widely used in industrial processes. Extracting such materials typically requires heating them to high temperatures (e.g., phosphorus from apatite-based minerals), followed by chemical processing (e.g., metallic lithium can be recovered from lithium chloride electrolysis). The energy-intensive extraction and synthesis routes also highlight the importance of evaluating their long-term sustainability and economic consequences in the context of the next-generation solid-state battery[40].

2.1.4 Halide-based SSEs

For decades, halide-based electrolytes have been known for their high ionic conductivity. Nevertheless, this was limited to high operating temperatures[46]. For example, the $LiAlCl_4$ spinel type, developed in 1976, couldn't illustrate high ionic conductivity at room temperature[47]. Only in 2018 did Asano et al. develop a room temperature operating, high conductivity trigonal Li_3YCl_6 and monoclinic Li_3YBr_6[48].

The high conductivity and good chemical stability of the halides have recently made them another alternative for SSBs[49], which provides potential with the combination of an uncoated cathode[50], and can positively affect the recyclability potential[34]. The instability of halides in contact with moisture and the ion-exchanging feature might add complexity to their recycling processes[49].

The crystallographic structure of metal halide is in the form of Li_3MX_6 (M = trivalent rare earth metal, X = F, Cl, Br, and I). There are three main production routes for halide-based SSEs; mechanochemical synthesis[51], comelting[52], and wet-chemistry[53]. The chosen production method can affect the particle size distribution, crystallinity, and ionic conductivity. Besides these factors, scalability, cost-effectiveness, and environmental impact can affect the selected production process[49].

Raw material	Electro-lyte	Stage1	Supply risk (SR)	Economic importance (EI)	EoL RIR (%)	Compared to 2020
Aluminium	Li_3AlF_6	Extraction	1.1	5.5	32	SR & EI ↑
Gallium	Li_3GaF_6	Pro-cessing	3.9	3.7	0	SR & EI ↑
Heavy REEs	Li_3YCl_6, Li_3YBr_6 Li_3HoCl_6, Li_3HoBr_6 Li_3ErCl_6, Li_3ErI_6,	Pro-cessing	5.1	4.2	1	SR ↓ & EI ↑
Indium	Li_3InCl_6 ,Li_3InBr_6	Pro-cessing	0.6	2.6	1	SR & EI ↓
Lithium	LLZO,β-Li_3PS_4, Li_6PS_5X LGPS	Pro-cessing	1.9	3.9	0	SR & EI ↑
Light REEs	Li_3LaI_6,	Pro-cessing	3.7	5.9	3	SR ↓ & EI ↑
PGMs	Li_3IrBr_6	Pro-cessing	2.7	7.1	12	SR & EI ↑
Scandium	Li_3ScCl_6, $LiSc_{2/3}Cl_4$	Pro-cessing	2.4	3.7	0	SR & EI ↓

The material requisition of halide-based SSEs needs to be considered thoroughly due to the insertion of rare earth elements with high costs and low availability. Considering the cobalt price (~33.34 $/kg, LME July 2025[54]) as a reference, most trivalent metals are significantly more expensive than cobalt (for example, holmium's price is ~ $65.165/kg, metal July 2025[55]), except for a few (Y, Eu, Gd, Er, Yb, Sn, La, and Ce). Also, the less expensive metals are still not abundant materials in the Earth's crust[49]. As it is illustrated in

Table 3, rather than Indium, all of the elements in the structure of halide-based SSEs are categorized as CRM list of EU, which emphasizes the necessity for recycling and circular economic design in SSB batteries.

2.1.5 Polymer-based SSEs

Although the inorganic solid-state electrolytes (oxide, sulfide, and halide-based SSEs) exhibit better performance in terms of ionic conductivity, combined with safety[56], [57], organic-based electrolytes improve electrode compatibility, cost-effectiveness, and durability, and environmentally friendly structure. These, in turn, position polymer-based SSEs as potential candidates for storing energy on a large scale[58], [59], [60].

Unlike inorganic solid electrolytes, solid polymer electrolytes not only minimize safety issues arising from lithium dendrite growth but also exhibit greater adhesion and cohesion, resulting in improved electrode-electrolyte interface compatibility[56].

Table 3. EU CRM assessment for halide-based SSEs (Data from "Study on the critical Raw Materials for the EU 2023"[38]).

Raw material	Electro-lyte	Stage[1]	Supply risk (SR)	Economic importance (EI)	EoL RIR (%)	Compared to 2020
Aluminium	Li_3AlF_6	Extraction	1.1	5.5	32	SR & EI ↑
Gallium	Li_3GaF_6	Pro-cessing	3.9	3.7	0	SR & EI ↑
Heavy REEs	Li_3YCl_6, Li_3YBr_6 Li_3HoCl_6, Li_3HoBr_6 Li_3ErCl_6, Li_3ErI_6,	Pro-cessing	5.1	4.2	1	SR ↓ & EI ↑
Indium	Li_3InCl_6 ,Li_3InBr_6	Pro-cessing	0.6	2.6	1	SR & EI ↓
Lithium	LLZO,β-Li_3PS_4, Li_6PS_5X LGPS	Pro-cessing	1.9	3.9	0	SR & EI ↑
Light REEs	Li_3LaI_6,	Pro-cessing	3.7	5.9	3	SR ↓ & EI ↑
PGMs	Li_3IrBr_6	Pro-cessing	2.7	7.1	12	SR & EI ↑
Scandium	Li_3ScCl_6, $LiSc_{2/3}Cl_4$	Pro-cessing	2.4	3.7	0	SR & EI ↓

Solid polymer electrolytes were found in 1975 when Wright studied the ionic conductivity of metal salt complexes of polyethylene oxide (PEO)[57]. This was then preceded by Armand et al.'s proposal that mixtures of polymer and salts are utilized as solid electrolytes for electrochemical devices[58], which caused the rise of an increasing amount of research in this area. Standard polymer electrolytes being applied presently include PEO, polyvinylidene difluoride (PVDF), polyvinylidene fluoride-co-hexafluoropropylene (PVDF-HFP), polymethylmethacrylate (PMMA), and polyacrylonitrile (PAN). These materials have gained interest for their flexibility, low flammability, improved safety, and stable electrode interface. One of the largest limitations of solid polymer electrolytes is their comparatively lower ionic conductivity than inorganic SSEs and traditional liquid electrolytes, which presently hinders their broad commercialization[56].

Polymer-based SSEs are mainly composed of a Li-ion salt being added to the aforementioned polymeric hosts. Ceramic fillers are added to the polymer composites to increase the ionic conductivity of the material, such as $LiAlO_2$, Al_2O_3, SiO_2 or LLZO. The source of carbon in the monomers of these polymeric hosts in the SSEs determines the sustainability of the material. This can be considered in the recovery and recycling of the material[40].

Achieving simultaneous enhancement of electrochemical as well as mechanical solid-state electrolyte properties is a significant challenge. As a trial to satisfy this demand, composite solid-state electrolytes (CSSEs) that combine the benefits of both inorganic materials as well as polymers are gaining attention[56]. CSSEs have traditionally been categorized into two broad classes: polymer-based and ceramic-based solid electrolytes[59]. Ceramic-based CSSEs have been found to be non-flammable, along with a strong dendrite growth inhibitor for lithium. However, despite these advantages, high ceramics content CSSEs implementation are still limited by challenges in the production methods, and extensive scientific research in the area is needed[56].

Overall, considering all types of SSEs, Figure 3 depicts the share of the global supply of fundamental materials requisite for the extraction (E) and processing (P) stages of solid-state electrolytes (SSEs) manufacturing. Even though tin is regarded as non-critical in the EU's CRM 2023 report, its processing is shown to be highly reliant on non-EU territories. The figure highlights the geopolitical dependencies in the SSB supply chain, emphasizing the growing need to take actions towards materials recycling, substitution, and local processing for economic and enduring sustainability.

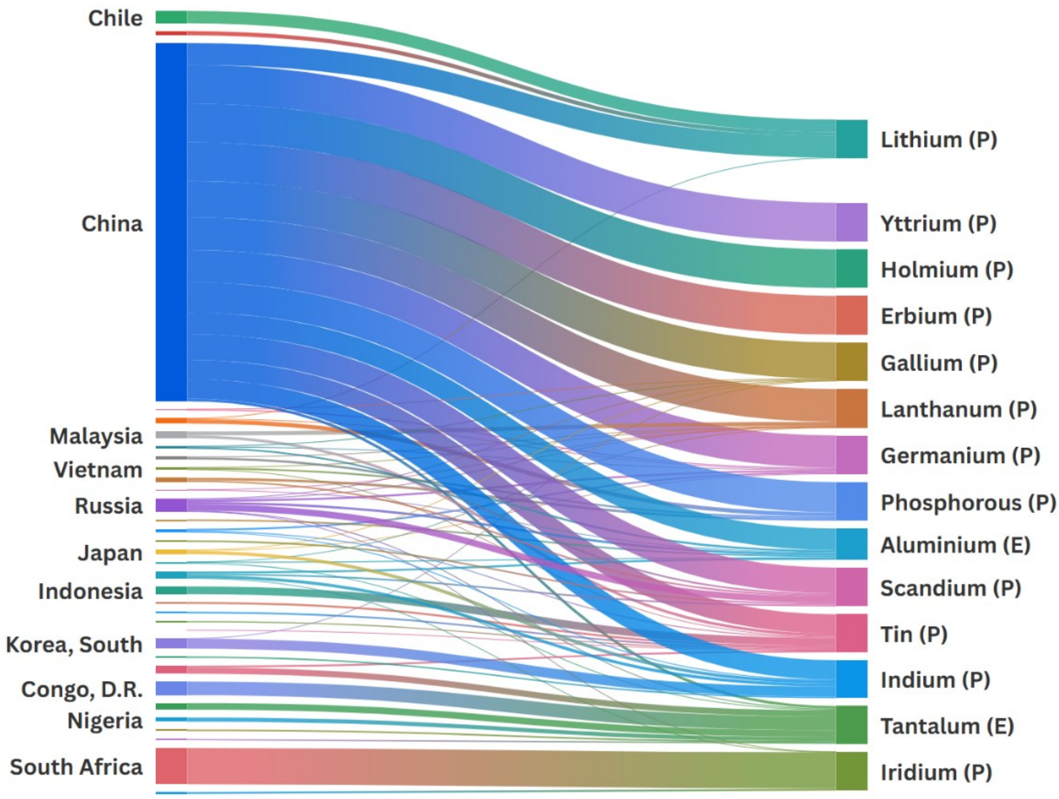

Figure 3. Global Supply share of materials involved in SSE (P = Processing, E = Extraction)(Data from "Study on the critical Raw Materials for the EU 2023"[38]).

Generally, environmental drawbacks stem from the mining and material scarcity of elements such as lithium, cobalt, and nickel, which compose the cathode materials and elements involved in SSEs. Furthermore, production of SSBs is being considered highly energy-intensive due to the sintering process being used for electrolyte production[16], [60]. The main advantage of SSBs is related to the end user phase, where these next-generation batteries with higher energy density, higher efficiency, and longer life span require a lower rate of replacement. This results in lower raw material usage, hand in hand with lower energy demand for the production itself[61], [62].

Figure 4, illustrates the comparative composition for LIB of a conventional NMC811 cell structure containing electrolyte, separator, current collectors, and binders. The structure of SSB contains a 5 μm thick metallic lithium anode, coupled with NMC811 cathode and 10 μm thick solid electrolyte (cathode: electrolyte volumetric ratio of 3:1). Copper is the current collector on the anode side with the thickness of 8 μm and aluminium as the current collector for cathode side with the thickness of 10 μm for both LIB and SSBs. In each of the SSE categories, one specific composition is being considered as the reference: PEO/LiTFSI for Polymer SSE, 10% $Li_{1.3}Al_{0.3}Ti_{1.7}(PO_4)_3$(LATP) filler in the PEO/LiTFSI hybrid SSE, Li_6PS_5Cl for sulfide SSE, Li_3InCl_6 for halide SSE, and for LATP oxide type, a cover layer of LLZO due to its instability in contact with the lithium anode[34].

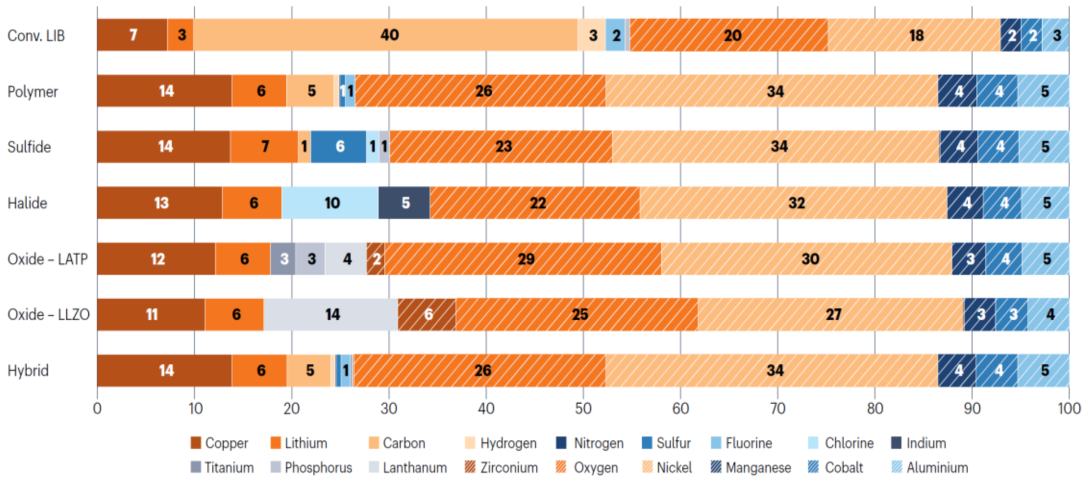

Figure 4. Comparative composition for LIB and different SSBs (%wt) for the theoretical capacity of 200 mAh g^{-1}[34].

Figure 4 indicates that SSBs are shifting the battery sector to more metal-dominant content with more complex chemistries. Compared to conventional LIBs, SSBs involve a broader range of elements, such as critical raw materials (CRMs) and even rare earth elements, as mentioned before, making sourcing and recyclability more complex. On the positive side, SSBs reduce carbon content and eliminate fluorine, which can be environmentally friendly and reduce emissions. However, the increased elemental diversity has major implications for cost, materials supply risk, and recycling practices, all of which need to be explored further to facilitate sustainable scaling of next-generation batteries.

2.2 Sodium-ion batteries

The three main criteria for a compatible energy storage solution are price of the stored energy (\$ $Wh^{-1}kg^{-1}$), lifetime (cycle life or years), and power (W kg^{-1})[63]. In the previous section, a future technology that aims to cover the enhancement in lifetime and energy efficiency has been assessed, while in this section, another main focus of future technologies related to cost reductions is being evaluated. For this purpose, reliance on abundant materials will not only reduce the cost of batteries but also can effect the environmental and geopolitical concerns.

Sodium is one of the elements with reserves that can be considered infinite globally. The first sparks of sodium ion batteries (SIBs) started with Faraday's observations on analysing the ionic conductivity with high-temperature solid state electrolyte (PbF_2 and Ag_2S) in 1839. With this inspiration, other researchers started focusing on the ionic conductivity of Na^+. Ford company was one of the early adopters looking for sodium-sulfur battery (NaS) in the late 1960s. This cell was operating at 300-350°C, and the main issue with this technology was related to the dense sintering of β-Al_2O_3 as a solid electrolyte, which indeed needs to show high temperature resistance in a reactive condition. With the emergence of the rocking chair battery concept and, further on, Sony commercializing the LIB, the focus of the research shifted toward LIBs. This, in turn, caused a delay in the development of the SIBs, while since 2008, an increasing number of researchers have focused on SIBs as a potential alternative for LIBs[63]. It is being predicted that the market share of SIBs would increase and potentially reach a yearly demand of 500 GWh by 2030[10].

There are different types of sodium batteries implementing the sodium ion technology in the main structure. Sodium metal batteries, Sodium-ion batteries (SIBs), all solid-state sodium metal batteries, Na-S, and Na-O_2 are types that may benefit from sustainable production in the precursors, secure supply of the raw materials, and, specifically, low cost[6]. SIBs are one of the most viable alternatives among the mentioned sodium-based types for next-generation batteries due to their similar design and operational mechanism to LIBs[10]. SIBs include a cathode with a sodium composition, a solid anode free from sodium and mainly carbon-based structure (such as hard carbon material), and an electrolyte, which is typically in a liquid state[64]. Figure 5 illustrates different structures of the above-mentioned sodium-based batteries.

The structure of the cathode is an important factor in the performance of SIBs, in terms of providing sodium ions and voltage. There are various types of cathode materials for SIBs, such as layered metal oxides, polyanionic compounds, Prussian blue analogous (PBAs), and organic compounds[65].

Just like LIBs, the electrochemical process of intercalation and deintercalation of ions between the cathode and anode governs the corresponding charge/discharge cycles, with sodium ions instead of lithium ions. Due to the larger ionic radius and higher atomic weight of sodium compared to lithium, different challenges are being introduced to the battery structure. Regarding these properties, graphite becomes an incompatible choice for integration into SIBs as the ions can get trapped or can cause mechanical stress to the structure, and hard carbon is instead being used as the anode[66], [67]. Thus, the material selection and battery design optimization, along with the proper ion transport, have recently been the main focus of research on SIBs[68].

On the other hand, lithium and sodium are both elements of the first group in the periodic table, so they share many features. Both of them have a single electron in their valence shell that is readily interacting in the vicinity of other elements, donating the electron and turning into an ionic form. In other words, both have very high reactive features[66].

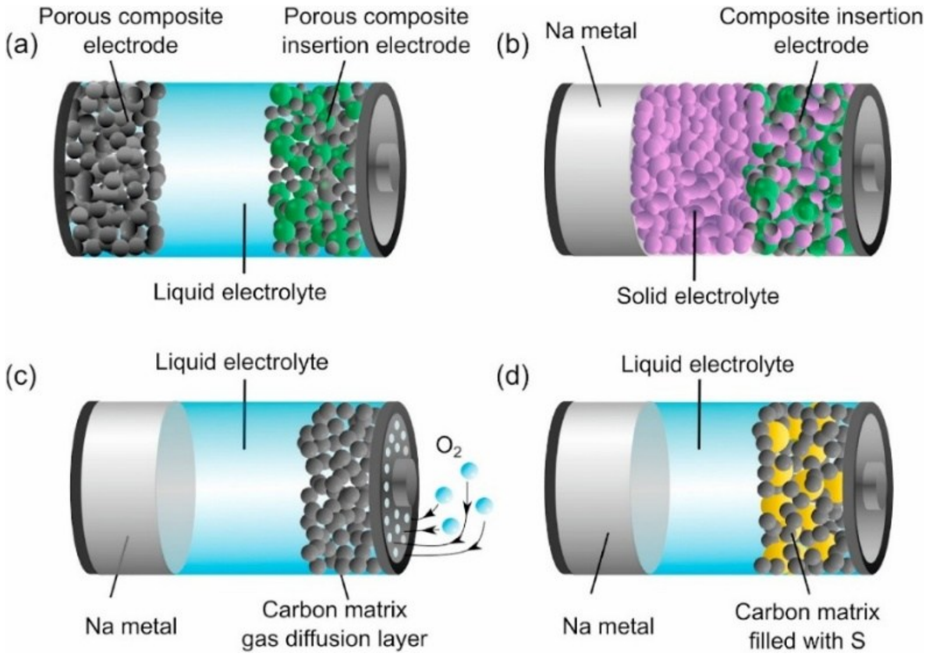

Figure 5. Schematic illustration of the common architectures of sodium-based batteries: (a) sodium-ion battery (SIB); (b) all-solid-state sodium battery with sodium metal anode; (c) Na/O2 battery (d) Na/S battery[64].

Similar to the development of the materials from the $LiCoO_2$ to polyanion $LiFePO_4$, sodium ion-based technology is mimicking the same patterns in the research, such as Na_xCoO_2, $NaFePO_4$, or ternary sodium layered oxides[69], [70]. For both solid and liquid electrolytes, the same electrolyte types of LIB can be used, with the replacement of the lithium ion with sodium ion. Similar to the basic structure of sodium ion batteries resembling the LIBs, the cell formats also follow the same patterns (pouch, cylindrical, and prismatic). These similarities in the main structures provide a great potential for the LIB production infrastructure to be used in SIBs as well. Thus, SIBs can benefit from existing plants for their scaling up to get accelerated[66].

2.2.1 Cathode

Cathode materials in SIBs can vary from layered metal oxides to polyanions and Prussian blue analogous, all consisting of inexpensive elements[10]. The basic characteristic of sodium metal oxides is in the form of $NaTMO_2$, in which TM represents the transition metals in the structure, like Ti, Ni, Cu, Mn, and Fe[71]. The manufacturing of these layered metal oxides will have several advantages due to the similarity of the sodium metal oxide with their predecessors in LIBs, such as $LiCoO_2$ and $LiNi_{0.33}Co_{0.33}Mn_{0.33}O_2$ (NMC111). While Faradion and TerraPower are implementing $NaNi_{0.33}Fe_{0.33}Mn_{0.33}O_2$, Hina Battery is using $Na_{0.9}Cu_{0.22}Fe_{0.3}Mn_{0.48}O_2$[10].

One of the most important factors in assessing SIB cathode materials is their chemical instability in contact with air and/or water. This is mainly due to the intrinsic characteristics of sodium with high alkalinity, large ionic radius, and hydrophilic potential of sodium salt, compared to lithium[62]. For instance, layered transition metal oxides have a higher tendency to react with moisture and carbon dioxide than their lithium counterparts. These cause structural damage through Na^+/H^+ exchange and surface complexation using compounds such as NaOH, Na_2CO_3, and $NaHCO_3$[63], which need to be considered in terms of integrating into the recycling processes.

Another type of cathode material is polyanion cathodes with a stable structure, high ionic conductivity, and high cycling life. This type of cathode material is comparable to $LiFePO_4$ in LIBs. Due to the proven stability of over 10,000 cycles for $Na_3V_2(PO_4)_3$ (Nasicon) and $NaVPO_4F$, various companies have been looking to commercialize batteries using polyanions, such as Guangzhou Great Power Energy & Technology[10].

While polyanionic compounds are readily acknowledged as being more stable due to their three-dimensional covalent frameworks, they can undergo strong moisture absorption. For example, $Na_2Fe_2(SO_4)_3$, when exposed to moisture in the air, forms $Na_2Fe(SO_4)_2 \cdot 4H_2O$ hydrate[64].

Cathode materials with prussian blue analogous containing the structure of $(Na_xM_a[M_b(CN)_6]$, where M_a and M_b stand for transition metals, have demonstrated faster charging patterns with higher ion diffusion. This is mainly because of their 3D Na^+ channels and higher stability[72]. CATL and Natron Energy are two of the companies working on the commercialization of batteries using Prussian blue technology in cathode materials[10].

Analogous of Prussian blue shows its own unique feature of significant hygroscopicity. Water molecules may exist in different forms, incorporated into the crystal lattice, residing in interstitial positions, or adsorbed to a surface, which in turn changes their electrochemical activity[65]. In general, compared to LIBs, SIB cathode active material shows higher sensitivity to air due to the tendency to react with water[59].

2.2.2 Anode, Electrolyte, and Other Parts

While the typical anode for LIB is graphite, its structure is not proper for SIBs due to the differences in lithium and sodium ions[73]. Prevention of intercalation and deintercalation of sodium ions to the packed layer structure of graphite causes irreversible ion transfer, reducing the cycle life, and causing capacity decay. Hard and soft carbon are being used in commercialized SIBs. It is foreseen that in the future, sodium alloys or sodium metal can be used, similar to silicon and lithium metal in LIBs[74].

SIBs use the same organic solvents based on liquid electrolytes as LIBs, a combination of ethylene carbonate, dimethyl carbonate, ethyl methyl carbonate, propylene carbonate, fluoroethylene carbonate, and/or vinyl carbonate[75], with $LiPF_6$ being replaced by $NaPF_6$[10].

Except for the binders and current collectors, the same shell, conductive agents, and separators as LIBs are being used in SIBs, too. The common binder for SIBs is PVDF for both electrodes, while in LIBs, it is only used for cathode materials, and sodium carboxymethyl cellulose/styrene-butadiene rubber is being used for the anode. Current collectors of SIBs can be made of aluminum for both of the electrodes, while for LIBs, Cu is being implemented in the anode. Although SIBs utilize a safer and more environmentally friendly alternative to lithium-ion batteries from the perspective of material availability and cost, they still contain toxic or flammable substances. Specifically, SIBs consist of ca. 13 wt.% flammable materials, 26 wt.% carbon-containing components, and ca. 1.4 mol kg^{-1} fluorine-containing compounds[10].

If SIB wastes are disposed of improperly, considering landfilling or incineration, they would pose severe fire hazards, result in a high carbon footprint, and release toxic substances, causing risks to the environment and human health. Therefore, recycling technologies need to be implemented at this early stage of SIB commercialization. These actions will not only minimize environmental and safety risks but also help optimize SIB material systems and create a more sustainable, circular battery value chain in the future[76]. Thus, the focus on recovering elements involved in current collectors (aluminum), binders, and electrolytes, which are not being targeted for LIB recycling at the moment, can be considered in recycling methods of these batteries. But how a low economic potential can cover the gap for the feasibility of the SIBs recycling is still a case that needs to be investigated.

3 Recycling Technologies and Future Batteries' Recyclability

Considering a LIB cell as the market-dominant battery type, the cathode material, which stands for the highest economic value, is around 40% of the whole battery cell weight[77]. The main target of the recycling plants is the recovery of the most valuable elements (e.g. Li, Co, Ni, …)[15]. For this purpose, different methods based on pyrometallurgy, hydrometallurgy, and direct recycling have been developed so far, in which some pyrometallurgical and hydrometallurgical processes have already been commercialized, while direct recycling methods are still under further investigation[40]. Figure 6, illustrates the general recycling units.

Prior to any recycling process, pre-treatment activities such as discharging and dismantling of battery packs and modules are required for any type of battery cell[78]. Discharging with thermal, chemical, or electrochemical processes is carried out in order to minimize safety risks such as electric shock, fire, explosion, or chemical exposure from the organic liquid electrolyte[79]. Dismantling then follows, where mechanical processes are employed to remove current collectors (e.g., Cu and Al foil), separators, and electrode materials based on properties like hydrophobicity, hydrophilicity, and density[78]. Various techniques can be employed to recycle and recover cathode active material from used lithium-ion batteries[40].

Chains of battery recycling processes, such as the resynthesis and reconditioning of active material, are still at the development stage[80]. These process cycles employ different combinations of mechanical, thermal, hydrometallurgical, and pyrometallurgical processes, each having its respective pros and cons[81]. Recycling can be generally classified into indirect processes, which decompose functional materials into their elemental precursors, and direct processes, which maintain the material's crystal structure at the functional level[34]. The effectiveness of recycling and subsequent resynthesis technology depends on factors such as recycling levels, cost-efficiency, and quality of reclaimed secondary materials[15], [81].

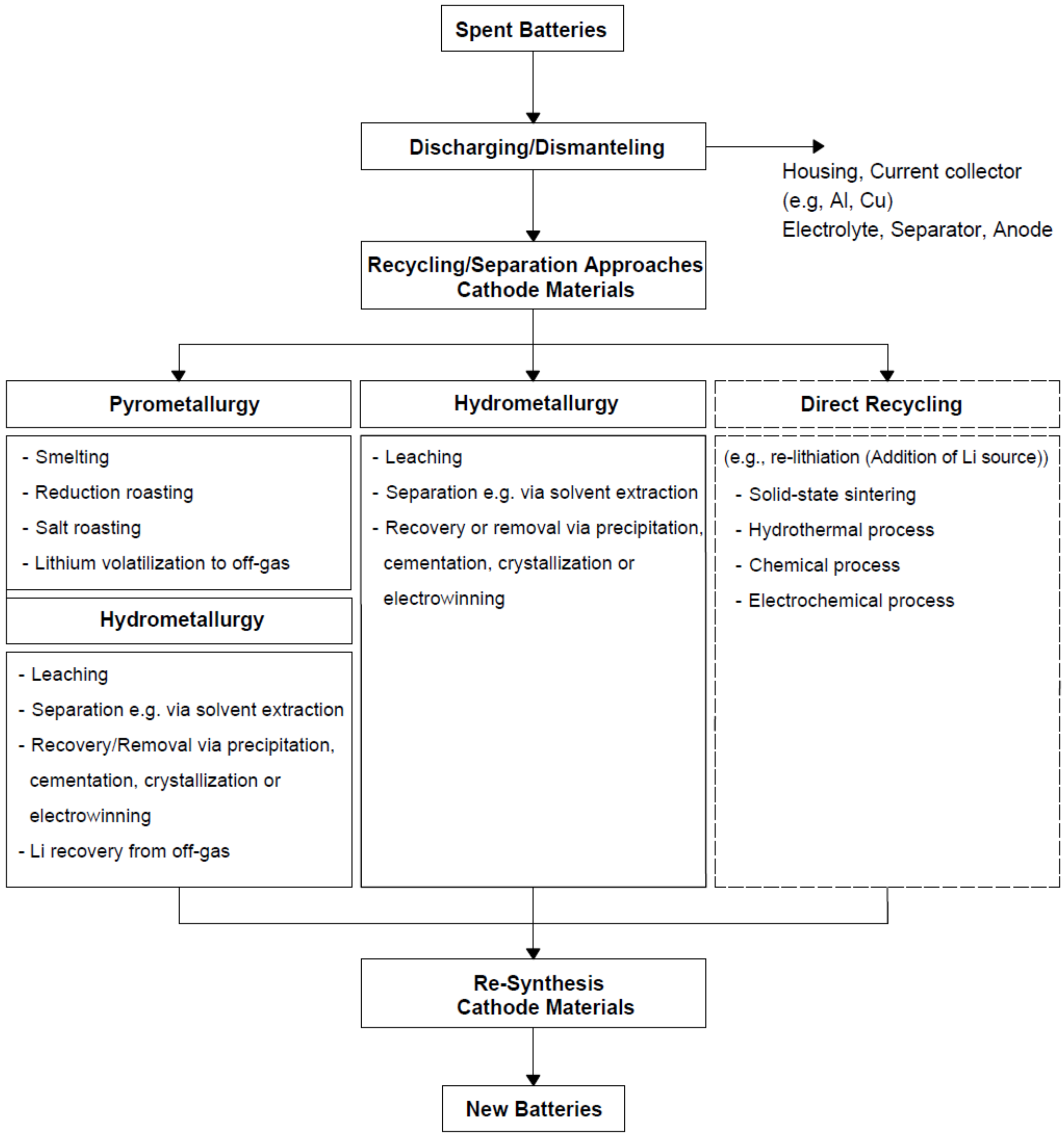

Figure 6. Generalized schematic illustrating key recycling pathways for spent batteries. Pyrometallurgical and hydrometallurgical recycling are industrially feasible recycling routes (high TRL). Direct recycling is not mature technology (low TRL)[2], [40], [82], [83].

To ensure that composite cathode materials enter recycling streams with minimal impurities, selective material separation is required. Since solid-state batteries (SSBs) employ nearly identical cathodes as lithium-ion batteries (LIBs), existing recycling methods, direct recycling, resynthesis, and reconditioning are still valid. However, protective coatings over cathodes, including $LiNbO_3$, ZrO_2, Al_2O_3, SiO_2, $LiTaO_3$, Li_2SiO_3, and Li_3PO_4, introduce additional material types, complicating recycling[82]. After initial separation steps such as discharging and disassembling, SSB's black mass would contain both CAM and SSE particles[40]. This increases the complexity of the materials to be integrated into the recycling plants.

Although the economic motivation for recycling SIBs is lower due to their reduced battery value, the initial focus should be on recovering the cathode active material (CAM), followed by anode and electrolyte recovery in subsequent steps. Among the various CAM types in SIBs, layered metal oxides (Na_xTMO_2) share similar compositions with their LIB counterparts[10]. This similarity increases the feasibility of integrating SIB recycling into existing LIB processes, while also enabling assessment of recovery efficiency, required process adaptations, material degradation, and potential contamination from precious material recovery.

3.1 Hydrometallurgical Recycling

Hydrometallurgy refers to the chemical process of extraction that involves leaching or dissolution of powder forms of substances (in case of battery recycling, “black mass”) followed by solution purification unit processes (e.g. via cementation or precipitation), separation processes (e.g. solvent extraction) and recovery unit processes via precipitation, crystallization, reduction or electrowinning for single-element or high-purity salt recovery. Leaching is most commonly carried out by using sulfuric acid (H_2SO_4) or hydrochloric acid (HCl), respectively. Other acids, such as nitric acid (HNO_3) or phosphoric acid (H_3PO_4), and different organic acids such as citric acid ($C_6H_8O_7$) and acetic acid ($C_2H_4O_2$) have also been studied in scientific literature [83], [84], [85], [86]. To improve leaching efficiency for a specific electrode material containing transition metals, redox-active agents like hydrogen peroxide (H_2O_2) (reductant) and sodium bisulfite ($NaHSO_3$) (reductant) are added to enhance dissolution of transition metal oxides from Li-ion battery waste, e.g., Co^{3+}

present in the LCO or NMC material needs to be reduced to Co^{2+} to enable dissolution [87], [88].

In addition, alkali leaching with ammonia may enable selective extraction of battery metals, due to the fact that it prefers the formation of stable metal ammonia complexes (Ni, Co). This may potentially simplify the process by reducing the number of precipitation and purification steps [89], [90], [91]. Sodium hydroxide (NaOH), sodium carbonate (Na_2CO_3), and sodium phosphate (Na_3PO_4) allow the precipitation/crystallization of transition metals as hydroxides, carbonates, or phosphates, respectively, depending on the specific pH conditions used[89], [90], [91], [92].

The main advantages of hydrometallurgical recycling have been reported as high element recovery rates, making it an alternative and/or complementary process to pyrometallurgical processes[93]. Challenges still exist, such as co-precipitation issues arising from the common solution chemistry of Fe, Co, and Mn, which can complicate the element separation. Certain reaction pathways can also produce gas emissions, such as chlorine (Cl_2) and nitrogen oxides (NO_x), which require proper containment and management. Another significant issue is aqueous waste treatment, since hydrometallurgical processing creates a large quantity of liquid residue that needs to be treated safely[94]. Also, high environmental load of solvent extraction and neutralization chemicals may challenge the hydrometallurgical operations[95].

Different industrial recycling plants are operating around Europe. One of the emerging hydrometallurgical recycling processes has been implemented by LithoRec, Germany. By combining different recycling approaches from mechanical and electrical to thermal and hydrometallurgical methods, this plant has been specifically designed to recover the NMC cathode material for LIBs[2]. Overall, recycling efficiency has been reported being 75-80% of battery mass, while the potential for graphite recycling has also been suggested[2], [96]. There is also increasing interest towards electrolyte salt removal, on the method studied on lab scale. Initial mechanical pretreatment starts with discharging and manual disassembly, followed by crushing and electrolyte extraction using CO_2. Different steps of crushing, air classification, and sieving are implemented to recover the steel and Al casing, besides light plastic particles, Cu, and Al foils. The extracted black mass is then fed to the hydrometallurgical treatment. The hydrometallurgical treatment is designed based on the co-precipitation of Ni, Co, and Mn in the form of hydroxides and Li_2CO_3. These precursors then get sintered to form NMC powder[2].

Figure 7, illustrates the hydrometallurgical recycling flow sheet for LithoRec. In this master's thesis, the leaching condition of LithoRec has been considered for the integration potential of different components of emerging battery types, and recommended steps for the separation of the CRMs have been investigated from literature sources. Figure 7 shows no separation (solvent extraction) for single transition metals, indicating that solution purification via impurity removal should be of high level in order to reach battery purity in co-precipitation stage. Alternatively, intermediates could be further purified by other operators.

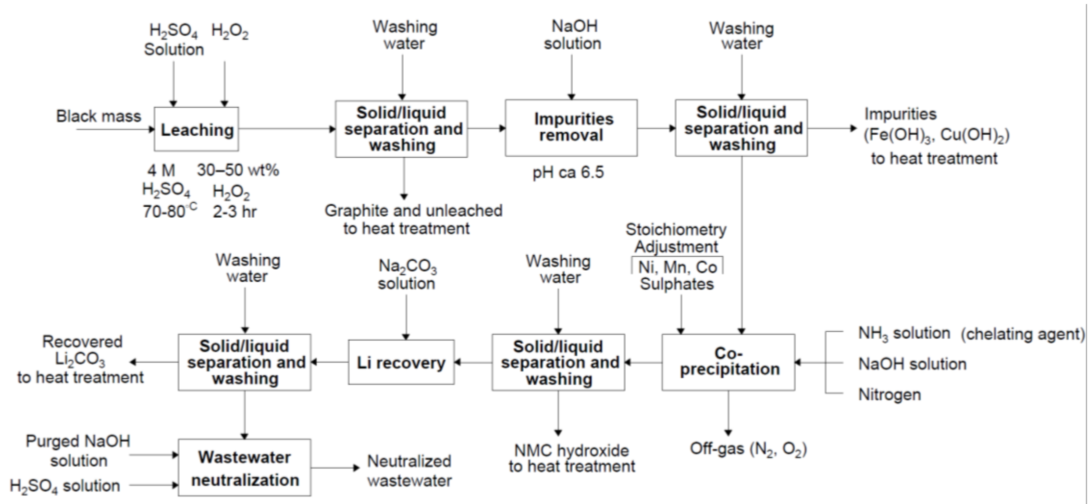

Figure 7. LithoRec hydrometallurgical recycling flow sheet[2].

3.1.1 Hydrometallurgical Recyclability of Oxide-based SSBs

Understanding the degradation pattern of SSBs is essential for an efficient and safe integration into the recycling methods. SSBs would generally reach the end of their useful life following degradation mechanisms associated with the interface between the solid electrolyte and electrode. Many mechanisms may exist, including the existence of a space charge region, interdiffusion of elements, and electrochemical shocks on the interfaces of the active materials and electrolyte[97], [98]. The SSE layer may experience cracking and voiding because of volume changes that accompany the cathode on electrochemical cycling, and thereby experience degradation in the ionic conductivity of the cell[99]. Besides, SSEs cannot effectively prohibit the growth of lithium dendrites, which have the potential to grow along grain boundaries and lead to internal short circuits[100].

Although the disassembly and discharge process of solid-state battery (SSB) is similar to that of lithium-ion batteries (LIBs), there are structural differences in their design that generate new challenges and opportunities in recycling. The differences follow largely from anode designs and the use of solid instead of liquid electrolytes. As mentioned before, various SSB anode designs exist, and lithium metal and, to some extent, silicon-based anodes are highly reactive, an issue that must be addressed at an early stage of recycling. Mechanical separation is impossible due to adhesive properties, especially for the lithium foil, excluding its direct reuse. Hydrometallurgical pathways involving solvents or acids have a potential solution, allowing recovery of lithium as a salt compound, e.g., Li_2CO_3, with secondary lithium metal reprocessing prospects [101], [102].

Utilization of lithium metal anodes enhances cell energy density, while presenting challenges in recycling due to potential internal short circuits within modules, leading to significant residual lithium that complicates mechanical separation methods and poses safety hazards due to its reactivity in non-ideal environments. Even conventional lithium-ion batteries, despite not employing lithium metal anodes, have historically presented safety hazards owing to their intrinsic reactivity, with numerous incidents arising from the accumulation of substantial lithium-ion battery waste over the last ten years. Mainly, in SSBs reaching their end of life, the metallic lithium anode is completely converted to non-elemental form, and, at most, only a small portion of the initial anode is left. Regarding the reactive nature of the metallic anode, these types of batteries need to be discharged in a way that all of the metallic lithium is reacted before disassembling. With this in mind, the main focus of the recycling approach is basically the recycling of CAM and SSE. EoL battery failure monitoring depicts that SSEs undergo solid electrolyte interphase (SEI) and cathode electrolyte interface (CEI) decompositions[103], [104].

Another challenge in SSB battery recycling is related to the composition of the inorganic electrolytes, which includes a wider range of elements. This, in turn, might cause some difficulties in terms of co-precipitation and also the synthesis of pure precursors[40].

An advantage of recycling SSBs is that the same CAM is used as in LIBs. This means that the recovery and resynthesis of the CAM would not be different from an existing plant's focus. However, the coatings being used in these types of batteries can increase the complexity. Not to mention that the mass percentage of different parts of SSBs differs from those of LIBs. As electrolytes occupy 20-25 wt% of an SSB cell, recycling of these electrolytes needs to be studied in advance[35]. Additionally, the target recovery of Li is 80% in regulation (EU) 2023/1542 regardless of Li being in cathode, anode, or electrolyte[105].

The structure of oxide-based solid-state electrolytes (SSEs) presents greater complexity compared to conventional lithium-ion batteries (LIBs) due to the greater number of elements. Solid oxide electrolyte recycling is critically hindered due to its ceramic structure and hardness (200 GPa elastic modulus)[106]. Mechanical treatment by conventional means may lead to severe wear on equipment and fine fraction contamination[34].

Following discharge, oxide-based SSBs can undergo mechanical treatment, wet, dry room, or cryogenic conditions, to maximize recycling. Though oxide layer brittleness restricts processing, it also promotes efficient shredding into a 'black mass-like fraction' consisting of oxide electrolyte and cathode. The fraction is separated by screening or density-based processes before hydrometallurgical treatment [104].

The next step, considering the hydrometallurgy, is highly dependent on the solubility of the metals in the structure. Complete dissolution or selective separation can be applied based on material composition[86,87]. One major disadvantage of hydrometallurgical processing of SSBs is, however, material complexity, with high costs of selective precipitation of precious elements[94].

Dissolution behaviour of oxide-based SSEs, specifically garnet-type $Li_{7-3x}M_xLa_3Zr_2O_{12}$ (M = Al or Ta-substituted LLZO), has been examined in the literature under various acidic solutions. Table 4, illustrates the elemental composition of different LLZO electrolytes.

Schwich et al. have examined water leaching as the most cost-effective and available lixiviant, prior to any other lixiviants. Based on their analysis, 40% of Al and 57% of Li were leached out in deionized water leaching, while La, Ta, and Zr could not be leached out due to forming more stable oxide structures[107]. Different literature has examined the stability of LLZO in contact with humidity, which confirms the water leaching results. For instance, Xia et.al, have admitted the unstable nature of Ta-substituted LLZO and leaching of Li in contact with moisture, due to the ion exchange of Li^+/H^+ [108]. Thus, the leaching of LLZO would follow the reaction below:

$$Li_7La_3Zr_2O_{12} + xH_2O \leftrightarrow Li_{7-x}H_xLa_3Zr_2O_{12} + xLiOH \ (1)$$

Table 4. Elemental weight distribution in LLZO-Type garnet electrolytes

Element	LLZO($Li_7La_3Zr_2O_{12}$)	Ta-LLZO($Li_{6.5}La_3Zr_{1.5}Ta_{0.5}O_{12}$)	Al-LLZO($Li_{6.25}Al_{0.25}La_3Zr_2O_{12}$)
Li	5.79%	5.12%	5.16%
La	49.62%	47.29%	49.53%
Zr	21.72%	15.53%	21.69%
Ta	-	10.27%	-
Al	-	-	0.80%

Based on Feng Yow et al., increasing the pH to 11-12 will lead the above-mentioned ion exchange reaction to shift toward the formation of LiOH in the water lixiviant. Based on their observations, longer contact with CO_2-containing air would result in the creation of Li_2CO_3 as a byproduct[109].
The findings of Schneider et al. indicate that a two-stage water and acid leaching with 1 M hydrochloric (HCl) or sulfuric (H_2SO_4) acid, with the S/L ratio of 50 g/L at 25°C, would result in leaching efficiency of 100% for Li and Al, followed by 95% La, 94% Zr, and 91% of Ta[107]. Adding specific steps for precipitating elements like Zr, La, and Ta in hydrometallurgical LIB recycling would enhance the extractive hydrometallurgy in LLZO recycling.

Figure 8, demonstrates the behavior of the Ta modelled with the HSC database, in different pH values. Based on the graph, precipitation of Ta is independent of the pH, and no clear border is identified.

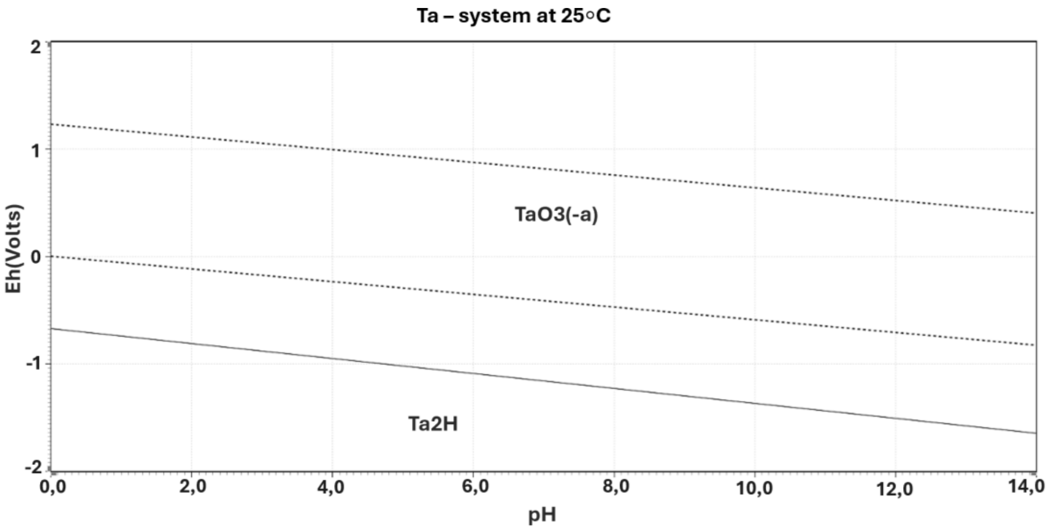

Figure 8. EpH diagram of Ta dependent on pH at 25 °C and 1 atm – Ta Concentration: 1 mol/l. HSC database

Based on the observations by Deblonde et al., alkaline leaching combined with the pH adjustment of 2-7 would result in the precipitation of Ta[110]. Considering this, Schwich et al. concluded that Ta can be precipitated in acidic media, which in turn can cause contamination of the Cu-cementation or aluminum and iron hydroxide precipitation[111]. Due to this fact, Chen et al. conducted a pressure leaching with hydrofluoric acid and a solvent extraction method for Ta recovery. They reported a 98% efficiency in recovering Ta_2O_5 with above 99.9% purity[112]. Ta mainly gets decomposed from its ores with the use of HF, while 6-7% of HF can be lost due to high volatility, which is hazardous; besides that, the wastewater containing fluorine requires further treatment. Thus, another method has been developed recently using KOH (sub-molten salt) at atmospheric pressure, which increases the yield by 10%, although KOH solution evaporation and recycling are energy-intensive [113]. Tantalum pentoxide is highly insoluble in any solvent except for strong bases or HF[114].

$$3(Fe,Mn)O.(Ta,Nb)_2O_5 + 8KOH + (n-4)H_2O \rightarrow K_8[(Ta,Nb)_6O_{19}.nH_2O] + 3(Fe,Mn)O \quad (2)$$

Based on the equation $3(Fe,Mn)O.(Ta,Nb)_2O_5 + 8KOH + (n-4)H_2O \rightarrow K_8[(Ta,Nb)_6O_{19}.nH_2O] + 3(Fe,Mn)O \quad (2)$, in the presence of KOH at a temperature of 150-200°C in the first step, unstable $K_8[(Ta,Nb)_6O_{19}.nH_2O]$ is formed in the first step, which in the next reaction can turn into an insoluble $K(Ta,Nb)O_3$. The reaction conditions, such as the concentration of KOH and temperature, can control the evolution of the product types[113].

Three different tantalum purification methods exist: distillation (or chlorination), solvent extraction, and ion exchange. The distillation method involves the lixiviant and carbon, reacting with chlorine gas at 600-800 °C. In the presence of niobium, separation can face difficulties due to the close boiling points of niobium chloride (249 °C) and tantalum chloride (239 °C). Thus, solvent extraction and ion exchange are recommended for a high degree of purity. Due to the difficult dissolution behavior of tantalum pentoxide, even when using HF, a long contact dissolution process is needed, while greater amounts of HF compared to the stochiometric values are needed[115]. Due to the structural difference of Ta-substituted LLZO compared with Ta_2O_5, the leaching behavior needs to be further investigated. The next steps are La and Zr precipitation, which also happen in acidic conditions.

Although a high ratio for leaching has been reported in the literature mentioned above for all elements involved in Ta-LLZO, Schwich et al. admitted that leaching of Ta would not be possible even in the case of using highly strong acid, except for the HF and pressure leaching[111]. This, in turn, supports their recommended process as illustrated in Figure 12 b. in which unleached Ta is being recovered by filtration after the leaching with strong acid.

Figure 9, illustrates Zr precipitation based on two different studies. Schwich et al. modelled the EpH diagram for Zr using StabCal with the Helgeson (SupCrt) database. Figure 9 left), demonstrates that Zr ions can undergo precipitation at pH of ~4.5[111]. Figure 9 right), Ma et al. reported the precipitation of ZrO_2 from the PLS at pH of 2.5 with Na_2CO_3[116].

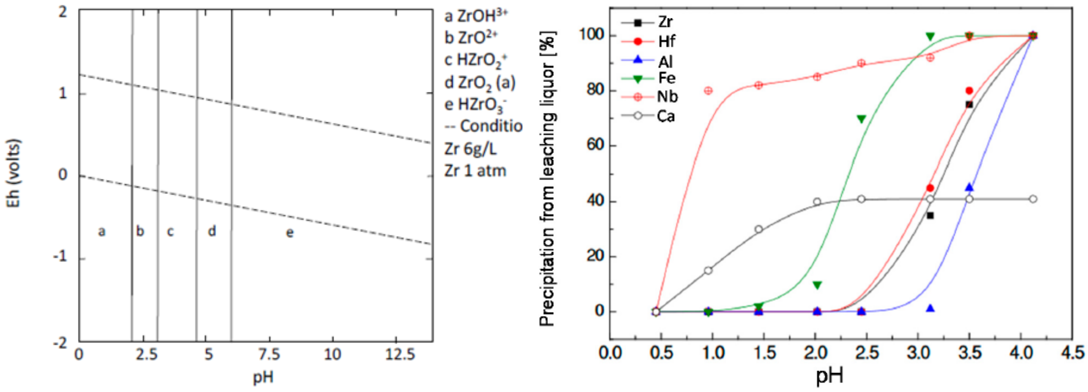

Figure 9. left) EpH diagram of Zr dependent on pH at 25 °C and 1 atm - Zr Concentration: 6 g/l. StabCal and Helgeson (SupCrt) databases[98]. right) pH effect on the precipitation of Zr, in H_2SO_4 with Na_2CO_3[100].

Figure 10, using LLNL database and StabCal, Schwich et al. reported that La-ions can be precipitated at pH 7.4 at a concentration of 18 g/l[111]. Yahya et al. have reported that at 25°C and a concentration of 0.01 M, La can precipitate at approximately pH 8[117]. Figure 11. Precipitation diagram of hydroxides at 25 °C[118], supports that in low concentrations, below 1 M, La can precipitate above a pH of 8. Overall, it illustrates that the La precipitation can occur under the basic condition above pH of 7.

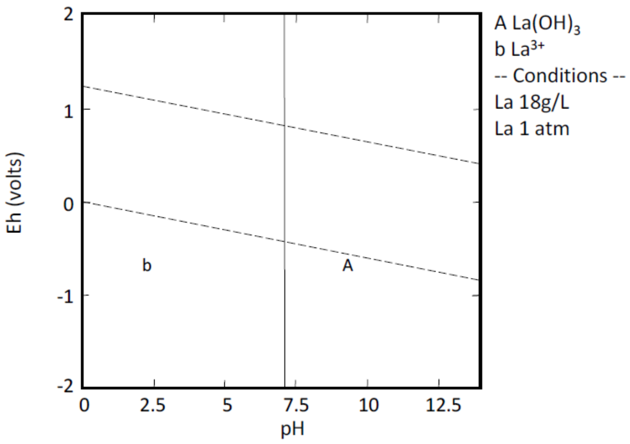

Figure 10. EpH diagram of La dependent on pH at 25 °C and 1 atm - La Concentration: 18 g/l. StabCal LLNL (Cp(T)) database[98].

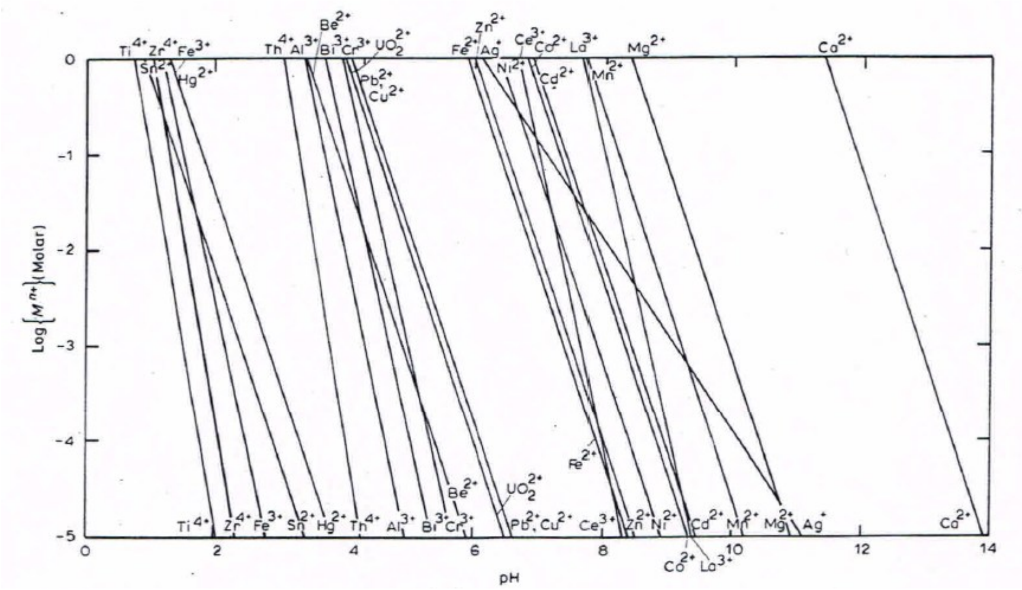

Figure 11. Precipitation diagram of hydroxides at 25 °C[118].

Figure 11, illustrates the precipitation of different elements' hydroxides at ambient temperature. This graph illustrates how the co-precipitation of different elements can be a challenge in more complex environments.

Nowroozi et al., demonstrated that leaching of $Li_{7-3x}Al_xLa_3Zr_2O_{12}$, $LiFePO_4$, and $Li_4Ti_5O_{12}$ by hydrochloric acid treatment and NaOH precipitation results in relatively pure recovery of La_2O_3 and ZrO_2, but at the cost of having to use extremely long precipitation sequences. They declared that the coprecipitation of Fe and La can cause the formation of $LaFeO_3$ perovskite type[119].

Figure 12, proposes two theoretical recovery processes for a system of LLZO + NMC: one by complete dissolution of both electrode and electrolyte materials in a single-step leaching process under strong acidic solution, followed by chemical precipitation in multi-steps at predetermined pH values; and another by selective leaching, where the electrode material dissolves first under mild acidity, but the electrolyte remains dissolved in a stronger acidic solution. The selective process minimizes co-precipitation, enabling efficient separation and recovery of the individual elements[111].

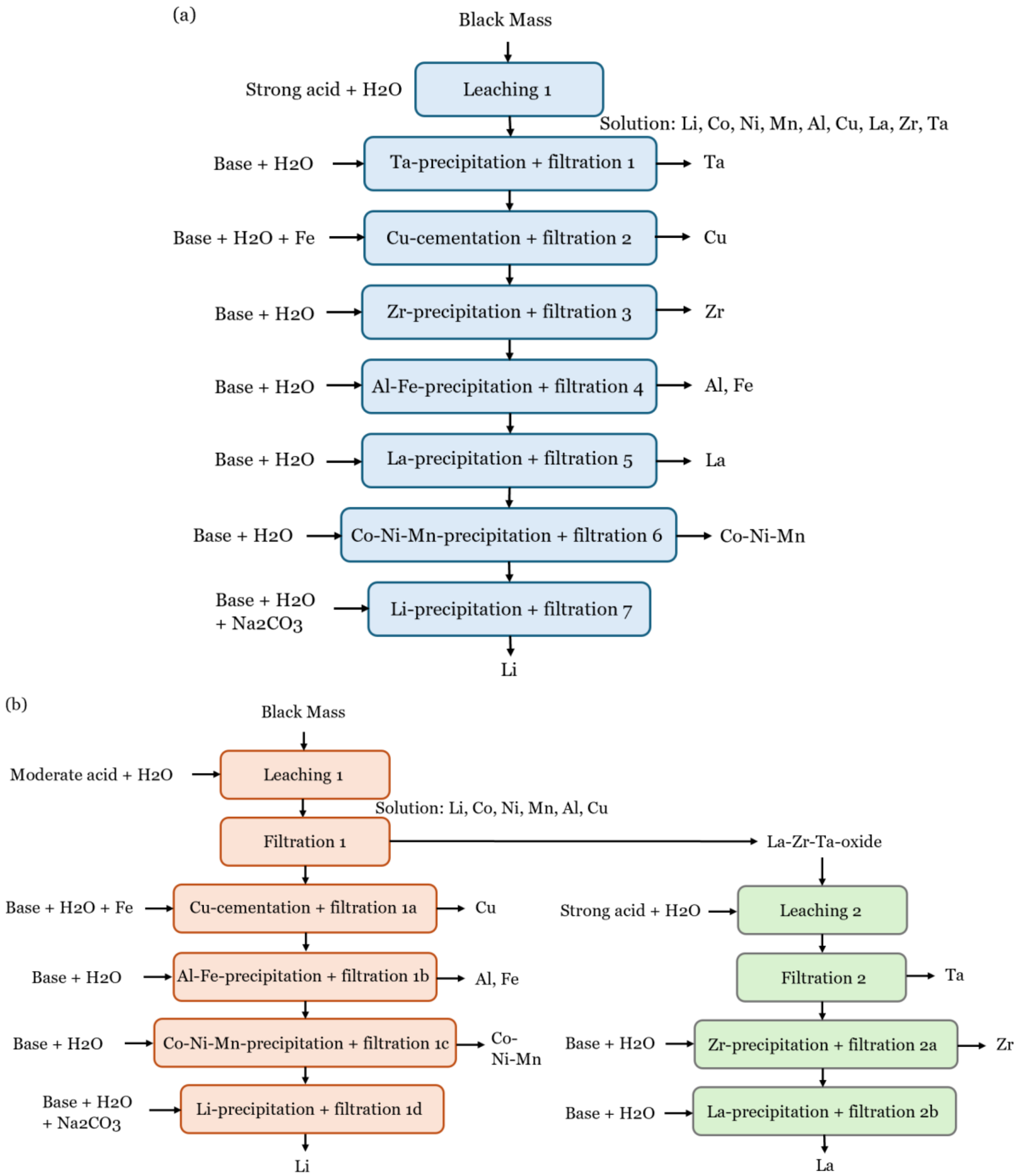

Figure 12. The proposed hydrometallurgical recycling process for an LLZO + NMC cell system following two paths:(a) Complete dissolution, where both the electrode and electrolyte materials are subjected to a single leaching in a highly acidic medium.(b) Selective leaching, which first leaches the electrode material under mild acidic conditions without leaching the electrolyte. The electrolyte is then treated separately with a strong acid[111].

Table 5. Precipitation pH windows of key elements in LLZO-type garnet electrolytes.

Element	Precipitating species	Approx. Precipitation pH	Notes	Reference
Li	LiOH or Li_2CO_3	>11 (as LiOH); with $CO_2 \rightarrow Li_2CO_3$	Leaches even with water; can form LiOH in alkaline pH, converts to Li_2CO_3 in air	[109]
La	$La(OH)_3$	~6.5 (HSC), ~7.4 (LLNL/StabCal), 9-9.5 (Hydroxide precipitation diagram)	Different pH values have been reported	[111], [118]
Zr	ZrO_2	≥2.5, 4.5, 2-2.5 (Hydroxide precipitation diagram)	Different pH reported for ZrO_2 precipitation	[111], [116], [118]
Ta	TaO_5	2-7 (precipitation possible), No border (HSC)	pH-independent trend; can precipitate even in acidic conditions	[110]
Al	$Al(OH)_3$	~4-5 (Hydroxide precipitation diagram)	-	[118]

Based on Table 5, the integration of Al- and Ta-substituted LLZO into the LithoRec hydro process requires a re-evaluation of the metal separation strategy to enable selective recovery of elements such as La, Al, Ta, and Zr. In the original process, copper was removed via precipitation as $Cu(OH)_2$. However, the overlap in precipitation pH between $Cu(OH)_2$ and $La(OH)_3$ or $Al(OH)_3$[111], (typically around pH 4-7) introduces the risk of co-precipitation, thereby lowering the separation selectivity. Therefore, copper cementation under acidic conditions (low pH) is now recommended to prevent this interference and enhance downstream recovery of LLZO-related dopants.

According to various studies, the precipitation mechanisms for these elements can involve oxides, hydroxides, or sulfides, depending on the pH, redox potential, and reagent availability. For example, La and Al are predominantly precipitated as hydroxides, while Zr and Ta may form oxides or mixed solid phases depending on conditions[111], [120].

Furthermore, due to the potential formation of complex compounds between oxide-based solid electrolytes and cathode elements, co-recycling is not recommended. Even though hydrometallurgical processing can enable leaching to a range, the presence of dopants and different elements in the electrolyte can reduce the purity of recycled CAM elements and complicate downstream separation. However, as noted earlier, the brittleness of the oxide electrolyte allows for effective mechanical comminution, and sieving or density separation becomes an effective pre-step to chemical treatment. Therefore, dedicated recycling streams with physical separation are preferred in order to prevent cross-contamination and to ensure material purity.

3.1.2 Hydrometallurgical Recyclability of Sulfide-based SSBs

Although sulfide-based electrolytes have higher ionic conductivity compared to the previous oxide-based category of SSEs, their chemical instability in contact with the cathode causes challenges in the battery life cycle. During this phenomenon, the lithium content decreases, and elemental sulfur can be formed on the SSE surface as an irreversible structure[103].

As it was discussed before, in the sulfide-based SSE category, argyrodite thiophosphates Li_6PS_5X (X=Cl, Br, I), have showed a superior ionic conductivity[121]. Recycling sulfide-based solid-state batteries (SSBs) is especially difficult because sulfide/thiophosphate electrolytes are unstable in room temperature atmosphere or humidity. They can react with water molecules to produce toxic hydrogen sulfide (H_2S), and thus require strict safety protocols for handling and processing. Sulfide-based electrolytes also become non-electrolytic when exposed to water, so production in an inert environment is a significant cost factor[122].

To eliminate H_2S formation, researchers have explored dry mechanical processing under a water-free environment and solvent stabilization. Introducing M_xO_y nanoparticles (such as Fe_2O_3 or ZnO) into sulfide electrolytes can inhibit H_2S formation[123].

Mechanical processing, however, needs special requirements such as inert gas or dry room conditions, which can be energy-intensive, or inert gas resource-consuming, and is therefore expensive and potentially hazardous in the event of H_2S gas leaks. On the other hand, the flexible structure of these electrolytes can cause some problems in comminution. Considering the less adhesive structure of these materials compared to the other LIB electrodes, the separation of compounds can be more feasible. This, in turn, leads to higher recoveries in terms of purity and yield of both electrodes and electrolytes[124].

A pretreatment method based on solvents is a good option as it dissolves the SSE with negligible safety issues. Suitable solvents such as ethanol, acetonitrile, or N-methyl formamide (NMF) can deactivate sulfide electrolytes, but their interaction with lithium and other components of the battery must be considered strictly [125], [126]. Solvent-based recycling also offers the benefit of enabling direct resynthesis and reconditioning from solution, and hence enabling material recovery optimization[127], [128].

Finally, these elements can be recovered using a hydrometallurgical approach. Because of the stringent safety conditions and technical advancement of sulfide-based SSB recycling, a hybrid process incorporating mechanical separation, hydrometallurgical extraction, and solvent-based resynthesis offers an economically viable route for high recovery rates[119], [120].

Ten et al. were the early researchers reporting the dissolution technique for the recovery of the sulfide-based SSEs with organic solvents. In their model, dissolution of SSB with lithium anode, Li_6PS_5Cl SSE, and $LiCoO_2$ cathode has been studied[128]. Their studies contributed to the possibility of the separation of electrode and electrolyte. However, the effect of the organic solvent type to be chosen, the ratio of electrolyte concentration to the solvent, and, importantly, the contact time, as well as the effect of different electrode materials, was not investigated[121].

Wissel et al. declared that the contact of different electrode materials with the dissolved sulfide-based electrolytes can lead to various chemical reactions. This is basically due to the chemically unstable nature of Li_6PS_5X(X=Cl, Br, I) with a narrow electrochemical window. The dissolution of argyrodite electrolytes follows the reaction below:

$$Li_6PS_5X(X = Cl, Br, I) \rightarrow 6Li^+ + PS^{3-}_4 + S^{2-} + X^- (3)$$

Existing Cl-, Br-, I-, and S- in the solution can interact with the electrode material surface and generate complex chemicals. In this regard, different aspects need to be studied, such as the redox potentials, the effect of different factors in forming complex compounds, and the stability, including solubili-ty and precipitation, etc. Divalent cations such as Mn, Fe, Co, and Ni form sulfides with a low solubility, while the halides can have a higher solubility[121].

In conclusion, while sulfide-based electrolytes recycling can face different challenges, especially in terms of safety, it can be considered economically feasible with mechanical disassembling followed by hydrometallurgical recycling[129].

Considering the LithoRec Flow Diagram (Section 3.1, Figure 7)[130], integration of these materials into the flow sheets is incompatible with an initial pretreatment step. After manually disassembling the battery packs and separating the parts, the cells get shredded under an inert atmosphere of nitrogen purging at around 100-140 °C. The processed black mass then passes through several sequential steps, such as an air classifier to separate the lighter parts. Although the solid sulfide-based electrolytes would remain after the heating step, which has been designed for removing the volatile liquid electrolytes in LIB counterparts, contact with the air humidity would cause H_2S gas generation as discussed before. Not only does the weak stability of these types of electrolytes lead to the generation of H_2S gas, but they also undergo side reactions in the presence of lithium to form LiCl, Li_2S, and $LiPO_4$[131]. Considering the leaching of these electrolytes, higher levels of safety need to be considered, especially in terms of gas scrubbers or incinerators. Phosphorus also needs to be washed away from the NMC precursor compositions, as it can deteriorate the quality of the CAM[132].

The EU's report on the potential of recycling the sulfide-based solid-state batteries shows that Li_6PS_5Cl argyrodite can be dissolved in solvents like ethanol and methanol, while cathodes would stay unleached. Based on their report, approximately 90% of the electrolyte dissolution is achievable, while the CAM can be leached out with following acid leaching[133].

3.1.3 Hydrometallurgical Recyclability of Halide-based SSBs

Halides represent a novel family of SSEs that exhibit high ionic conductivities (>1 mS cm^{-1}) and superior (electro)chemical oxidation stability[49]. Such stability enables their application as catholytes for an uncoated cathode, potentially enabling recycling simplification[50]. However, halides are unstable in contact with metallic lithium, which necessitates hybrid cell designs with sulfide separators or anode-side protective layers, both introducing complexity for recycling. Having an elastic modulus of around 20 GPa[134], halides also have similar advantages when compared to sulfides, but introduce difficulties in comminution[34].

Copper is the dominant metal in the battery due to the anode current collector. Chloride solution attacks copper surfaces by corroding them and forming CuCl, which is highly insoluble. However, this can be prevented by optimal exposure[40]. Another consideration in halide recycling is the acidification of aqueous solutions due to the influence of strongly charged metal cations as Lewis acids. It proceeds through the reaction:

$$M(H_2O)_6{}^{z+} + H_2O \rightarrow M(H_2O)_5(OH)^{(z-1)^+} + H_3O^+ \; (4)$$

As a result, acidification influences the solubility of cathode materials such as phospho-olivine ($LiFePO_4$) or layered structures such as Li(Ni, Co, Mn)O_2, which have been found to dissolve at moderate pH levels[135]. Understanding these interactions is important for optimizing halide separation and the recovery processes in battery recycling[40].

Acid leaching is not required for the extraction of the metals from these types of SSEs. Water dissolution provides a great potential for the extraction of the metals, skipping the electrode dissolution simultaneously and in this way providing inexpensive, selective leaching[136].

Due to their moisture sensitivity and tendency for ion-exchange reactions, recycling of halides has to be conducted in a controlled dry-room facility after mechanical disassembly[49]. Subsequent treatment depends on the cell design. For hybrid cell types with polymer components, mechanical treatment tends to be ineffective, and thermal or solvent-based processes need to be employed. On the other hand, pure halide SSEs can undergo dry comminution and electrolyte separation, similar to that with sulfide SSEs. Separation based on density is difficult due to halides' relatively high densities, e.g., 2.71 g cm^{-3} for Li_3InCl_6 [137].

Halides, excluding fluorides, are found to be extremely soluble in water or alcohols providing a viable route for recycling. Most metal chlorides are soluble except for AgCl, $PbCl_2$, $HgCl_2$, TiCl, and CuCl. But since the majority of metals cannot be stabilized in a solution as chloride complexes, the direct precipitation of pure metal chlorides (MCl_y) is not feasible. Thus, additional purification steps, i.e., distillation or reaction with ammonium chloride (NH_4Cl), are required[40].

Based on the literature, Li_3OCl is an electrolyte type highly soluble in water and methanol. This would lead to the formation of LiCl and Li_2CO_3. Separating these two compounds is possible using selective ethanol leaching of LiCl. Heating the remaining Li_2CO_3 above the decomposition point under a vacuum condition converts the Li_2CO_3 to Li_2O[40].

3.1.4 Hydrometallurgical Recyclability of Polymer-based SSBs

The drawbacks of using inorganic SSEs are complicated preparation procedures, high expense, low durability, and low mechanical properties. In contrast, implementing the polymeric solid-state electrolyte shows excellent electrode interface stability as well as flexibility, thereby effectively resolving the interfacial problems of the inorganic solid-state electrolyte. Moreover, due to its favourable ductility, simplicity in the formation of a film, and simple preparation procedure, the polymer can be prepared on a large scale and is hence readily available for further commercialization. Although lots of research has been focused on the advancement of these types of electrolytes, a single structure (organic or inorganic-based) can not help achieve good performance. Thus, a combined organic/inorganic structure is generally required to achieve the best performance[138].

Regarding non-toxic nature and less safety requirements, polymer-based SSEs enable the simpler recycling process compared to other SSEs. Due to the solubility of the polymer-based SSE in acidic or basic solutions, it is predictable that co-precipitation would occur with CAM elements in following precipitation process. Ether groups can break up in contact with strong acids or bases, which, in turn, can affect the recovery of the elements from the CAM, as well as from the filler and the lithium salt, and also slow down the recovery of the polymers. Some of the salts being used in the structure of the polymers, such as LiTFSI (Lithium bis trifluoromethanesulfonyl imide), are highly soluble in water, and they can interact with the CAM. Not to mention that the existence of the filler materials in the electrolytes can lead to unwanted side reactions and co-precipitation. Thus, the separation of the polymers before the leaching of the electrodes would be beneficial[40], [139]. Mechanical shredding, sieving, and mechanical separation from the current collectors can face similar challenges as sulfide-based SSEs, due to the flexible nature of the polymer-based SSEs[104].

Although there are different types of polymer-based SSEs under investigation, one of the widely investigated old species is polyethylene oxide (PEO). PEO and almost all of the involved phases are water-soluble, except for the ceramic fillers (Oxide-based SSE section). Although this can be a viable approach to separate the electrolyte and other components involved in the black mass, it is essential to consider that possible side reactions with the existing phases need to be investigated[139], [140], [141], [142].

Due to the high viscosity of dissolved PEO, the dissolution procedure of PEO can be done by using water or a water/alcohol mixture at 50 °C[143]. The filtered leachate would have high viscosity, which has a repelling effect on the precipitation of the metals. The dissolved solution would contain PEO monomers and the dissolved lithium salt, which can later be recovered by evaporating the solvent. However, the quality and purity level are uncertain[104], [144].

According to Thielen et. al, contact with water can lead to above 98% decoating of the material in long runs (360 minutes) while using the wet agitated media mill, PEO dissolution efficiency can reach the same level in 10 minutes [144]. Different methods for recovering the PEO from the leachate are available. Adding an anti-solvent to reduce the solubility of PEO in water and precipitation is one of the methods[145]. Additionally, PEO can be separated through temperature-induced precipitation[146]. Also, PEO recrystallization can take place following the evaporation–concentration of the solution [144].

While not yet reaching the cycle stability of traditional LIBs, current SSBs are still undergoing research and are not yet commercialized. Not to mention that all above mentioned possible recycling paths are theoretically evaluated and need to be experimentally investigated for practical proof.

Overall, considering all types of SSB cell packs using metallic lithium anode, water leaching might not be practical. This is basically due to the safety concerns and the leaching efficiency. Contact of water and lithium can cause an exothermic reaction, which can lead to thermal runaway or even fire.

Moreover, this reaction would generation of H_2 gas, which is also combustible and can cause safety risks. As a solution, controlled reaction either under an inert atmosphere using N_2, Ar, or even CO_2 leading to lithium carbonate development is recommended. In all of the cases, proper gas ventilation and monitoring are required[144].

3.1.5 Hydrometallurgical Recyclability of SIBs

Due to the similarities in the structure of both LIB and SIB batteries, besides the material compositions, generally, the developed recycling routes for LIBs can be used for SIBs as well, with some adjustments regarding the recoverable materials. On the other hand, the safety risks are similar in both of these battery types, firstly due to the same procedure of metal plating in the anode, followed by the short circuits and gas generation. Considering the highly exothermic sodium reaction with water, full discharge is required before recycling. Due to the less complex structures and more abundant material integration, the subsequent steps for recycling of SIBs are more straightforward than in LIB recycling[10].

Although sodium is mainly considered abundant and economically of lower value compared to lithium, the presence of Ni, Cu, Mn, V, P, and F highlights the importance of recycling. Not to mention that the economic value of SIBs is 30-40% lower than that of LIBs, but still in theory, recycling of these types of batteries can be economically viable[10]. The degradation of SIBs mainly follows the same patterns as with LIBs, and is mainly due to the loss of sodium, material interface degradation, and structural damage to the battery[147].

Among different types of cathode active materials, transition metal oxide types (M = Mn, Ni, Co, Fe, Cr, Ti, V, and their combined forms) show the most promising performance for SIBs. This is mainly because of their simple structure, easy synthesis process, and feasibility of industrialization, besides the good operating potential. In contrast to their lithium counterparts, in which only lithium ions can intercalate into $LiCoO_2$ and $LiNiO_2$, intercalation of sodium ions is possible in almost all types of Na_xMO_2. Further, various transition metal species are blended to synthesize Na_xMO_2 compounds with variable properties[148], [149].

Based on the literature, the layered sodium oxide type of NFM (sodium iron manganese oxide) is unstable in contact with air and moisture. This should be considered in any aqueous leaching process as the presence of sodium ions in contact with moisture can form NaOH. Furthermore, NaOH contacting to aluminum current collector can cause the formation of AlO^{2-}, hence degrading the current collector. Battery degradation patterns show that the EoL salts such as NaF, Na_2CO_3, Na_2O, and organic compounds are highly water-soluble. Thus, immersing these materials of CAM in the water can help with the separation from the current collector i.e., dissolution and removal of EoL salts and leaving residual Al. Nevertheless, some CAM material loss is possible being adhesive to the aluminum current collector. On the other hand, the surface analysis on the cathode shows that using water can completely remove the Cathode Electrolyte Interface (CEI) layer from the CAM surface[76].

Mechanical separation is less challenging for SIBs compared to the LIBs. This is mainly because of the limited number of integrated materials, for example, the current collector in SIBs being only aluminum-based. This increases the possibility of pulverizing both SIBs and LIBs together. It needs to be noted that the main purpose of recycling in this concept needs to be the same, and based on the recovery of the most valuable components for both battery types[10], [150].

Although the recycling of SIBs seems to be less technically challenging, modifications to the existing recycling paths are required to align with the materials integrated. As it was mentioned, hydrometallurgical recycling of SIBs can follow LIBs, particularly for layered oxide cathodes. As an example, cathode materials such as P2-$Na_{2/3}Ni_{1/3}Mn_{2/3}O_2$ can be leached using inorganic acids in the presence of a reductant, using the same procedure used for LCO or NMC CAMs in LIBs. However, an important distinction exists in the economic drivers: sodium is inexpensive and abundant, reducing the incentive to recycle it. Therefore, only high-value metals such as Al, Ni, and Mn are typically targeted for recycling from SIBs with layered metal oxide cathodes, whereas in LIBs, Li, Cu, Al, Co, Ni, and Mn are recycled. Another advantage of SIBs processing is that Al impurities can be more easily eliminated due to the amphoteric character of Al. However, there are still problems. For instance, while $Na_2V_2(PO_4)_3$ cathode materials readily dissolve in 1 M HCl at room temperature, vanadium does not precipitate easily through neutralization. Thus, vanadium recycling from such PLS will require the further development of new separation techniques[10].

Zhang et al. conducted an evaluation of the recycling process for the layered oxide-type cathode material $NaNi_{1/3}Fe_{1/3}Mn_{1/3}O_2$ (NFM), drawing parallels to the well-known $LiNi_{1/3}Co_{1/3}Mn_{1/3}O_2$ type. Their findings indicate that while the pretreatment of NFM cathode active material is comparatively easier than that of its lithium counterpart, several challenges remain in achieving efficient leaching. Their investigation revealed that water can effectively separate the cathode active material (CAM) from the aluminum foil current collector, as well as wash away the solid electrolyte interphase (SEI) layer. This method has also proven effective for separating the anode from its current collector. However, the presence of high sodium concentrations in the cathode results in an alkaline wash, which can lead to the reduction of aluminum. This effect is less important in the anode due to its lower sodium content and, consequently, a lower pH. During the battery's charge and discharge cycles, nickel transitions between oxidation states of 2^+ and 3^+, while iron and manganese remain relatively stable. When the battery reaches a fully discharged state prior to recycling, the nickel is predominantly in the 2^+ state, and sodium ions are intercalated within the CAM layers. As sodium is washed away from the CAM, the nickel oxidation state shifts to 3^+. This change makes the nickel structure more resistant to leaching, necessitating the use of a reducing agent such as hydrogen peroxide (H_2O_2)[76].

Based on their observation, water can effectively be used for moving the CEI layer out of the CAM surface while also helping the effective separation of the current collector and CAM. During water leaching, H/Na exchange takes place. This phenomenon reduces the leaching efficiency of transition metals with 1 M H_2SO_4 containing 5% H_2O_2, reaching roughly 15% at 80 °C, while without initial water leaching, it can reach 57% . After removing the CEI and sodium from the CAM surface, instead of leaching, the filtrate can be regenerated using Na_2CO_3, which is sintered at 900 °C[76].

Figure 13, illustrates two potential processing strategies for recycling of metal layered oxide SIB cathode materials (M referring to Fe, Mn, Ni), in which an integration to the LithoRec is suggested by the author. Considering there is a significant potential for effective CEI removal and the re-sodiation of the water-leached residue, the integration of these CAM materials into the LithoRec recycling plant with strong acid leaching seems not to be logical. Given the low economic value of sodium, its removal with water leaching could be practical not only for reducing complexity in lithium-ion battery (LIB) material recycling but also for minimizing acid usage. While Zhang et al. found that the recycled CAM exhibits high electrochemical performance[76], this strategy not only enhances the sustainability of the recycling process but also maximizes the recovery of valuable materials, thereby contributing to a circular economy in battery technology.

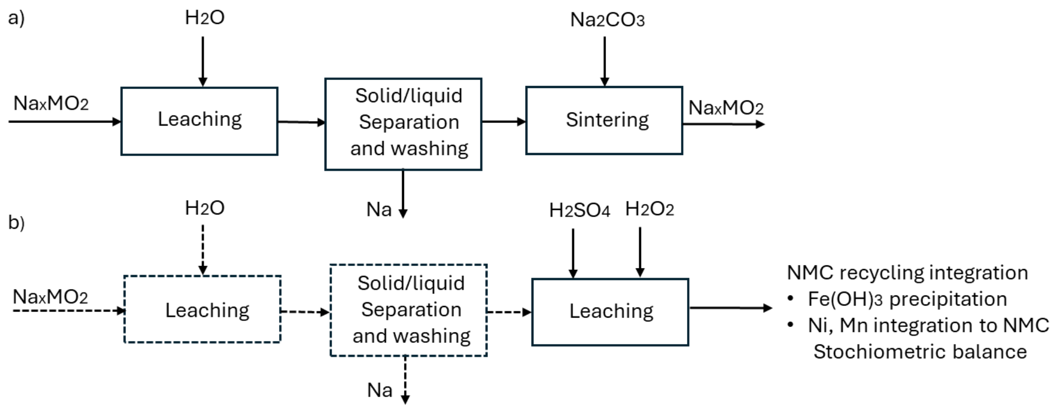

Figure 13. Potential processing approach for Na_xMO_2 type CAM recycling: a) Direct recycling[76], and b) an additional step for integration to LithoRec flow sheet.

Considering the characteristics of black mass, as it was mentioned, the structure composition of SIBs generally follows that of LIBs but with less complexity (e.g., substituting copper current collectors with aluminum). Furthermore, given the present status of recycling initiatives for LIBs, where components such as carbon-based anodes and electrolytes are typically excluded from the recycling scope, the integration of SIBs into the existing recycling infrastructure appears to be doable. It should be noted that other compositions of CAM, integrating with different elements such as vanadium, would need further adjustments to the flow diagram for recycling them.

3.2 Pyrometallurgical Recycling

Pyrometallurgical recycling represents a well-established and predominant methodology within the realm of industrial battery recycling processes[77]. The process can be either a direct thermal battery cell processing or a combined process with a preliminary mechanical treatment stage, followed by pyrometallurgical processing of the recovered black mass. Pyrometallurgical processes are high-temperature processes involving roasting and melting, ultimately yielding battery slag and metal alloy[151]. The pyrometallurgical recycling of lithium-ion batteries begins with the heating of 150-500°C to break down the electrolyte and organic solvents. The substances are then subjected to high temperature treatment to as high as 1450°C, where reducing agents like graphite, coke, or other salts ($NaHSO_4$, $CaCl_2$, NH_4Cl) facilitate the recovery of battery alloy and slag, including lithium compounds like Li_2O and Li_2CO_3[152], [153], [154].

Pyrometallurgical treatment is typically integrated with hydrometallurgical processing to recover single elements from transition-metal alloys containing iron, cobalt, and copper. The process generates by-products such as slag and gases, some of which are toxic, such as carbon dioxide emissions from reductants based on carbon. Other gases are derived from electrolyte and binder degradation. As lithium ends up in mineral-based slag, further hydrometallurgical processing is required for final recovery. Smelting is widely applied across industries due to its efficiency and established use for the extraction of metals from ores. Its drawback is a heavy CO_2 impact, release of poisonous gases (e.g., those resulting from incomplete removal of fluoride), a high energy input and cost, as well as a need for additional purification stages[79], [94]. Although if the entering feed contains high aluminium content, the process can be considered autothermal, while the existing of graphite providing the reduction capability[155], [156].

In addition, lithium's volatility at high temperatures is a problem in this process. LiOH can readily be generated when oxidic samples come into contact with atmospheric moisture. Due to its low melting and evaporation points, it is susceptible to chemical vapor transport and consequent losses since it will disperse in the air[40]. Although this might have previously been considered a disadvantage, recent studies have proved the possibility of recovering lithium from off-gas. Adding enough chloride sources can result in the recovery of lithium from the dust in the form of volatile LiCl. $CaCl_2$ or $MgCl_2$ can be considered as the main sources of the chloride, which have the boiling points of 1935 °C and 1412 °C, and can provide a good contact of chloride with the Li_2O in the smelter[157]. Based on Rinne et al. recovering the lithium from the off-gas being followed by leaching and carbonate precipitation, is environmentally beneficial compared to primary production[158].

The principles of the pyrometallurgical reduction are based on the Ellingham diagram and Gibbs free energy. The Ellingham diagram is a thermodynamic tool that illustrates the stability of various metal oxides as a function of temperature, providing essential insight into their reducibility in the presence of a reducing agent like coke (carbon). Figure 14 illustrates the Ellingham diagram being used in pyrometallurgical reduction and slag formation principles. Metals whose oxide curves lie above the carbon monoxide (CO or CO_2) line at a given temperature can be thermodynamically reduced by coke, whereas metals below this line form oxides that are too stable to undergo reduction under those conditions. For example, oxides of transition metals such as iron (FeO), copper (CuO), and nickel (NiO) lie above the carbon line at around 1400°C, indicating that they can be reduced to their metallic forms. In contrast, oxides of aluminum or magnesium remain below the carbon line, meaning they resist reduction, and instead, the metals themselves may oxidize[159].

Figure 15, illustrates the Umicore pyrometallurgical recycling plant, where not shredded batteries enter the furnace shaft. Battery wastes initially get mixed with an efficient amount of coke and slag former, and based on the feed, silicon or limestone also might be added. The shaft furnace consists of three different zones, the first one is the low temperature section with around 300 °C, in which the liquid electrolyte of the traditional LIB batteries evaporates. The stepwise heating is due to the safety requirements, as the fast increase in the heating temperature might indeed cause an explosion. The second zone is the mid-temperature zone with the temperature reaching 700 °C. In this section, organic materials such as binders and separators undergo pyrolysis. And lastly, the materials flow enters to the high temperature zone with 1200-1450 °C. In this section of the furnace, smelting and the reduction of inorganic components take place[160].

The preliminary thermal treatment guarantees that combustible or volatile substances are eliminated and burned in a controlled manner prior to the completion of the smelting process. When material reaches the highest temperature zone, residual metals such as cobalt, nickel, copper, and iron, melt and get separated from lighter fractions. The furnace operation utilized by Umicore is based on a reducing atmosphere boosted with carbon, frequently from decomposed plastic wastes or added coke, in order to reduce metal oxides to their elemental metal forms[160].

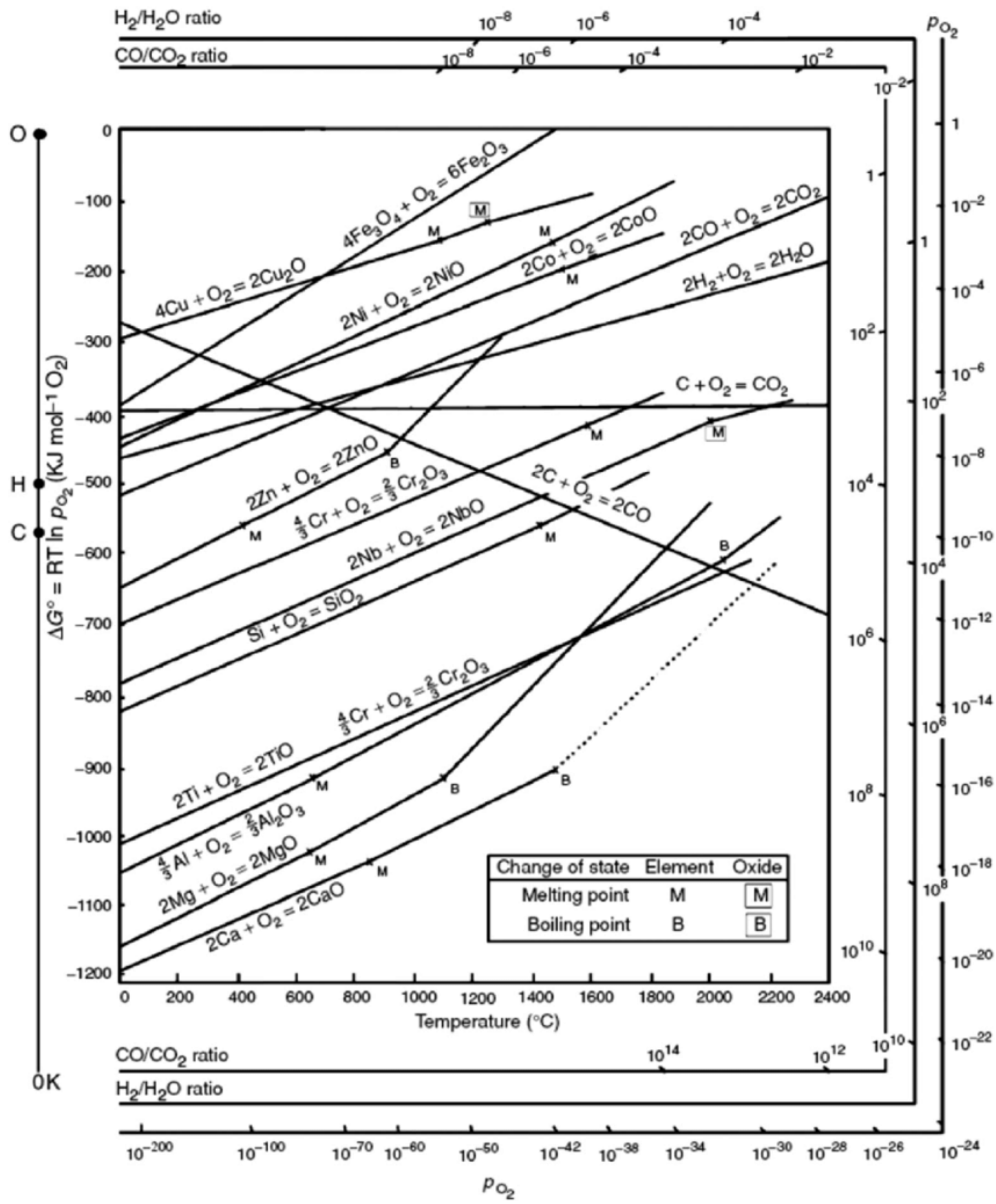

Figure 14. Ellingham diagram, ΔG vs T(°C), calculated under the atmospheric pressure[161].

Figure 15 demonstrates the gas preheating and treatment in the Umicore Pyrometallurgical process. Gases emitted by the furnace are treated through an afterburner and a scrubbing system. Umicore recycles a part of the emissions from the mid-temperature zone back to the low-temperature zone, enabling vaporization of the electrolyte and improvement in overall energy efficiency. The furnace design in Umicore's flow diagram contains mitigations of emissions and captures them from the off-gas. For this purpose, Na, Ca, or ZnO are being added to the slag to trap halogens and the volatile compounds. The high-temperature off-gas gets cooled quickly to quench the dioxins/furans formation (from plastic burning), and after that is filtered[160]. Sulfur in some feedstocks is oxidized to SO_2, which is then converted into sulfuric acid as a byproduct[162]. Umicore claims that carbon dioxide emissions as well as energy consumption for the production of $LiCoO_2$ can be up to 70% lower using the recycled materials rather than using virgin materials from ores and mining[160].

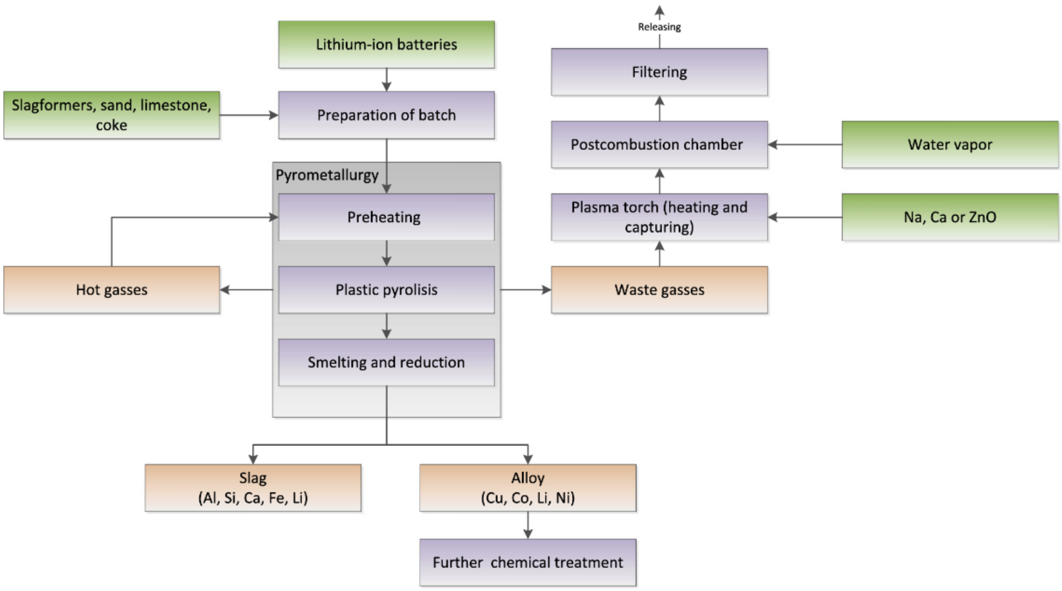

Figure 15 Umicore battery recycling flow diagram[160].

3.2.1 Pyrometallurgical Recyclability of Oxide-based SSBs

Pyrometallurgy is the mainstream method for conventional lithium-ion battery (LIB) recycling, and its adaptation for recycling SSBs should be considered.

One of the major benefits of recycling SSBs using pyrometallurgy lies in the elimination of the need for sorting or pre-treatment procedures, as complete battery packs and modules can be fed directly as input materials. Additionally, the process poses minimal reactivity concerns and safety risks to workers and reactivity concerns, since the elevated furnace temperatures effectively neutralize potential hazardous components[104].

Pyrometallurgical recycling of oxide-based SSBs involves the heating of electrode and solid electrolyte materials along with carbon, which leads to elemental redistribution and cross-reactions, which have been reported due to the fabrication of the SSBs [163], [164], [165]. While late transition metals (Cu, Ni, and Co) may be easily separated due to their greater reducibility [166], earlier transition metals (Ti, Zr, Nb, Ta) and rare earth metals (La) would remain in the slag. Moreover, excess carbon in the process can convert titanium-group metals to carbides, which complicates extraction [167]. Such carbides require further treatment by chlorine and form metal chlorides, which must be reduced by magnesium, making the process highly energy-intensive[40]. The effect of this cross-contamination during the recycling process is still unclear and needs to be further investigated.

Schirmer et al. suggested an engineered artificial mineral (EnAM) method, making a synthetic slag by adding Ca, Al, Si, Ti, and P oxides to the mixture containing Li, La, Zr, and Ta of oxide-based SSB electrolyte. Flotation is an effective processing technique for efficiently separating individual mineral phases when crystal sizes are sufficiently large. Beside the crystal formation, complex mixtures with thermodynamically stable phases have been detected after the heating and controlled cooling process, which needs to be further investigated in non-equilibrium thermodynamic modelling[168].

Furthermore, mixing different solid-state electrolytes (SSEs) e.g., $Li_{1+x}Al_xTi_{2-x}(PO_4)_3$ and $Li_{7-3x}Al_xLa_3Zr_2O_{12}$ may result in an element redistribution that makes recycling more complex compared to processing a single SSE type.

This will, in turn, add more branches in the flow chart for conversion steps[168].

Considering all solid-state batteries that do not undergo an exothermic reaction due to the lack of combustible compositions, using pyrometallurgy to recycle these materials would result in the formation of large amounts of slags. Although one of the main disadvantages of SSBs over LIBs is their complex structures, the absence of fluorine or phosphorus species is an advantage considering ecotoxicity. This would, in turn, result in less hazardous gas emissions from thermal treatments[111]. The formed slag can later be treated by hydrometallurgical recycling, considering the terms mentioned in the previous section for material recovery.

3.2.2 Pyrometallurgical Recyclability of Sulfide-based SSBs

Considering the recycling of sulfide-based SSEs, pyrometallurgical treatment is not appropriate, as sulfide-based electrolytes will either get burned or become a part of the slag beside generating gases as a hydrolysing byproduct, which needs to be scrubbed[104]. This makes the processing of these materials in industrial plants less attractive. The problem can be targeted with mechanical processing under an inert or dry atmosphere[40].

This highlights the importance of bringing these types of batteries into the recycling process without prior shredding, enabling direct feeding into the furnace, as at Umicore's plant. Considering the Umicore recycling plant, in which the battery cells enter to the furnace without being shredded[122], these types of SSEs can be fed into the process.

In the presence of humidity, the hydrolysis reaction in equation 5 for argyrodite-type SSEs is predicted. The following equation 6 is the neutralization of LiOH, in which, as a byproduct, Li_2CO_3 is formed by the reaction of LiOH with atmospheric CO_2[169].

$$Li_6PS_5Cl + 6H_2O \rightarrow LiCl + Li_3PO_4 + 5H_2S + 2LiOH \quad (5)$$

$$2LiOH + CO_2 \rightarrow Li_2CO_3 + H_2O \quad (6)$$

Li_2SO_4 can be created by the reaction between argyrodite and H_2O and O_2 in the atmosphere, as demonstrated in equation 7 [169].

$$Li_6PS_5Cl + 4H_2O + 2O_2 \rightarrow LiCl + Li_3PO_4 + 4H_2S + Li_2SO_4 (7)$$

On the other hand, other procedures highlight the conversion of thiophosphates to their oxide analogues. This permits lithium, phosphorus, and other metals to be recovered in secondary operations, even though the production of sulfur dioxide (SO_2) necessitates gas-washing in order to prevent environmental pollution while facilitating sulfur recovery[170].

On the other hand, regarding the presence of halides in these types of SSEs, Na, Ca, or ZnO are typically added to capture halogens and volatile species during processing. However, if alkaline batteries are part of the feed, then their original ZnO content will typically be sufficient for this function[160].

Unlike conventional lithium-ion battery recycling, sulfide-based SSE recycling will have to overcome the challenge of re-forming Li/P/Ge/Sn-S bonds. Fortunately, sulfur supply is not facing supply risk in the near future due to collusive reserves from natural gas, oil, and coal desulfurization[38], [171].

While the flexibility of the Umicore recycling plant enables the processing of these types of SSEs, there are some uncertainties regarding the environmental impacts, material usage, and economic feasibility. By integrating these materials into the Umicore pyrometallurgical process, sulfur is converted to SO_2 with subsequent sulfuric acid production[162] and lithium is potentially recovered from off-gas[157]. These offset some of the economic burdens, however, further investigation is needed to assess the extent of valuable material losses. This raises a critical question: does the combined recovery of sulfur dioxide and lithium, sufficiently justify the pyrometallurgical recycling of sulfide-based SSEs.

3.2.3 Pyrometallurgical Recyclability of Halide-based SSBs

Pyrometallurgical processing of chloride-type material is especially daunting compared to oxides or thiophosphates. Chloride molten salts are corrosive and will react with other components of the battery. Humidity also comes into focus in a significant way because exposure at elevated temperature can lead to the formation of corrosive hydrogen chloride (HCl) gas, thus rendering processing even more difficult[40].

Even with such limitations, pyrometallurgy can have potential in some of the metal chlorides with similarly low melting points and high vapor pressure. In strictly controlled heating process, such molecules could be separated from other residues, such as oxides, so that unwanted cross-reaction is prevented. For instance, $ZrCl_4$ sublimes at only 331°C, providing the potential of chloride elimination at similarly modest thermal inputs without excessive thermal application[40].

Not all chlorides can be separated successfully by thermal methods. Some chlorides, such as YCl_3, have much higher melting and boiling points (721°C and 1507°C, respectively), and therefore are more difficult to be separated. At such high temperatures, YCl_3 can also chemically react with other components of the battery and reduce pyrometallurgical treatment efficiency[40].

Generally, while pyrometallurgy may be a possible processing option for a few chlorides, tight temperature control and reaction condition observation is necessary to ensure material degradation and unwanted chemical contamination are not incurred[40].

3.2.4 Pyrometallurgical Recyclability of Polymer-based SSBs

In the cutting-edge smelters, aside from copper and precious metals, plastics or polymeric organics can efficiently be utilized to reduce the coke and energy consumption. The Umicore smelter uses a submerged lance combustion system in which the oxygen-rich air is injected together with the fuel and coke into the molten bath. So, the modern smelters have a significant impact not only on the elements being recycled but also on the value that is being recovered[162].

Based on the literature, introducing these polymer-based SSEs to the pyrometallurgical recycling plants would not result in the recovery of the materials from them, and instead, they would be burnt just the same as their sulfide counterparts[104]. This is basically due to the presence of oxygen in the furnace, which in turn would end in burning of polymers and emitting the CO_2, CO, NO_x, and aromatic hydrocarbons, etc[172].

Burning these types of materials in pyrometallurgical recycling plants would negligibly reduce their environmental footprint in terms of CO_2 emissions to the air. One important ecological term to be considered is the potential of the fluorinated organic compounds in their structure, which can cause the formation of volatile fluorinated organics. This can be eliminated by considering the appropriate incinerations[173].

The presence of the fluorinated lithium salt in the structure of these types of electrolytes raises the importance of the pretreatment in order to prevent HF formation. As mentioned earlier, mechanical separation from the current collectors can face similar challenges as with the sulfide-based SSEs, due to the flexible nature of the polymer-based SSEs[40].

Polymers and the conducting salts tend to break down at comparatively low temperatures. For instance, poly(ethylene oxide) (PEO) decomposes at around 200 °C, polyvinylidene fluoride-hexafluoropropylene (PVDF-HFP) copolymer at around 450 °C, pentaerythritol tetraacrylate (PAN) below 300 °C, poly(methyl methacrylate) (PMMA) under 360 °C, and lithium bis(trifluoromethanesulfonyl)imide (LiTFSI) at around 300 °C. Additionally, these materials can potentially react with the active components at high temperatures[34].

Cryogenic comminution offers a promising approach for processing polymer-based electrolytes. By cooling the battery components to cryogenic temperatures (e.g., ~85 K), typically with liquid argon, solid or gel electrolytes undergo a ductile-to-brittle transition. This allows for effective mechanical comminution, enabling subsequent separation steps. The resulting fine polymer fragments can be selectively removed, incinerated, or chemically digested[174].

Considering the chemical properties of the polymers, heating them up in the high temperatures of pyrometallurgical recycling process would not be beneficial in terms of recycling. This, as mentioned before, would be an exothermic reaction and generate heat, as well as off-gas. In turn, considering the circular economy, integrating these materials into the pyrometallurgical plants only would only add to the gas treatment; besides, the circularity only means that the carbon is from renewable sources. The ceramic fillers being used in these types of SSEs would accordingly follow the same path as the oxide-based SSEs mentioned previously.

3.2.5 Pyrometallurgical Recyclability of SIBs

Pyrometallurgical recycling seems to be more beneficial for SIBs compared to LIBs. The main reason for this arises from that sodium has a lower potential for volatilization than lithium and sodium is an abundant element. In addition, as tabs and current collectors are all out of aluminium in SIBs, there is less complexity in integration to pyrometallurgy while for LIBs, the anode current collector is made of copper and tabs can contain nickel coatings. According to Zhang et al., the pulverization and shredding of SIBs can be done simultaneously with LIBs, with the goal of recovering valuable elements[10].

Due to the lack of studies on the possibility of pyrometallurgical recycling, no scientific proof for the behaviour of the material in detailed studies exists. Theoretically based on the Ellingham diagram in Figure 14, mainly all elements except iron (Na, V, P) will end in the slag. Therefore, further treatments considering hydrometallurgical leaching and recovery of elements from slag need to be considered for increasing the recycling yield.

In thermal treatment, the fluorinated substances in SIBs can cause problem, stemming from $NaPF_6$ and PVDF. These substances accounts for only 3% of the total battery mass. However, monitoring these materials and implementing proper removal methods needs to be considered. Although the recycling and circular economy are basically based on the principle of following the same recycled materials for the battery manufacturing itself, downgraded materials such as extracted carbon can be converted for other structures as well[10].

4 Research Material and Methods

4.1 Sample Origin and Classification

The novel industrial prototype battery studied in this master's thesis has a structural basis close to lithium-SO_2 batteries, which are typically made of a lithium metal anode, porous carbon-based cathode, and highly conductive SO_2-containing inorganic electrolyte. In these types of batteries, electrolytes are in the form of $LiAlCl_4 \cdot xSO_2$. Electrochemical discharge normally yields solid products such as LiCl and $Li_2S_2O_4$[175].

The end-of-life battery sample in this master's thesis differs in two general respects from lithium-SO_2 peers: sodium is replaced as active metal, and the cathode composition includes a metal oxide as cathode active material with carbon black to increase the conductivity by implementing a binder. The cathode material sample sourced from end-of-life cells contains residual $NaAlCl_4$, possible dithionates, and NaCl as a discharge product, with trace metallic sodium (potentially passivated) and possible other byproducts. The main focus of this master's thesis is the characterization and leaching of the elements out of cathode composite samples (CAM, EoL salts, etc), with the main focus on sodium and sulfur leaching efficiency.

4.2 Safety Precautions and Sample Handling

Due to the manual disassembling of the battery cell under the lab conditions, the presence of metallic sodium particles from the anode as contamination in the cathode composite is possible. Sample processing was performed under a fume hood with full Personal Protective Equipment (PPE), that is, nitrile gloves, safety glasses, and lab jackets. Regarding the potential reactivity of metallic sodium in the vicinity of air and humidity, a container of dry sand was also available under the fume hood in order to control any consequent sodium-related fire incidents. Samples were visually monitored for apparent metallic fragments before any further analysis prior to any treatment.

4.3 Sodium Deactivation

To eliminate the potential risk of residual metallic sodium, the cathode composite sample undergoes a sodium contamination deactivation. The procedure was designed to eliminate reactivity of metallic sodium but keep other cathode component morphologies intact.

The cathode composite sample was soft crushed to a fine powder using an agate mortar and pestle, selected for its hardness and chemical inertness. During the grinding, the EoL salts and agglomerated hard particles were observed. The material was crushed gently in small quantities and at low pressure to avoid friction heating or accidental burning.

The ground material was transferred to a borosilicate glass beaker in a fume hood that was ventilated. Spraying of deionized water was done using a pipette at a distance of 20-30 cm on small chunks of the sample. No sign of bubbling or heat evolution was observed, showing the absence of metallic sodium in the sample. The material was gently stirred with a spatula to wet evenly and prevent any localized reaction.

Following the spraying of water, a bulk dissolution process was undertaken to neutralize safely any remaining reactive sodium and evaluate the water solubility of cathode materials. Water was selected as the initial lixiviant for several reasons: it is a low-cost and environmentally benign solvent, and its use allows an initial assessment of the dissolution behavior of the metal species present. Moreover, because of the potential reactive metallic sodium presence, water is a safer solution for controlled dissolution in terms of both chemical compatibility and safety. On the other hand, although this step is initially undertaken due to the inactivation of sodium, the leaching of the elements is also studied.

Subsequently, powdered cathode material was mixed with deionized water under steady stirring using a VWR Advanced magnetic stirrer (model VMS-C7, MoT 5) reaching a solid-to-liquid ratio of approximately 100 g/L. Room temperature dissolution over 2 hours was conducted to allow sufficient interaction and avoid any further delayed reactions due to trapped sodium.

Right after the dissolution time, the liquid sample was taken and immediately diluted 10 times with 2% HNO_3 to avoid precipitation in the sample for further examination by ICP-OES. ICP-OES analysis was conducted using the Agilent 5900 SVDV, located at Aalto University School of Chemical Engineering.

After the dissolution, solid and liquid separation using vacuum filtration in a Büchner funnel with filter paper(Whatman Grade 1 - pore size of 11 µm - filter paper 150 mm diameter), was unsuccessful. This was due to the immediate clogging of the filter medium. Separation by decantation was applied to separate the supernatant from the settled solids.

Following the water dissolution and deactivation for 2 hours, thirteen successive decantation cycles were performed using deionized water to further purify the cathode composite material from the water-soluble species. In each cycle, the slurry was diluted to a total volume of approximately 1500 mL, and 600-700 mL of the supernatant liquid was carefully separated using a syringe, leaving the settled solids behind. This was repeated until the decanted liquid was clear and colorless, which indicated that most water-soluble species had been removed.

Following the final decantation, the leftover slurry was stirred at 300 rpm using a magnetic stirrer and heater (model VMS-C7, MoT 5) while gently heated to 30-40 °C for around 24 hours to allow partial evaporation of water and achieving a concentrated mixture. The concentrated slurry was poured into plastic weighing boats and allowed to stay in a drying oven at 60 °C for one whole day to dry completely, evaporating any leftover moisture. The dried material was obtained, ground with a mortar, and then reserved for further solid-phase analysis. Dried residue is named as sodium deactivated residue (SDR).

4.4 Raw Material Characterization

A series of analytical processes was utilized to analyze the chemical and structural properties of the cathode material at different stages of processing. These characterizations help to identify significant compounds associated with discharge reactions, remains of electrolytes, and alterations due to deactivation and leaching processes.

4.4.1 X-ray Diffraction (XRD)

X-ray diffraction (XRD) was applied to identify crystalline phases present in the cathode material before and after sodium deactivation. The technique was employed to perform non-destructive structural analysis of salts, discharge products, and residual impurities.

All XRD analysis was conducted at Aalto University School of Chemical Engineering with a PANalytical X'Pert PRO MPD Alpha1 diffractometer. The scan was performed using a normal 90-minute scanning program. Resulting diffraction patterns were properly baseline corrected using HighScore Plus software in order to increase peak clarity and eliminate background noise.

4.4.2 Raman Spectroscopy

Raman spectroscopy was also performed to investigate the carbon structure and disorder degree on both CAM, and SDR samples. The analysis was conducted at the School of Chemical Engineering, Aalto University, using a Renishaw inVia™ Qontor Raman microscope equipped with two laser wavelengths (532 nm green and 785 nm NIR). In this case, a 532 nm laser was employed to enhance the Raman signal of carbon-containing materials. Live Track™ for real-time focus optimization and Wire 5.3 software for spectral acquisition and data processing are components of the system.

Raman spectra were measured in the 100× solid sample objective, with the spectral range set between 100-3000 cm^{-1} to measure the dominant D (~1350 cm^{-1}) and G (~1580 cm^{-1}) bands. ID/IG intensity ratio was used to evaluate the structural disorder of carbon black. Baseline correction and noise filtering were also done during post-processing of the data to maximize spectral purity. These data reveal the nature of the carbonaceous matrix within the CAM, and how structural ordering is impacted by the process of SDR sample.

4.4.3 Particle Size Distribution (PSD) Analysis

For the investigation of the size distribution of the solid powder in the SDR, laser diffraction particle size analysis was conducted by Malvern Mastersizer 3000 (Malvern Instruments, UK) in the School of Chemical Engineering, Aalto University. The analysis was performed using the Hydro EV wet dispersion unit, and deionized water was used as a dispersant. Fraunhofer Spherical Model (MS2000/MS2000E) optical analysis was selected.

Only the SDR example was treated due to safety limitations associated with the untreated CAM, which may still contain reactive sodium and dissolve during the measurement. The deactivated and dried SDR material in powder form was gradually introduced into the dispersion unit in order to avoid agglomeration. Partial flotation of particles, which can be explained by the hydrophobic character of carbonaceous components (e.g., carbon black)[176], was visually observed during dispersion and can affect dispersion uniformity.

Homogenization was achieved during measurement by the instrument's internal stirrer. All of the analyses were conducted under standard conditions, and the results were analyzed with Mastersizer software for volume-based distribution outputs (Dx10, Dx50, Dx90).

4.4.4 X-ray Fluorescence (XRF) Spectroscopy

Elemental analysis of the CAM and SDR samples was also performed using the Hitachi X-MET8000 Expert Geo handheld XRF analyzer in the School of Chemical Engineering, Aalto University. Even though the instrument is very sensitive to elements from magnesium (Mg) through uranium (U), it cannot analyze sodium (Na) since the element has a low atomic number, less than the detection zone of the device. The absence of sodium in the XRF spectra should therefore not be taken as the absolute evidence that it had been eliminated. Further analysis conducted with ICP-OES can complete the gaps and prove the XRF results.

4.5 Leaching

4.5.1 Aqua Regia Leaching Test

Two aqua regia tests were conducted to evaluate the elemental composition of the CAM and SDR. Due to that, a mixture of concentrated hydrochloric acid (HCl) 37% (16 ml) and nitric acid (HNO_3) 65% (4 ml) were prepared. The molar ratio of the aqua regia was 1:3 for HCl to HNO_3. Approximately 0.5 g of the SDR sample, and CAM was leached in 20 ml of Aqua Regia using a 50 ml volumetric flask and a magnetic stirrer (model VMS-C7, MoT 5) for approximately 2 hr. Finally, deionized water was added to reach the volume of 50 ml. . Table 6, depicts the list of chemicals being used in the experiments.

The leachate was allowed to settle for 1.5 hr without being stirred. This step was introduced to reduce clogging and ensure separation. After that, the fine and insoluble particles were removed using a syringe of 20 ml and a Sartorius Minisart® NML sterile syringe filter equipped with a hydrophilic cellulose acetate membrane (pore size 0.2 µm, REF 16592). Immediately, the sample was diluted 10, 100, 1000, and 10000 times using 2% HNO_3 for further analysis using AAS and ICP-OES.

4.5.2 Leaching of SDR Sample

The leaching behavior of the SDR sample was investigated at three different conditions using water, 1 M H_2SO_4, and 1 M HCl as lixiviants. This series of tests was designed to analyze the dissolution behavior of the SDR sample in resembling the industrial leaching at low temperature with moderate agitation. For each leaching test, 16 g of SDR powder was added to 160 mL of the corresponding leaching solution in a glass reactor placed in a water bath to control the temperature. Leaching was performed in an approximately 30 °C water bath, and the mixture was agitated using a mechanical overhead stirrer of VWR model VOS 16 at 300 rpm. Figure 16, illustrates the experimental set-up.

Sampling was conducted at selected time points (5, 15, 30, 60, 90, and 120 min). A sample was taken at each interval, and it was diluted 10-folds with 2 wt% HNO_3 solution immediately before filtration. This method has mainly been considered to avoid the clogging of the syringe filter. The diluted sample was filtered through a 0.2 µm hydrophilic syringe filter (Sartorius Minisart NML). The filtrates were reserved for analysis. Also, redox potential was measured in the intervals using a redox probe (mV vs. Ag/AgCl in 3 M KCl, Mettler Toledo, Germany) and Wavetek 5XL multimeter.

Table 6. Stock chemicals used for preparation of solutions for leaching experiments

Chemical	Formula	Purity	Manufacturer
Hydrochloric acid	HCl	37%	Supelco
Sulfuric acid	H_2SO_4	95-97%	Supelco
Nitric acid	HNO_3	65%	Supelco
Deionized(DI) water	H_2O	ion exchanged	-

Figure 16. Leaching setup with temperature-controlled water bath, and overhead stirrer.

Table 6 shows the list of chemicals used for the leaching and dilution of the samples. The original 10 times diluted samples were further diluted to 1:100, 1:1,000, and 1:10,000 using 2 wt% HNO_3 prepared for the metals scanning by ICP-OES.

4.5.3 ICP-OES

The elemental composition of the PLS from aqua regia digestion and SDR leaching tests were analyzed by Inductively Coupled Plasma Optical Emission Spectrometry (ICP-OES). The analysis was performed at the School of Chemical Engineering, Aalto University, using an Agilent 5900 SVDV ICP-OES instrument.

All filtered samples of aqua regia and leaching tests were submitted to the system after further dilution in 2 wt% HNO_3. The calibration was done using multi-metal standards and a special sulfur (S) standard for the precise quantitation of Al, Na, S, Fe, and other detectable metals.

4.6 Calculations

Leaching extraction efficiency has been calculated using equation 8 below;

$$Me_{extr} = \left(\frac{C_i.V}{m_0.W_i}\right).100\% \quad (8)$$

C_i is the metal concentration in the PLS

V is the solution volume

m_o is the mass of the sample added to the leaching

w_i is the metal concentration in the raw material

5 Results and Discussion

5.1 Raw Material Characterization Results

5.1.1 X-ray Diffraction (XRD) Results

Figure 17, presents the XRD patterns of the untreated cathode active material (CAM), sodium-deactivated residue (SDR), and acid-leached residue (ALR). All samples present broad and sharp diffraction features, indicating the existence of crystalline and possibly amorphous components. The CAM sample has numerous strong peaks, especially in the 20-40° 2θ range, char-

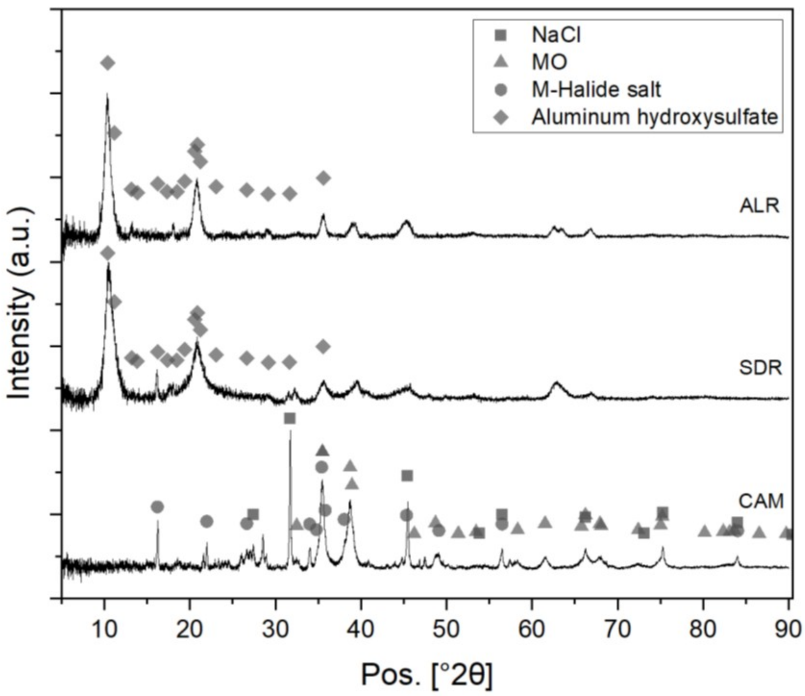

acteristic of crystalline residues from the cell operation and discharge phases.

Figure 17. XRD patterns of untreated CAM, SDR, and ALR with reference peak positions for identified compounds.

To facilitate phase identification, reference peak positions of known materials were overlaid as symbol markers.

Squares (■) represent peaks of sodium chloride (NaCl), a common discharge product. Triangles (▲) denote reflections of a metal oxide (MO) phase, which is expected to be associated with the original cathode composition. Circles (●) represent metal-halide salts, and diamonds (◆) show the position of aluminum hydroxysulfate, which has been detected after the sodium deactivation and drying of the residue as well as in the ALR.

The SDR sample contains lower-intensity and wider features, reflecting partial dissolution or loss of some crystalline salts following the aqueous treatment. Elimination of NaCl-derived peaks in the SDR sample is evidence of the efficiency of the leaching process in eliminating soluble electrolyte residues, as was predicted due to high solubility of NaCl[177]. The halide's elimination also indicates solubility or decomposition in mild aqueous conditions. Sodium-deactivated residue (SDR) demonstrated the development of novel diffraction peaks not found in the untreated cathode composite sample. The changes in the composition of the SDR over CAM, can basically stem from the dissolution of NaCl, MO, and M-Halide salts, which removes more soluble phases, and the presence of the dissolved Al and sulfate ions lead to the precipitation of Al hydroxysulfate visible in the XRD patterns.

The presence of the same peaks of aluminum hydroxysulfate in ALR sample, indicates incomplete leaching of the phase in acidic solution.

5.1.2 Raman Spectroscopy Results

Figure 18 displays the Raman spectra for the untreated CAM, and SDR samples. The D and G bands are illustrated at around 1350 cm^{-1} and 1580 cm^{-1}, respectively pinpointing of graphitic and disordered carbon structures. The ratio of the intensity of the D to G bands (ID/IG) gives an indication of structural disorder in the carbon structure.

The ID/IG ratio of the CAM sample is 1.057, while that of the SDR sample is slightly higher at 1.098. The modest improvement can be considered negligible, and the exposure to water leaching and drying has not changed or damaged the structure. Furthermore, both spectra have a weak 2D band at ~2700 cm^{-1}, revealing the presence of few-layer graphitic domains.

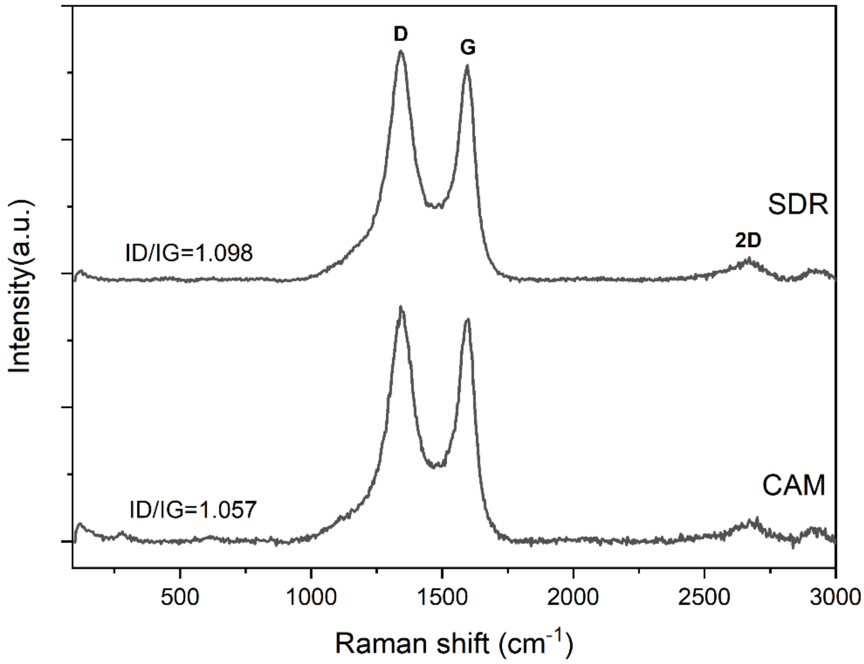

Figure 18. Raman spectra of CAM and SDR samples showing D, G, and 2D bands.

5.1.3 Particle Size Distribution (PSD) Analysis Results

Figure 19 reveals the PSD of SDR sample possessing a wide distribution from tens to over a thousand micrometres. The wide range represents the morphology of carbon black composite cathode materials, where nanometre-sized carbon nodules agglomerate into larger bundles. Looking at Figure 20, based on the literature, the particle size of carbon black is primarily in the range of 10 nm, while due to the Van der Waals forces, they can agglomerate to form larger particles in the size range of microns[178].

The presence of large agglomerates, indicated by the high D90 value (1230 µm) as depicted in

Table 7, is an indication of poor dispersion or re-agglomeration during drying caused by the hydrophobicity of carbon black or poor deagglomeration in water during particle size measurement. Agglomeration principles in carbon black are illustrated in Figure 20. It is also explained by visual flotation behavior under wet dispersion conditions in the PSD test, where certain hydro-

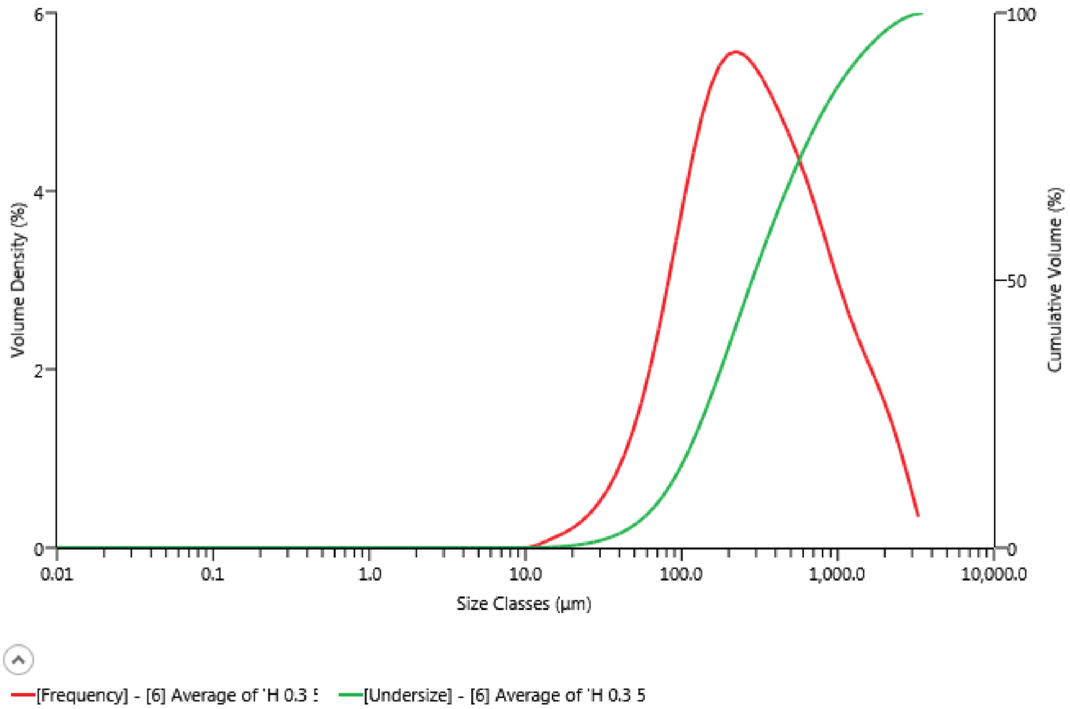

Figure 19. Particle size distribution of SDR

phobic particles were found to resist complete wetting and floated suspended at the surface.

Table 7. Percentile-based particle size distribution parameters of SDR

Percentile	Diameter (µm)
Dx(10)	77.3
Dx(50)	282

Dx(90)	1230

5.1.4 X-ray Fluorescence (XRF) Spectroscopy Results

The weight percentages of the elements detected in CAM and SDR are shown in the Table 8, as measured by XRF. Regarding normalized results (wt%) from XRF, variation between CAM and SDR samples is a relative change in abundance, not a definite indication of element loss or gain. These values need to be interpreted in terms of changes in composition after the other components were eliminated.

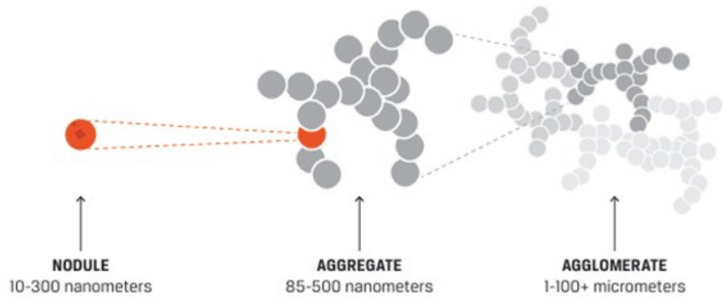

Figure 20. Structure of carbon black particles[178].

For instance, Cl content in the CAM was 5.32 wt%, and the absence of Cl in the SDR sample strongly points to the removal of chlorine-bearing salts such as $NaAlCl_4$ or NaCl during deactivation. Conversely, the observed Al and S wt% increase is likely to be attributed to their incrementation of the normalized value in the solid matrix, since more soluble species were removed. Although the initial CAM composite depicts the presence of Mg, the disappearance of the element during the sodium deactivation process proves that Mg salts in the CAM are water-soluble.

Similarly, the determined decrease in the unknown metal (M) grade from 10.02% to 7.68% may show partial dissolution or redistribution. Based on the XRD comparative results in

Figure 17, the presence of the MO or M-Halide salt species in the SDR could not be confirmed, which initially suggested complete dissolution of those phases. The results illustrated in the Table 8, indicates that not all of the species containing the M have been dissolved. However, without corroborative mass balance information, this observation by itself is insufficient to prove dissolution as there are other elements involved in the mass balance. This is further investigated by the ICP-OES test reported in the next sections.

Table 8. Elemental composition of CAM and SDR samples measured by XRF (wt%).

Element	**CAM**	**CAM(**SD**)**	**SDR**	**SDR(**SD)
M(wt%)	10.02	0.82	7.68	0.31
Cl(wt%)	5.32	0.64	NA	NA
Al(wt%)	3.38	0.28	6.45	0.18
Mg(wt%)	1.18	0.06	NA	NA
S(wt%)	0.46	0.14	2.01	0.08
Other(wt%)	Trace	NA	Trace	NA

[1] NA refers to not applicable; the values are out of the range of the validation.

[2] SD refers to the standard deviation.

[3] M refers to an unknown metal.

[4] Trace values are below 0.1 wt%.

[5] The values are the average of three measurements.

5.2 Leaching efficiency via ICP-OES

The results in this section are divided into two main scopes: (1) evaluation of the initial elemental content of CAM and SDR samples before leaching, and (2) investigation of leaching efficiency in different media via ICP-OES data.

As was mentioned before, the immediate clogging of the paper and syringe filters was evident during the filtration of pregnant leach solution (PLS) and samples. This issue hindered standard vacuum filtration and prevented proper monitoring of the mass balance. As a result, decantation was chosen for the methodology instead of filtration. Looking at the main reason for this phenomenon, the basic studies have shown that this has stemmed from the presence of carbon black particles in high amounts in the CAM.

Looking at the carbon black structure, Donnet et al. (1993) described vacuum densification as a process where fine carbon black powder is pressed against porous rollers under vacuum pressure, and this, coupled with the fine particle size, leads to a very dense material layer[179]. The same effect can be observed in vacuum filtration of suspensions of carbon black, where finer particles deposit rapidly onto the surface of the filter paper. The filter cake layer forms rapidly and clogs the filter, hindering the free flow of liquid through it and ultimately making the filtration impossible. As another observation during the analysis, grinding the sample with pressing by pestle was inefficient and resulted in the film like layer formation. This is aligned also with the development of carbon black cake under the pressure.

During aqua regia test, the low wettability of SDR sample was observed, Figure 21. This phenomena was due to the high carbon content, which is intrinsically hydrophobic[180].

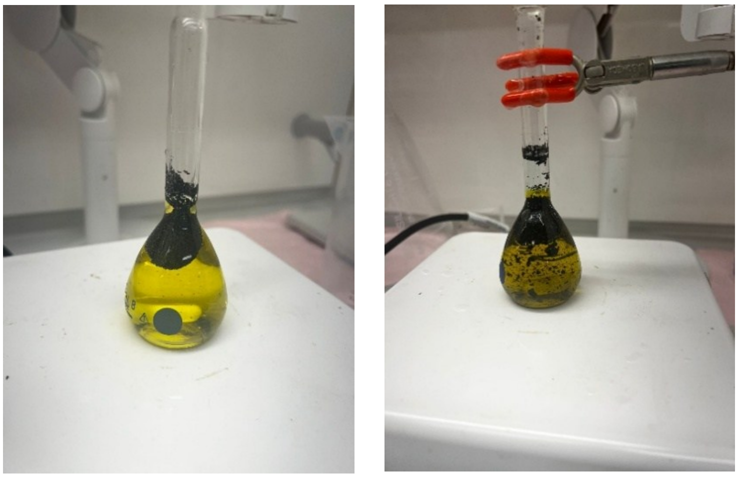

Figure 21. Observation of solid residue hydrophobic behavior during aqua regia leaching of SDR before, and after long time mixing.

Error! Reference source not found., depicts the elemental composition of t he CAM and SDR samples, by ICP-OES, out of the aqua regia analysis. The discrepancy of the values between the XRF and ICP-OES aqua regia can be related to the technics of the evaluation they have for analyzing the sample. In XRF mainly the surface of the samples is being analyzed, and the density of the elements might affect the presence of the elements on the surface. On the other hand, samples of CAM are possibly heterogenous and this also might have an effect on the discrepancy in the results of XRF and ICP-OES. Not to mention that the presence of the elements like sodium, which is not detectable in XRF, can have a high contribution on the deviations of the values precent in the surface evaluation of the XRF. The main purpose of the XRF in this thesis was initial investigation on the presence of other types of elements.

Table 9. Elemental composition of CAM and SDR samples measured by ICP-OES(wt%).

Element	CAM	SDR
M(wt%)	22.40	12.55
S(wt%)	8.27	5.50
Na(wt%)	5.92	0.28
Al(wt%)	5.73	11.48
Fe(wt%)	0.10	0.03

The sodium in CAM is derived from EoL battery salt, identified as NaCl during initial XRD testing. NaCl is highly soluble in water, and therefore it was expected that excessive sodium would be dissolved during sodium deactivation and decantation processes[177]. Other potential EoL sodium salts, such as dried electrolyte ($NaAlCl_4$)[181] or EoL sodium polysulfides[182], are all water-soluble species as well. During sodium deactivation the metal (M) element was partially leached out from the sample.

Figure 22, illustrates the extraction efficiencies for both aluminum and sulfur in 2 hr leaching. The primary source of the aluminum is from the dried electrolyte with minor possibility of small pieces, from current collector possibly present during the disassembly. Figure 22 a) 1 M H_2SO_4 demonstrates the highest aluminum extraction efficiency, reaching nearly 90% within the first 20 minutes, suggesting rapid initial leaching kinetics. 1 M HCl also facilitates substantial Al extraction, between 60% and 70%, in 5 minutes. In contrast, water as a lixiviant exhibits negligible Al extraction (<5%). The observed fluctuations in extraction efficiency, particularly in acidic media, can be related to experimental uncertainties arising from the presence of residual carbon in the sample matrix, clogging the syringes during sampling. Not to mention that during all the intervals, the samples taken out of the reactor were allowed to wait to be decanted and then diluted, to avoid any clogging of the filter happening during the test. However, this approach might introduce uncertainties to the analysis. Based on the observations of Partinen et al. leaching behavior of aluminum current collectors out of the black mass at 30°C with 2M H_2SO_4 and S/L 200 g/L can approximately reach 35% after 2 hours[183]. Joulié et al. have examined the leaching behavior of aluminum out of the

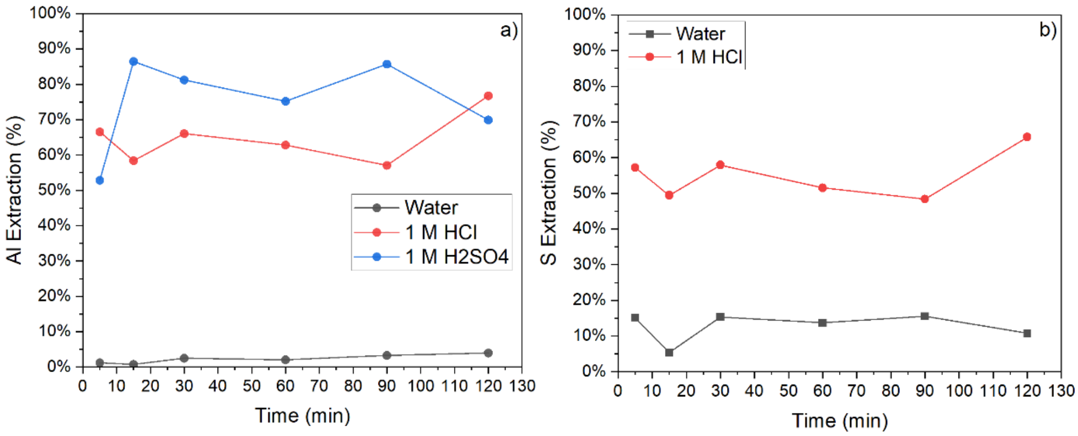

NCA cathode material. Based on their observations using 1M HCl, the leaching efficiency of aluminum can approximately reach 37% at 25°C after 18 hours with S/L = 5%(w/v), while with 2M H_2SO_4 under the same conditions, it roughly reaches 37%[184]. The contrast in the results with the current study can stem from the material structure of the species under investigation.

Figure 22. Effect of leaching time on the extraction efficiency of, a) aluminum (Al) and, b) sulfur (S) using different lixiviants.

Figure 22 b), presents sulfur extraction efficiency based on time. While 1 M HCl enables moderate S extraction (50-65%), water again shows poor performance (<15%). It can be interpreted as 15% of the containing sulfur is in the form of water-soluble compounds still existing in the SDR sample. The extracted ratio of sulfur in water shows higher values than the aluminum, indicating that there might be a difference in the solubility of the salt types. Notably, sulfur extraction using 1 M H_2SO_4 is not reported. This is due to the high sulfate background inherent in sulfuric acid, which interferes with accurate sulfur quantification in solution.

Figure 23, demonstrates redox potential evolution of the leaching solution during water, 1 M HCl, and 1 M H_2SO_4 leaching over 120 minutes. The trend suggests that leaching was largely proton-driven, as opposed to redox-driven by electron transfer reactions. The acidic medium (HCl and H_2SO_4) had higher redox potentials than water. This is due to the fact that acids contain a larger concentration of protons (H^+), thus it becomes easier to dissolve oxides and salts using acid-base reactions.

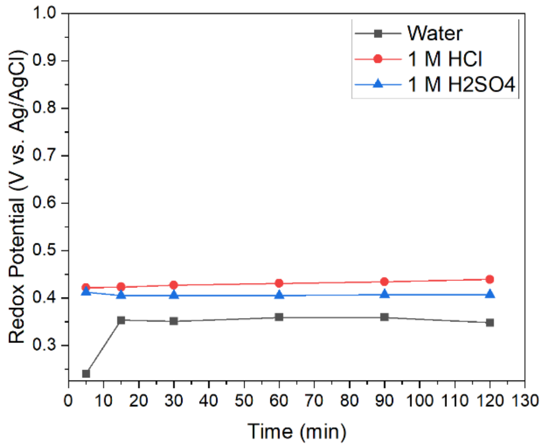

Figure 23. Redox potential vs. time in H_2O, HCl, and H_2SO_4 leaching

6 Conclusions and Future Directions

Future battery recyclability is not only dependent on process compatibility but also on the range of chemistries being developed, unpredictability of dominant battery types in the market, and evolving definition of circularity in the sector. Identifying the battery type, through methods like the battery passport, is still necessary in coordinating recycling strategies with material content and recovery potential.

- Future batteries integration to hydrometallurgical recycling processes: While hydrometallurgical processes have enhanced recovery efficiencies and selectivity, a lack of sufficient knowledge regarding the decomposition behavior of most novel cathode and electrolyte chemistries limits the understanding of the pathways during purification and separation. Without absolute data on the interaction between the materials in a solution, integration into existing hydrometallurgical lines involves both technical and quality risks. Not to mention that further purification steps need to be taken into consideration to recover all of the elements.
- Future batteries integration to pyrometallurgical recycling processes: Pyrometallurgical processes' broad compositional flexibility can provide greater potential for the digestion of different materials from next-generation batteries. However, the value derived from such routes, yielding downcycled products or conversion to energy, must be recalibrated on the basis of what constitutes a circular economy benefit.
- Selective water leaching, which is compatible with some types of SSEs, is a very attractive option as an initial lixiviant. Also, in sodium ion batteries CAM, if sodium can be removed from the CAM using water, this can reduce the contamination during CAM separation and decomposition, and in some cases, recover species such as lithium at an initial step. As in some structures, most significantly oxide-based SSEs, water is not a viable stand-alone strategy due to the low solubility of the major components. This also highlights the requirement of a standardized battery

passport, as incorrect identification can increase gas evolution risks with corresponding costly scrubbing systems and/or higher capital expenditure.

- Leaching results of experimental analysis show great potential for the CAM and EoL salts' leaching behavior. The sodium deactivation step can inherently remove NaCl while also decomposing water-soluble salts. Although the presence of sulfur ions, together with aluminum and halides, can lead to the formation of a new phase after the sodium deactivation step, the leaching behavior of aluminum from this structure exhibits fast dissolution with high leaching efficiency (90% with 1 M H_2SO_4 and nearly 60% with 1 M HCl), suggesting rapid initial leaching kinetics. This indicates that the aluminum phase generated is less stable against acid leaching compared to the aluminum present in NCA CAM or the aluminum current collector reported in the literature, thereby confirming its higher solubility.

The integration and recovery routes for most future battery chemistries remain extremely underdeveloped. Future research needs to take technical feasibility into account, while economic motivations, lifecycle trade-offs, and regulatory frameworks that would encourage recycling need to be studied.

References

[1] “Electric vehicles - European Commission.” Accessed: Feb. 19, 2025. [Online]. Available: https://transport.ec.europa.eu/transport-themes/clean-transport/clean-and-energy-efficient-vehicles/green-propulsion-transport/electric-vehicles_en

[2] D. Latini *et al.*, “A comprehensive review and classification of unit operations with assessment of outputs quality in lithium-ion battery recycling,” *Journal of Power Sources*, vol. 546, p. 231979, Oct. 2022, doi: 10.1016/j.jpowsour.2022.231979.

[3] M. Ge, J. Friedrich, and L. Vigna, “Where Do Emissions Come From? 4 Charts Explain Greenhouse Gas Emissions by Sector,” Dec. 2024, Accessed: Feb. 19, 2025. [Online]. Available: https://www.wri.org/insights/4-charts-explain-greenhouse-gas-emissions-countries-and-sectors

[4] F. Núñez, D. Canca, and Á. Arcos-Vargas, “An assessment of European electricity arbitrage using storage systems,” *Energy*, vol. 242, p. 122916, Mar. 2022, doi: 10.1016/j.energy.2021.122916.

[5] P. Alotto, M. Guarnieri, and F. Moro, “Redox flow batteries for the storage of renewable energy: A review,” *Renewable and Sustainable Energy Reviews*, vol. 29, pp. 325–335, Jan. 2014, doi: 10.1016/j.rser.2013.08.001.

[6] S. Passerini, L. Barelli, M. Baumann, J. Peters, and M. Weil, Eds., *Emerging Battery Technologies to Boost the Clean Energy Transition: Cost, Sustainability, and Performance Analysis*. in The Materials Research Society Series. Cham: Springer International Publishing, 2024. doi: 10.1007/978-3-031-48359-2.

[7] “EuropeanTechnologyandInnovationPlatformonBatteries:Strategicresearchagendaforbatteries(2020)Online.” [Online]. Available: :https://www.era-min.eu/sites/default/files/docs/batteries_europe_strategic_resea.pdf

[8] A. Nordelöf, S. Poulikidou, M. Chordia, F. Bitencourt De Oliveira, J. Tivander, and R. Arvidsson, “Methodological Approaches to End-Of-Life Modelling in Life Cycle Assessments of Lithium-Ion Batteries,” *Batteries*, vol. 5, no. 3, p. 51, Jul. 2019, doi: 10.3390/batteries5030051.

[9] “IEA (2022) Global EV Outlook 2022. IEA, Paris.”

[10] Y. Zhao *et al.*, “Recycling of sodium-ion batteries,” *Nat Rev Mater*, vol. 8, no. 9, pp. 623–634, Jul. 2023, doi: 10.1038/s41578-023-00574-w.

[11] F. Duffner, N. Kronemeyer, J. Tübke, J. Leker, M. Winter, and R. Schmuch, “Post-lithium-ion battery cell production and its compatibility with lithium-ion cell production infrastructure,” *Nat Energy*, vol. 6, no. 2, pp. 123–134, Jan. 2021, doi: 10.1038/s41560-020-00748-8.

[12] J. Janek and W. G. Zeier, “Challenges in speeding up solid-state battery development,” *Nat Energy*, vol. 8, no. 3, pp. 230–240, Feb. 2023, doi: 10.1038/s41560-023-01208-9.

[13] J. Baars, T. Domenech, R. Bleischwitz, H. E. Melin, and O. Heidrich, “Circular economy strategies for electric vehicle batteries reduce reliance on raw materials,” *Nat Sustain*, vol. 4, no. 1, pp. 71–79, Sep. 2020, doi: 10.1038/s41893-020-00607-0.

[14] S. Gifford, “Lithium, Cobalt and Nickel: The Gold Rush of the 21st Century,” no. 6.

[15] Y. Bai, N. Muralidharan, Y.-K. Sun, S. Passerini, M. Stanley Whittingham, and I. Belharouak, “Energy and environmental aspects in recycling lithium-ion batteries: Concept of Battery Identity Global Passport,” *Materials Today*, vol. 41, pp. 304–315, Dec. 2020, doi: 10.1016/j.mattod.2020.09.001.

[16] F. Degen, M. Mitterfellner, and A. Kampker, “Comparative life cycle assessment of lithium-ion, sodium-ion, and solid-state battery cells for electric vehicles,” *Journal of Industrial Ecology*, vol. 29, no. 1, pp. 113–128, 2025, doi: 10.1111/jiec.13594.

[17] J. Betz, G. Bieker, P. Meister, T. Placke, M. Winter, and R. Schmuch, “Theoretical versus Practical Energy: A Plea for More Transparency in the Energy Calculation of Different Rechargeable Battery Systems,” *Advanced Energy Materials*, vol. 9, no. 6, p. 1803170, Feb. 2019, doi: 10.1002/aenm.201803170.

[18] Z. Zhang *et al.*, “New horizons for inorganic solid state ion conductors,” *Energy Environ. Sci.*, vol. 11, no. 8, pp. 1945–1976, Aug. 2018, doi: 10.1039/C8EE01053F.

[19] “Polymer Electrolytes for Lithium-Based Batteries: Advances and Prospects - ScienceDirect.” Accessed: Mar. 17, 2025. [Online]. Available: https://www.sciencedirect.com/science/article/pii/S2451929419302190

[20] V. Thangadurai, H. Kaack, and W. J. F. Weppner, “Novel Fast Lithium Ion Conduction in Garnet-Type $Li_5 La_3 M_2 O_{12}$ (M = Nb, Ta),” *Journal of the American Ceramic Society*, vol. 86, no. 3, pp. 437–440, Mar. 2003, doi: 10.1111/j.1151-2916.2003.tb03318.x.

[21] W. G. Zeier, “Structural limitations for optimizing garnet-type solid electrolytes: a perspective,” *Dalton Trans.*, vol. 43, no. 43, pp. 16133–16138, 2014, doi: 10.1039/C4DT02162B.

[22] J. B. Bates *et al.*, “Electrical properties of amorphous lithium electrolyte thin films,” *Solid State Ionics*, vol. 53–56, pp. 647–654, Jul. 1992, doi: 10.1016/0167-2738(92)90442-R.

[23] W. Ju Kwon *et al.*, “Enhanced Li + conduction in perovskite Li 3x La 2/3−x □ 1/3−2x TiO 3 solid-electrolytes via microstructural engineering,” *Journal of Materials Chemistry A*, vol. 5, no. 13, pp. 6257–6262, 2017, doi: 10.1039/C7TA00196G.

[24] “Synthesis and Properties of NaSICON-type LATP and LAGP Solid Electrolytes - DeWees - 2019 - ChemSusChem - Wiley Online Library.” Accessed: Mar. 18, 2025. [Online]. Available: https://chemistry-europe.onlinelibrary.wiley.com/doi/full/10.1002/cssc.201900725

[25] “Synthesis, conductivity and structural aspects of Nd 3 Zr 2 Li 7−3x Al x O 12 - Journal of Materials Chemistry A (RSC Publishing) DOI:10.1039/C3TA13252H.” Accessed: Mar. 18, 2025. [Online]. Available: https://pubs.rsc.org/en/content/articlehtml/2013/ta/c3ta13252h

[26] K. Waetzig *et al.*, “Synthesis and sintering of Li1.3Al0.3Ti1.7(PO4)3 (LATP) electrolyte for ceramics with improved Li+ conductivity,” *Journal of Alloys and Compounds*, vol. 818, p. 153237, Mar. 2020, doi: 10.1016/j.jallcom.2019.153237.

[27] R. Djenadic *et al.*, “Nebulized spray pyrolysis of Al-doped Li7La3Zr2O12 solid electrolyte for battery applications,” *Solid State Ionics*, vol. 263, pp. 49–56, Oct. 2014, doi: 10.1016/j.ssi.2014.05.007.

[28] M. Botros, R. Djenadic, O. Clemens, M. Möller, and H. Hahn, “Field assisted sintering of fine-grained Li7−3xLa3Zr2AlxO12 solid electrolyte and the influence of the microstructure on the electrochemical performance,” *Journal of Power Sources*, vol. 309, pp. 108–115, Mar. 2016, doi: 10.1016/j.jpowsour.2016.01.086.

[29] S. Lobe, A. Bauer, D. Sebold, N. Wettengl, D. Fattakhova-Rohlfing, and S. Uhlenbruck, “Sintering of Li-garnets: Impact of Al-incorporation and powder-bed composition on microstructure and ionic conductivity,” *Open Ceramics*, vol. 10, p. 100268, Jun. 2022, doi: 10.1016/j.oceram.2022.100268.

[30] L. Chen, Y. Li, S.-P. Li, L.-Z. Fan, C.-W. Nan, and J. B. Goodenough, “PEO/garnet composite electrolytes for solid-state lithium batteries: From ‘ceramic-in-polymer’ to ‘polymer-in-ceramic,’” *Nano Energy*, vol. 46, pp. 176–184, Apr. 2018, doi: 10.1016/j.nanoen.2017.12.037.

[31] "Capacity Fade in Solid-State Batteries: Interphase Formation and Chemomechanical Processes in Nickel-Rich Layered Oxide Cathodes and Lithium Thiophosphate Solid Electrolytes | Chemistry of Materials." Accessed: Mar. 18, 2025. [Online]. Available: https://pubs.acs.org/doi/full/10.1021/acs.chemmater.7b00931

[32] R. Koerver *et al.*, "Chemo-mechanical expansion of lithium electrode materials – on the route to mechanically optimized all-solid-state batteries," *Energy & Environmental Science*, vol. 11, no. 8, pp. 2142–2158, 2018, doi: 10.1039/C8EE00907D.

[33] D. T. Schmaltz, "Solid-State Battery Roadmap 2035+".

[34] M. Ahuis, S. Doose, D. Vogt, P. Michalowski, S. Zellmer, and A. Kwade, "Recycling of solid-state batteries," *Nat Energy*, vol. 9, no. 4, pp. 373–385, Mar. 2024, doi: 10.1038/s41560-024-01463-4.

[35] A. Jetybayeva, D. S. Aaron, I. Belharouak, and M. M. Mench, "Critical review on recently developed lithium and non-lithium anode-based solid-state lithium-ion batteries," *Journal of Power Sources*, vol. 566, p. 232914, May 2023, doi: 10.1016/j.jpowsour.2023.232914.

[36] A. Müller *et al.*, "Influence of Au, Pt, and C Seed Layers on Lithium Nucleation Dynamics for Anode-Free Solid-State Batteries," *ACS Appl. Mater. Interfaces*, vol. 16, no. 1, pp. 695–703, Jan. 2024, doi: 10.1021/acsami.3c14693.

[37] K. Schneider and D. Goldmann, "Oxide-based lithium solid-state batteries from a recycling perspective".

[38] "Study on the Critical Raw Materials for the EU 2023 – Final Report".

[39] M. Fingerle, C. Loho, T. Ferber, H. Hahn, and R. Hausbrand, "Evidence of the chemical stability of the garnet-type solid electrolyte Li5La3Ta2O12 towards lithium by a surface science approach," *Journal of Power Sources*, vol. 366, pp. 72–79, Oct. 2017, doi: 10.1016/j.jpowsour.2017.08.109.

[40] M. Jacob, K. Wissel, and O. Clemens, "Recycling of solid-state batteries—challenge and opportunity for a circular economy?," *Mater. Futures*, vol. 3, no. 1, p. 012101, Jan. 2024, doi: 10.1088/2752-5724/acfb28.

[41] Q. Zhang, D. Cao, Y. Ma, A. Natan, P. Aurora, and H. Zhu, "Sulfide-Based Solid-State Electrolytes: Synthesis, Stability, and Potential for All-Solid-State Batteries," *Advanced Materials*, vol. 31, no. 44, p. 1901131, Nov. 2019, doi: 10.1002/adma.201901131.

[42] “Anomalous High Ionic Conductivity of Nanoporous β-Li3PS4 | Journal of the American Chemical Society.” Accessed: Mar. 19, 2025. [Online]. Available: https://pubs.acs.org/doi/full/10.1021/ja3110895

[43] H.-J. Deiseroth *et al.*, “Li6PS5X: A Class of Crystalline Li-Rich Solids With an Unusually High Li+ Mobility*”.

[44] Y. Li *et al.*, “A lithium superionic conductor for millimeter-thick battery electrode,” *Science*, vol. 381, no. 6653, pp. 50–53, Jul. 2023, doi: 10.1126/science.add7138.

[45] A. J. Pearse, “DEPOSITED THREE DIMENSIONAL ALL-SOLID-STATE BATTERIES”.

[46] X. Nie, J. Hu, and C. Li, “Halide-based solid electrolytes: The history, progress, and challenges,” *Interdisciplinary Materials*, vol. 2, no. 3, pp. 365–389, 2023, doi: 10.1002/idm2.12090.

[47] W. Weppner and R. A. Huggins, “Ionic conductivity of alkali metal chloroaluminates,” *Physics Letters A*, vol. 58, no. 4, pp. 245–248, Sep. 1976, doi: 10.1016/0375-9601(76)90087-6.

[48] T. Asano, A. Sakai, S. Ouchi, M. Sakaida, A. Miyazaki, and S. Hasegawa, “Solid Halide Electrolytes with High Lithium-Ion Conductivity for Application in 4 V Class Bulk-Type All-Solid-State Batteries,” *Advanced Materials*, vol. 30, no. 44, p. 1803075, 2018, doi: 10.1002/adma.201803075.

[49] C. Wang, J. Liang, J. T. Kim, and X. Sun, “Prospects of halide-based all-solid-state batteries: From material design to practical application,” *Science Advances*, vol. 8, no. 36, p. eadc9516, Sep. 2022, doi: 10.1126/sciadv.adc9516.

[50] X. Li *et al.*, “Progress and perspectives on halide lithium conductors for all-solid-state lithium batteries,” *Energy Environ. Sci.*, vol. 13, no. 5, pp. 1429–1461, May 2020, doi: 10.1039/C9EE03828K.

[51] R. Schlem *et al.*, “Mechanochemical Synthesis: A Tool to Tune Cation Site Disorder and Ionic Transport Properties of Li3MCl6 (M = Y, Er) Superionic Conductors,” *Advanced Energy Materials*, vol. 10, no. 6, p. 1903719, 2020, doi: 10.1002/aenm.201903719.

[52] J. Liang *et al.*, “Site-Occupation-Tuned Superionic LixScCl3+xHalide Solid Electrolytes for All-Solid-State Batteries,” *J. Am. Chem. Soc.*, vol. 142, no. 15, pp. 7012–7022, Apr. 2020, doi: 10.1021/jacs.0c00134.

[53] X. Li *et al.*, “Water-Mediated Synthesis of a Superionic Halide Solid Electrolyte,” *Angewandte Chemie International Edition*, vol. 58, no. 46, pp. 16427–16432, 2019, doi: 10.1002/anie.201909805.

[54] T. L. M. Exchange, “Metals | London Metal Exchange,” Lme. Accessed: Jun. 25, 2025. [Online]. Available: https://www.lme.com/Metals

[55] “Rare Earth Metals Prices, Price of Lanthanum, Cerium, Neodymium, Yttrium, Scandium| SMM Metal Market.” Accessed: Jul. 16, 2025. [Online]. Available: https://www.metal.com/Rare-Earth-Metals/

[56] J. Li *et al.*, “Development of solid polymer electrolytes for solid-state lithium battery applications,” *Materials Today Energy*, vol. 43, p. 101574, Jul. 2024, doi: 10.1016/j.mtener.2024.101574.

[57] P. V. Wright, “Electrical conductivity in ionic complexes of poly(ethylene oxide),” *British Polymer Journal*, vol. 7, no. 5, pp. 319–327, 1975, doi: 10.1002/pi.4980070505.

[58] M. Armand, “Polymer solid electrolytes - an overview,” *Solid State Ionics*, vol. 9–10, pp. 745–754, Dec. 1983, doi: 10.1016/0167-2738(83)90083-8.

[59] Q. Hu, Z. Sun, L. Nie, S. Chen, J. Yu, and W. Liu, “High-safety composite solid electrolyte based on inorganic matrix for solid-state lithium-metal batteries,” *Materials Today Energy*, vol. 27, p. 101052, Jul. 2022, doi: 10.1016/j.mtener.2022.101052.

[60] L. Nastasi and S. Fiore, “Environmental Assessment of Lithium-Ion Battery Lifecycle and of Their Use in Commercial Vehicles,” *Batteries*, vol. 10, no. 3, Art. no. 3, Mar. 2024, doi: 10.3390/batteries10030090.

[61] H. Zhang *et al.*, “Recent progress in advanced electrode materials, separators and electrolytes for lithium batteries,” *J. Mater. Chem. A*, vol. 6, no. 42, pp. 20564–20620, Oct. 2018, doi: 10.1039/C8TA05336G.

[62] P. B. Bobba, L. S. H. Yerraguntla, S. Pisini, H. P. Bhupathi, S. D, and M. M. Hassan, “Performance analysis of solid-state batteries in Electric vehicle applications,” *E3S Web Conf.*, vol. 552, p. 01149, 2024, doi: 10.1051/e3sconf/202455201149.

[63] C. Delmas, “Sodium and Sodium-Ion Batteries: 50 Years of Research,” *Advanced Energy Materials*, vol. 8, no. 17, p. 1703137, Jun. 2018, doi: 10.1002/aenm.201703137.

[64] I. Hasa *et al.*, “Challenges of today for Na-based batteries of the future: From materials to cell metrics,” *Journal of Power Sources*, vol. 482, p. 228872, Jan. 2021, doi: 10.1016/j.jpowsour.2020.228872.

[65] H. Rostami, J. Valio, P. Suominen, P. Tynjälä, and U. Lassi, “Advancements in cathode technology, recycling strategies, and market dynamics: A comprehensive review of sodium ion batteries,” *Chemical Engineering Journal*, vol. 495, p. 153471, Sep. 2024, doi: 10.1016/j.cej.2024.153471.

[66] X. Cai, Y. Yue, Z. Yi, J. Liu, Y. Sheng, and Y. Lu, “Challenges and industrial perspectives on the development of sodium ion batteries,” *Nano Energy*, vol. 129, p. 110052, Oct. 2024, doi: 10.1016/j.nanoen.2024.110052.

[67] H. Moriwake, A. Kuwabara, C. A. J. Fisher, and Y. Ikuhara, “Why is sodium-intercalated graphite unstable?,” *RSC Adv.*, vol. 7, no. 58, pp. 36550–36554, Jul. 2017, doi: 10.1039/C7RA06777A.

[68] P. Phogat, S. Dey, and M. Wan, “Comprehensive review of Sodium-Ion Batteries: Principles, Materials, Performance, Challenges, and future Perspectives,” *Materials Science and Engineering: B*, vol. 312, p. 117870, Feb. 2025, doi: 10.1016/j.mseb.2024.117870.

[69] F. Xiong *et al.*, “Revealing the atomistic origin of the disorder-enhanced Na-storage performance in NaFePO4 battery cathode,” *Nano Energy*, vol. 57, pp. 608–615, Mar. 2019, doi: 10.1016/j.nanoen.2018.12.087.

[70] J.-M. Kim *et al.*, “Stearoyl lysophosphatidylcholine prevents lipopolysaccharide-induced extracellular release of high mobility group box-1 through AMP-activated protein kinase activation,” *International Immunopharmacology*, vol. 28, no. 1, pp. 540–545, Sep. 2015, doi: 10.1016/j.intimp.2015.07.010.

[71] Y.-F. Liu *et al.*, “Layered oxide cathodes for sodium-ion batteries: From air stability, interface chemistry to phase transition,” *InfoMat*, vol. 5, no. 6, p. e12422, 2023, doi: 10.1002/inf2.12422.

[72] J. Peng *et al.*, “Prussian Blue Analogues for Sodium-Ion Batteries: Past, Present, and Future,” *Advanced Materials*, vol. 34, no. 15, p. 2108384, 2022, doi: 10.1002/adma.202108384.

[73] H. S. Hirsh, Y. Li, D. H. S. Tan, M. Zhang, E. Zhao, and Y. S. Meng, “Sodium-Ion Batteries Paving the Way for Grid Energy Storage,” *Advanced Energy Materials*, vol. 10, no. 32, p. 2001274, 2020, doi: 10.1002/aenm.202001274.

[74] E. Irisarri, A. Ponrouch, and M. R. Palacin, “Review—Hard Carbon Negative Electrode Materials for Sodium-Ion Batteries,” *J. Electrochem. Soc.*, vol. 162, no. 14, p. A2476, Oct. 2015, doi: 10.1149/2.0091514jes.

[75] C. Bommier and X. Ji, “Electrolytes, SEI Formation, and Binders: A Review of Nonelectrode Factors for Sodium-Ion Battery Anodes,” *Small*, vol. 14, no. 16, p. 1703576, 2018, doi: 10.1002/smll.201703576.

[76] J. Zhang *et al.*, “Cathode Recycling of Spent Sodium Ion Batteries,” *Energy Material Advances*, vol. 5, p. 0128, Nov. 2024, doi: 10.34133/energymatadv.0128.

[77] M. Chen *et al.*, “Recycling End-of-Life Electric Vehicle Lithium-Ion Batteries,” *Joule*, vol. 3, no. 11, pp. 2622–2646, Nov. 2019, doi: 10.1016/j.joule.2019.09.014.

[78] D. Yu, Z. Huang, B. Makuza, X. Guo, and Q. Tian, “Pretreatment options for the recycling of spent lithium-ion batteries: A comprehensive review,” *Minerals Engineering*, vol. 173, p. 107218, Nov. 2021, doi: 10.1016/j.mineng.2021.107218.

[79] X. Zhang *et al.*, “Toward sustainable and systematic recycling of spent rechargeable batteries,” *Chem. Soc. Rev.*, vol. 47, no. 19, pp. 7239–7302, Oct. 2018, doi: 10.1039/C8CS00297E.

[80] F. Larouche *et al.*, “Progress and Status of Hydrometallurgical and Direct Recycling of Li-Ion Batteries and Beyond,” *Materials*, vol. 13, no. 3, p. 801, Feb. 2020, doi: 10.3390/ma13030801.

[81] S. Doose, J. K. Mayer, P. Michalowski, and A. Kwade, “Challenges in Ecofriendly Battery Recycling and Closed Material Cycles: A Perspective on Future Lithium Battery Generations,” *Metals*, vol. 11, no. 2, p. 291, Feb. 2021, doi: 10.3390/met11020291.

[82] S. P. Culver, R. Koerver, W. G. Zeier, and J. Janek, “On the Functionality of Coatings for Cathode Active Materials in Thiophosphate-Based All-Solid-State Batteries,” *Advanced Energy Materials*, vol. 9, no. 24, p. 1900626, 2019, doi: 10.1002/aenm.201900626.

[83] S. P. Barik, G. Prabaharan, and L. Kumar, “Leaching and separation of Co and Mn from electrode materials of spent lithium-ion batteries using hydrochloric acid: Laboratory and pilot scale study,” *Journal of Cleaner Production*, vol. 147, pp. 37–43, Mar. 2017, doi: 10.1016/j.jclepro.2017.01.095.

[84] W. Tang, X. Chen, T. Zhou, H. Duan, Y. Chen, and J. Wang, “Recovery of Ti and Li from spent lithium titanate cathodes by a hydrometallurgical

process," *Hydrometallurgy*, vol. 147–148, pp. 210–216, Aug. 2014, doi: 10.1016/j.hydromet.2014.05.013.

[85] C. K. Lee and K.-I. Rhee, "Preparation of LiCoO2 from spent lithium-ion batteries," *Journal of Power Sources*, vol. 109, no. 1, pp. 17–21, Jun. 2002, doi: 10.1016/S0378-7753(02)00037-X.

[86] E. G. Pinna, M. C. Ruiz, M. W. Ojeda, and M. H. Rodriguez, "Cathodes of spent Li-ion batteries: Dissolution with phosphoric acid and recovery of lithium and cobalt from leach liquors," *Hydrometallurgy*, vol. 167, pp. 66–71, Jan. 2017, doi: 10.1016/j.hydromet.2016.10.024.

[87] H. Li, S. Xing, Y. Liu, F. Li, H. Guo, and G. Kuang, "Recovery of Lithium, Iron, and Phosphorus from Spent LiFePO4 Batteries Using Stoichiometric Sulfuric Acid Leaching System," *ACS Sustainable Chem. Eng.*, vol. 5, no. 9, pp. 8017–8024, Sep. 2017, doi: 10.1021/acssuschemeng.7b01594.

[88] P. Meshram, B. D. Pandey, and T. R. Mankhand, "Hydrometallurgical processing of spent lithium ion batteries (LIBs) in the presence of a reducing agent with emphasis on kinetics of leaching," *Chemical Engineering Journal*, vol. 281, pp. 418–427, Dec. 2015, doi: 10.1016/j.cej.2015.06.071.

[89] M. Yu, Z. Zhang, F. Xue, B. Yang, G. Guo, and J. Qiu, "A more simple and efficient process for recovery of cobalt and lithium from spent lithium-ion batteries with citric acid," *Separation and Purification Technology*, vol. 215, pp. 398–402, May 2019, doi: 10.1016/j.seppur.2019.01.027.

[90] J. R. Almeida *et al.*, "Composition analysis of the cathode active material of spent Li-ion batteries leached in citric acid solution: A study to monitor and assist recycling processes," *Science of The Total Environment*, vol. 685, pp. 589–595, Oct. 2019, doi: 10.1016/j.scitotenv.2019.05.243.

[91] H. Setiawan, H. T. B. M. Petrus, and I. Perdana, "Reaction kinetics modeling for lithium and cobalt recovery from spent lithium-ion batteries using acetic acid," *Int J Miner Metall Mater*, vol. 26, no. 1, pp. 98–107, Jan. 2019, doi: 10.1007/s12613-019-1713-0.

[92] L. Li, J. Ge, F. Wu, R. Chen, S. Chen, and B. Wu, "Recovery of cobalt and lithium from spent lithium ion batteries using organic citric acid as leachant," *Journal of Hazardous Materials*, vol. 176, no. 1, pp. 288–293, Apr. 2010, doi: 10.1016/j.jhazmat.2009.11.026.

[93] M. He *et al.*, "Combined pyro-hydrometallurgical technology for recovering valuable metal elements from spent lithium-ion batteries: a review

of recent developments," *Green Chemistry*, vol. 25, no. 17, pp. 6561–6580, 2023, doi: 10.1039/D3GC01077E.

[94] "Sustainable Recycling Technology for Li-Ion Batteries and Beyond: Challenges and Future Prospects | Chemical Reviews." Accessed: Apr. 19, 2025. [Online]. Available: https://pubs.acs.org/doi/10.1021/acs.chemrev.9b00535

[95] M. Rinne, H. Elomaa, A. Porvali, and M. Lundström, "Simulation-based life cycle assessment for hydrometallurgical recycling of mixed LIB and NiMH waste," *Resources, Conservation and Recycling*, vol. 170, p. 105586, Jul. 2021, doi: 10.1016/j.resconrec.2021.105586.

[96] "Vianode launches first recycled graphite product for more sustainable…," Vianode. Accessed: Sep. 22, 2025. [Online]. Available: https://www.vianode.com/news/vianode-launches-first-recycled-graphite-product-for-more-sustainable-evs-and-batteries

[97] J. G. Kim *et al.*, "A review of lithium and non-lithium based solid state batteries," *Journal of Power Sources*, vol. 282, pp. 299–322, May 2015, doi: 10.1016/j.jpowsour.2015.02.054.

[98] J. Ma, B. Chen, L. Wang, and G. Cui, "Progress and prospect on failure mechanisms of solid-state lithium batteries," *Journal of Power Sources*, vol. 392, pp. 94–115, Jul. 2018, doi: 10.1016/j.jpowsour.2018.04.055.

[99] Q. Tu, L. Barroso-Luque, T. Shi, and G. Ceder, "Electrodeposition and Mechanical Stability at Lithium-Solid Electrolyte Interface during Plating in Solid-State Batteries," *Cell Reports Physical Science*, vol. 1, no. 7, p. 100106, Jul. 2020, doi: 10.1016/j.xcrp.2020.100106.

[100] Q. Zhao, S. Stalin, C.-Z. Zhao, and L. A. Archer, "Designing solid-state electrolytes for safe, energy-dense batteries," *Nat Rev Mater*, vol. 5, no. 3, pp. 229–252, Mar. 2020, doi: 10.1038/s41578-019-0165-5.

[101] X. Zheng *et al.*, "A Mini-Review on Metal Recycling from Spent Lithium Ion Batteries," *Engineering*, vol. 4, no. 3, pp. 361–370, Jun. 2018, doi: 10.1016/j.eng.2018.05.018.

[102] J. Dube, "(75) Inventors: Francois Cardarelli, St-Leonard (CA);".

[103] X. Wu, G. Ji, J. Wang, G. Zhou, and Z. Liang, "Toward Sustainable All Solid-State Li–Metal Batteries: Perspectives on Battery Technology and Recycling Processes," *Advanced Materials*, vol. 35, no. 51, p. 2301540, 2023, doi: 10.1002/adma.202301540.

[104] L. Azhari, S. Bong, X. Ma, and Y. Wang, "Recycling for All Solid-State Lithium-Ion Batteries," *Matter*, vol. 3, no. 6, pp. 1845–1861, Dec. 2020, doi: 10.1016/j.matt.2020.10.027.

[105] "Regulation (EU) 2023/ of the European Parliament and of the Council of 12 July 2023 concerning batteries and waste batteries, amending Directive 2008/98/EC and Regulation (EU) 2019/1020 and repealing Directive 2006/66/EC".

[106] K. J. Kim, M. Balaish, M. Wadaguchi, L. Kong, and J. L. M. Rupp, "Solid-State Li–Metal Batteries: Challenges and Horizons of Oxide and Sulfide Solid Electrolytes and Their Interfaces," *Advanced Energy Materials*, vol. 11, no. 1, p. 2002689, 2021, doi: 10.1002/aenm.202002689.

[107] K. Schneider, V. Kiyek, M. Finsterbusch, B. Yagmurlu, and D. Goldmann, "Acid Leaching of Al- and Ta-Substituted Li7La3Zr2O12 (LLZO) Solid Electrolyte," *Metals*, vol. 13, no. 5, Art. no. 5, May 2023, doi: 10.3390/met13050834.

[108] "Reaction mechanisms of lithium garnet pellets in ambient air: The effect of humidity and CO2 - Xia - 2017 - Journal of the American Ceramic Society - Wiley Online Library." Accessed: Apr. 20, 2025. [Online]. Available: https://ceramics.onlinelibrary.wiley.com/doi/full/10.1111/jace.14865

[109] Z. F. Yow, Y. L. Oh, W. Gu, R. P. Rao, and S. Adams, "Effect of Li+/H+ exchange in water treated Ta-doped Li7La3Zr2O12," *Solid State Ionics*, vol. 292, pp. 122–129, Sep. 2016, doi: 10.1016/j.ssi.2016.05.016.

[110] G. J.-P. Deblonde, A. Chagnes, V. Weigel, and G. Cote, "Direct precipitation of niobium and tantalum from alkaline solutions using calcium-bearing reagents," *Hydrometallurgy*, vol. 165, pp. 345–350, Oct. 2016, doi: 10.1016/j.hydromet.2015.12.009.

[111] L. Schwich *et al.*, "Recycling Strategies for Ceramic All-Solid-State Batteries—Part I: Study on Possible Treatments in Contrast to Li-Ion Battery Recycling," *Metals*, vol. 10, no. 11, Art. no. 11, Nov. 2020, doi: 10.3390/met10111523.

[112] W.-S. Chen, H.-J. Ho, and K.-Y. Lin, "Hydrometallurgical Process for Tantalum Recovery from Epoxy-Coated Solid Electrolyte Tantalum Capacitors," *Materials*, vol. 12, no. 8, Art. no. 8, Jan. 2019, doi: 10.3390/ma12081220.

[113] H. Zhou, S. Zheng, Y. Zhang, and D. Yi, "A kinetic study of the leaching of a low-grade niobium–tantalum ore by concentrated KOH solution,"

Hydrometallurgy, vol. 80, no. 3, pp. 170–178, Dec. 2005, doi: 10.1016/j.hydromet.2005.06.011.

[114] “Tantalum pentoxide,” *Wikipedia*. May 24, 2025. Accessed: Aug. 07, 2025. [Online]. Available: https://en.wikipedia.org/w/index.php?title=Tantalum_pentoxide&oldid=1291898087

[115] R·P·星 and M·J·米勒, “Method for dissolution and purification of tantalum pentoxide,” CN1082935C, Apr. 17, 2002 Accessed: Aug. 09, 2025. [Online]. Available: https://patents.google.com/patent/CN1082935C/en

[116] Y. Ma, S. Stopic, X. Wang, K. Forsberg, and B. Friedrich, “Basic Sulfate Precipitation of Zirconium from Sulfuric Acid Leach Solution,” *Metals*, vol. 10, no. 8, Art. no. 8, Aug. 2020, doi: 10.3390/met10081099.

[117] F. Nasuha Yahya, L. Nadirah Mat Suli, W. Hanisah Wan Ibrahim, and R. Abdul Rasid, “Thermodynamic Evaluation of the Aqueous Stability of Rare Earth Elements in Sulfuric Acid Leaching of Monazite through Pourbaix Diagram,” *Materials Today: Proceedings*, vol. 19, pp. 1647–1656, Jan. 2019, doi: 10.1016/j.matpr.2019.11.193.

[118] “TransIMMCvol.861977p.C202-C206Precipitationdiagrams-formetalsalts.”

[119] M. Ali Nowroozi *et al.*, “Towards Recycling of LLZO Solid Electrolyte Exemplarily Performed on LFP/LLZO/LTO Cells,” *ChemistryOpen*, vol. 11, no. 3, p. e202100274, 2022, doi: 10.1002/open.202100274.

[120] Y. Zou, A. Chernyaev, S. Seisko, J. Sainio, and M. Lundström, “Removal of iron and aluminum from hydrometallurgical NMC-LFP recycling process through precipitation,” *Minerals Engineering*, vol. 218, p. 109037, Nov. 2024, doi: 10.1016/j.mineng.2024.109037.

[121] K. Wissel *et al.*, “Towards Recycling of All-Solid-State Batteries with Argyrodite Sulfide Electrolytes: Insights into Electrolyte and Electrode Degradation in Dissolution-Based Separation Processes,” *ChemSusChem*, vol. 18, no. 9, p. e202402128, 2025, doi: 10.1002/cssc.202402128.

[122] M. Batzer, C. Heck, P. Michalowski, and A. Kwade, “Current Status of Formulations and Scalable Processes for Producing Sulfidic Solid-State Batteries,” *Batteries & Supercaps*, vol. 5, no. 12, p. e202200328, 2022, doi: 10.1002/batt.202200328.

[123] A. Hayashi, H. Muramatsu, T. Ohtomo, S. Hama, and M. Tatsumisago, “Improvement of chemical stability of Li3PS4 glass electrolytes by

adding MxOy (M = Fe, Zn, and Bi) nanoparticles,” *J. Mater. Chem. A*, vol. 1, no. 21, pp. 6320–6326, May 2013, doi: 10.1039/C3TA10247E.

[124] M. Batzer, K. Voges, W. Wang, P. Michalowski, and A. Kwade, “Systematic evaluation of materials and recipe for scalable processing of sulfide-based solid-state batteries,” *Materials Today Communications*, vol. 30, p. 103189, Mar. 2022, doi: 10.1016/j.mtcomm.2022.103189.

[125] A. Miura *et al.*, “Liquid-phase syntheses of sulfide electrolytes for all-solid-state lithium battery,” *Nat Rev Chem*, vol. 3, no. 3, pp. 189–198, Mar. 2019, doi: 10.1038/s41570-019-0078-2.

[126] S. Chen *et al.*, “Sulfide solid electrolytes for all-solid-state lithium batteries: Structure, conductivity, stability and application,” *Energy Storage Materials*, vol. 14, pp. 58–74, Sep. 2018, doi: 10.1016/j.ensm.2018.02.020.

[127] D. H. S. Tan, A. Banerjee, Z. Chen, and Y. S. Meng, “From nanoscale interface characterization to sustainable energy storage using all-solid-state batteries,” *Nat. Nanotechnol.*, vol. 15, no. 3, pp. 170–180, Mar. 2020, doi: 10.1038/s41565-020-0657-x.

[128] D. H. S. Tan *et al.*, “Sustainable design of fully recyclable all solid-state batteries,” *MRS Energy & Sustainability*, vol. 7, no. 1, p. 23, Jul. 2020, doi: 10.1557/mre.2020.25.

[129] M. Ghidiu, J. Ruhl, S. P. Culver, and W. G. Zeier, “Solution-based synthesis of lithium thiophosphate superionic conductors for solid-state batteries: a chemistry perspective,” *Journal of Materials Chemistry A*, vol. 7, no. 30, pp. 17735–17753, 2019, doi: 10.1039/C9TA04772G.

[130] O. Velázquez-Martínez, J. Valio, A. Santasalo-Aarnio, M. Reuter, and R. Serna-Guerrero, “A Critical Review of Lithium-Ion Battery Recycling Processes from a Circular Economy Perspective,” *Batteries*, vol. 5, no. 4, Art. no. 4, Dec. 2019, doi: 10.3390/batteries5040068.

[131] “Enhancing the Moisture Stability and Electrochemical Performances of Li6PS5Cl Solid Electrolytes through Ga Substitution - ScienceDirect.” Accessed: Jun. 02, 2025. [Online]. Available: https://www.sciencedirect.com/science/article/pii/S0013468622019132

[132] Y. Zheng *et al.*, “The Effects of Phosphate Impurity on Recovered LiNi0.6Co0.2Mn0.2O2 Cathode Material via a Hydrometallurgy Method,” *ACS Appl Mater Interfaces*, vol. 14, no. 43, pp. 48627–48635, Nov. 2022, doi: 10.1021/acsami.2c12715.

[133] M. Stopic and C. Stallmeister, “Solid state sUlfide Based LI-MEtal batteries for EV applications”.

[134] S. Y. Kim *et al.*, “Lithium Ytterbium-Based Halide Solid Electrolytes for High Voltage All-Solid-State Batteries,” *ACS Materials Lett.*, vol. 3, no. 7, pp. 930–938, Jul. 2021, doi: 10.1021/acsmaterialslett.1c00142.

[135] Y. Nikodimos, C.-J. Huang, B. W. Taklu, W.-N. Su, and B. J. Hwang, “Chemical stability of sulfide solid-state electrolytes: stability toward humid air and compatibility with solvents and binders,” *Energy Environ. Sci.*, vol. 15, no. 3, pp. 991–1033, Mar. 2022, doi: 10.1039/D1EE03032A.

[136] M. Jacob *et al.*, “Direct Recycling of All-Solid-State Batteries with a Halide Solid Electrolyte via Water-Based Separation: Interactions of Electrode Materials in Aqueous Li3InCl6 Solutions,” *Batteries & Supercaps*, vol. n/a, no. n/a, p. 2500189, doi: 10.1002/batt.202500189.

[137] H. Kwak *et al.*, “Emerging Halide Superionic Conductors for All-Solid-State Batteries: Design, Synthesis, and Practical Applications,” *ACS Energy Lett.*, vol. 7, no. 5, pp. 1776–1805, May 2022, doi: 10.1021/acsenergylett.2c00438.

[138] L. Yue *et al.*, “All solid-state polymer electrolytes for high-performance lithium ion batteries,” *Energy Storage Materials*, vol. 5, pp. 139–164, Oct. 2016, doi: 10.1016/j.ensm.2016.07.003.

[139] N. Xin, Y. Sun, M. He, C. J. Radke, and J. M. Prausnitz, “Solubilities of six lithium salts in five non-aqueous solvents and in a few of their binary mixtures,” *Fluid Phase Equilibria*, vol. 461, pp. 1–7, Apr. 2018, doi: 10.1016/j.fluid.2017.12.034.

[140] “Polymer electrolytes for lithium ion batteries: a critical study | Ionics.” Accessed: Mar. 25, 2025. [Online]. Available: https://link.springer.com/article/10.1007/s11581-016-1908-6

[141] B. Ensing *et al.*, “On the origin of the extremely different solubilities of polyethers in water,” *Nat Commun*, vol. 10, no. 1, p. 2893, Jun. 2019, doi: 10.1038/s41467-019-10783-z.

[142] C. Özdemir and A. Güner, “Solubility profiles of poly(ethylene glycol)/solvent systems, I: Qualitative comparison of solubility parameter approaches,” *European Polymer Journal*, vol. 43, no. 7, pp. 3068–3093, Jul. 2007, doi: 10.1016/j.eurpolymj.2007.02.022.

[143] J. Meier-Haack, W. Lenk, D. Lehmann, and K. Lunkwitz, “Pervaporation separation of water/alcohol mixtures using composite membranes based on polyelectrolyte multilayer assemblies,” *Journal of Membrane Science*, vol. 184, no. 2, pp. 233–243, Mar. 2001, doi: 10.1016/S0376-7388(00)00618-9.

[144] A. Thielen, T. Leißner, T. Eisenmann, and U. A. Peuker, "On decoating of polymer electrolyte-based solid-state battery cathodes," *RSC Sustainability*, vol. 3, no. 5, pp. 2377–2389, 2025, doi: 10.1039/D5SU00082C.

[145] J. G. Poulakis and C. D. Papaspyrides, "Dissolution/reprecipitation: A model process for PET bottle recycling," *Journal of Applied Polymer Science*, vol. 81, no. 1, pp. 91–95, 2001, doi: 10.1002/app.1417.

[146] P. Pang and P. Englezos, "Phase separation of polyethylene oxide (PEO)–water solution and its relationship to the flocculating capability of the PEO," *Fluid Phase Equilibria*, vol. 194–197, pp. 1059–1066, Mar. 2002, doi: 10.1016/S0378-3812(01)00691-4.

[147] Y. Zhao *et al.*, "Regeneration and reutilization of cathode materials from spent lithium-ion batteries," *Chemical Engineering Journal*, vol. 383, p. 123089, Mar. 2020, doi: 10.1016/j.cej.2019.123089.

[148] J. M. Paulsen, C. L. Thomas, and J. R. Dahn, "Layered Li-Mn-Oxide with the O2 Structure: A Cathode Material for Li-Ion Cells Which Does Not Convert to Spinel," *J. Electrochem. Soc.*, vol. 146, no. 10, p. 3560, Oct. 1999, doi: 10.1149/1.1392514.

[149] Q. Liu *et al.*, "Recent Progress of Layered Transition Metal Oxide Cathodes for Sodium-Ion Batteries," *Small*, vol. 15, no. 32, p. 1805381, 2019, doi: 10.1002/smll.201805381.

[150] H. Du *et al.*, "Easily recyclable lithium-ion batteries: Recycling-oriented cathode design using highly soluble LiFeMnPO4 with a water-soluble binder," *Battery Energy*, vol. 2, no. 4, p. 20230011, 2023, doi: 10.1002/bte2.20230011.

[151] L. Brückner, J. Frank, and T. Elwert, "Industrial Recycling of Lithium-Ion Batteries—A Critical Review of Metallurgical Process Routes," *Metals*, vol. 10, no. 8, Art. no. 8, Aug. 2020, doi: 10.3390/met10081107.

[152] T. Georgi-Maschler, B. Friedrich, R. Weyhe, H. Heegn, and M. Rutz, "Development of a recycling process for Li-ion batteries," *Journal of Power Sources*, vol. 207, pp. 173–182, Jun. 2012, doi: 10.1016/j.jpowsour.2012.01.152.

[153] S. Xiao *et al.*, "Recovery of Valuable Metals from Spent Lithium-Ion Batteries by Smelting Reduction Process Based on MnO–SiO2–Al2O3 Slag System," *J. Sustain. Metall.*, vol. 3, no. 4, pp. 703–710, Dec. 2017, doi: 10.1007/s40831-017-0131-7.

[154] M. Assefi, S. Maroufi, Y. Yamauchi, and V. Sahajwalla, "Pyrometallurgical recycling of Li-ion, Ni–Cd and Ni–MH batteries: A minireview,"

Current Opinion in Green and Sustainable Chemistry, vol. 24, pp. 26–31, Aug. 2020, doi: 10.1016/j.cogsc.2020.01.005.

[155] D. c/o U. Cheret and S. Santén, “Battery recycling,” EP1589121B1, Dec. 31, 2008 Accessed: Jun. 27, 2025. [Online]. Available: https://patents.google.com/patent/EP1589121B1/en

[156] G. Ren *et al.*, “Recovery of valuable metals from spent lithium ion batteries by smelting reduction process based on FeO–SiO2–Al2O3 slag system,” *Transactions of Nonferrous Metals Society of China*, vol. 27, no. 2, pp. 450–456, Feb. 2017, doi: 10.1016/S1003-6326(17)60051-7.

[157] L. SCHEUNIS and W. CALLEBAUT, “Process for the recovery of lithium,” WO2020104164A1, May 28, 2020 Accessed: Jun. 27, 2025. [Online]. Available: https://patents.google.com/patent/WO2020104164A1/en

[158] M. Rinne, H. Lappalainen, and M. Lundström, “Evaluating the possibilities and limitations of the pyrometallurgical recycling of waste Li-ion batteries using simulation and life cycle assessment,” *Green Chem.*, vol. 27, no. 9, pp. 2522–2537, Feb. 2025, doi: 10.1039/D4GC05409A.

[159] “CM2200.Primary.Metals.fm.” Accessed: Sep. 25, 2025. [Online]. Available: https://www.chem.mtu.edu/chem_eng/faculty/kawatra/CM2200_Primary_Metals.pdf

[160] A. Vezzini, “Manufacturers, Materials and Recycling Technologies,” in *Lithium-Ion Batteries*, Elsevier, 2014, pp. 529–551. doi: 10.1016/B978-0-444-59513-3.00023-6.

[161] Oar-Arteta et al.,"Metal organic frameworks as precursors for the manufacture of advanced catalytic materials", Mater. Chem. Front., 2017, 1, 1709, 2017, doi: 10.1039/c7qm00007c.

[162] C. Hagelüken, “Recycling of Electronic Scrap at Umicore’s Integrated Metals Smelter and Refinery,” *World of Metallurgy*, no. 3, 2006.

[163] L. Miara *et al.*, “About the Compatibility between High Voltage Spinel Cathode Materials and Solid Oxide Electrolytes as a Function of Temperature,” *ACS Appl. Mater. Interfaces*, vol. 8, no. 40, pp. 26842–26850, Oct. 2016, doi: 10.1021/acsami.6b09059.

[164] M. Gellert, E. Dashjav, D. Grüner, Q. Ma, and F. Tietz, “Compatibility study of oxide and olivine cathode materials with lithium aluminum titanium phosphate,” *Ionics*, vol. 24, no. 4, pp. 1001–1006, Apr. 2018, doi: 10.1007/s11581-017-2276-6.

[165] M. Rumpel *et al.*, “Thermal stabilities of Mn-based active materials in combination with the ceramic electrolyte LATP for ASSB bulk cathodes,” *Mater. Adv.*, vol. 3, no. 9, pp. 4015–4025, May 2022, doi: 10.1039/D2MA00158F.

[166] E. Wiberg, “Lehrbuch der anorganischen Chemie,” in *Lehrbuch der anorganischen Chemie*, De Gruyter, 2019. Accessed: Apr. 19, 2025. [Online]. Available: https://www.degruyterbrill.com/document/doi/10.1515/9783111520285/html?lang=de

[167] E. Communications, “Zirconium.” Accessed: Apr. 19, 2025. [Online]. Available: https://roempp.thieme.de/lexicon/RD-26-00467?context=lexiconOverview

[168] T. Schirmer, H. Qiu, D. Goldmann, C. Stallmeister, and B. Friedrich, “Influence of P and Ti on Phase Formation at Solidification of Synthetic Slag Containing Li, Zr, La, and Ta,” *Minerals*, vol. 12, no. 3, Art. no. 3, Mar. 2022, doi: 10.3390/min12030310.

[169] H. Tsukasaki, H. Sano, K. Igarashi, A. Wakui, T. Yaguchi, and S. Mori, “Deterioration process of argyrodite solid electrolytes during exposure to humidity-controlled air,” *Journal of Power Sources*, vol. 524, p. 231085, Mar. 2022, doi: 10.1016/j.jpowsour.2022.231085.

[170] “Synthesis of Sulfide Solid Electrolytes through the Liquid Phase: Optimization of the Preparation Conditions | ACS Omega.” Accessed: Apr. 20, 2025. [Online]. Available: https://pubs.acs.org/doi/full/10.1021/acsomega.0c04307

[171] A. Heitmann and P. Reher, “Recycling-Prozessefür Schwefel-Verbindungen,” *Chemie Ingenieur Technik*, vol. 46, no. 14, pp. 589–594, 1974, doi: 10.1002/cite.330461403.

[172] J. Vohlídal, “Polymer degradation: a short review,” *Chemistry Teacher International*, vol. 3, no. 2, pp. 213–220, Jun. 2021, doi: 10.1515/cti-2020-0015.

[173] D. Jovell, J. O. Pou, F. Llovell, and R. Gonzalez-Olmos, “Life Cycle Assessment of the Separation and Recycling of Fluorinated Gases Using Ionic Liquids in a Circular Economy Framework,” *ACS Sustainable Chem. Eng.*, vol. 10, no. 1, pp. 71–80, Jan. 2022, doi: 10.1021/acssuschemeng.1c04723.

[174] F. CARDARELLI and J. Dub, “A method for recycling spent lithium metal polymer rechargeable batteries and related materials,” EP1269554B1, May 30, 2012 Accessed: Jul. 25, 2025. [Online]. Available: https://patents.google.com/patent/EP1269554B1/en

[175] H.-D. Lim *et al.*, “A New Perspective on Li–SO2 Batteries for Rechargeable Systems,” *Angewandte Chemie International Edition*, vol. 54, no. 33, pp. 9663–9667, 2015, doi: 10.1002/anie.201504306.

[176] S. Subramanian and G. Øye, “Aqueous carbon black dispersions stabilized by sodium lignosulfonates,” *Colloid Polym Sci*, vol. 299, no. 7, pp. 1223–1236, Jul. 2021, doi: 10.1007/s00396-021-04840-7.

[177] “Sodium Chloride | Solubility of Things.” Accessed: Aug. 10, 2025. [Online]. Available: https://www.solubilityofthings.com/sodiumchloride

[178] “carbon-black-user-guide.pdf.” Accessed: Jun. 21, 2025. [Online]. Available: https://cancarb.com/wp-content/uploads/2020/05/carbon-black-user-guide.pdf

[179] J.-B. Donnet, *Carbon Black: Science and Technology, Second Edition*, 2nd ed. Boca Raton: CRC Press LLC, 1993.

[180] D. Leistenschneider *et al.*, “Mechanochemical Functionalization of Carbon Black at Room Temperature,” *C*, vol. 4, no. 1, Art. no. 1, Mar. 2018, doi: 10.3390/c4010014.

[181] “NaAlCl4.” Accessed: Aug. 10, 2025. [Online]. Available: https://www.chembk.com/en/chem/NaAlCl4

[182] “Sodium polysulfide,” *Wikipedia*. Apr. 08, 2025. Accessed: Aug. 10, 2025. [Online]. Available: https://en.wikipedia.org/w/index.php?title=Sodium_polysulfide&oldid=1284557382

[183] J. Partinen, P. Halli, A. Varonen, B. P. Wilson, and M. Lundström, “Investigating battery black mass leaching performance as a function of process parameters by combining leaching experiments and regression modeling,” *Minerals Engineering*, vol. 215, p. 108828, Sep. 2024, doi: 10.1016/j.mineng.2024.108828.

[184] M. Joulié, R. Laucournet, and E. Billy, “Hydrometallurgical process for the recovery of high value metals from spent lithium nickel cobalt aluminum oxide based lithium-ion batteries,” *Journal of Power Sources*, vol. 247, pp. 551–555, Feb. 2014, doi: 10.1016/j.jpowsour.2013.08.128.